Institute of Hydrology

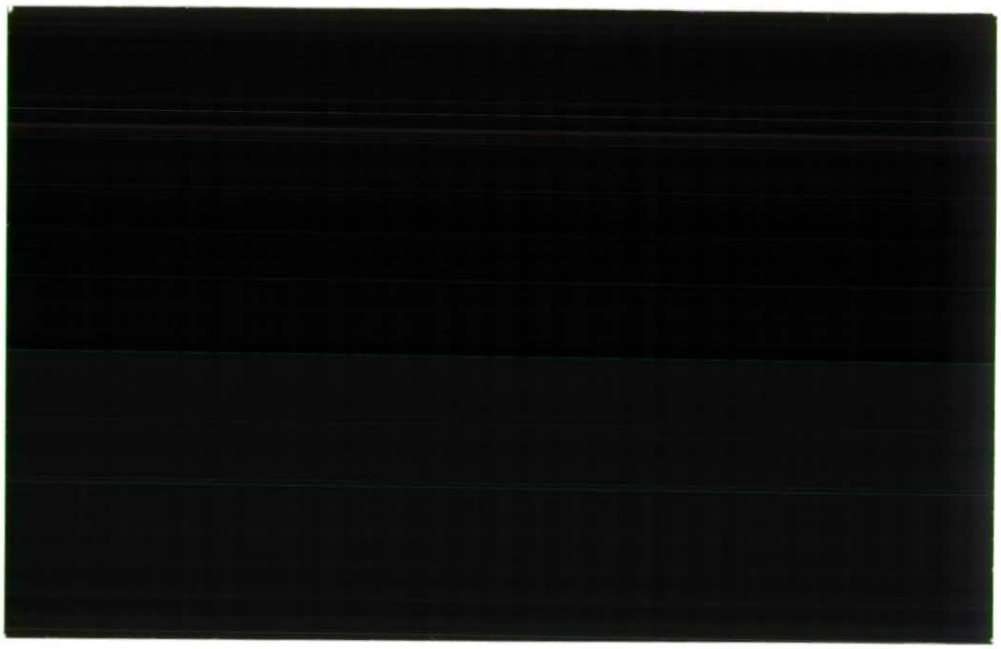

Natural Environment Research Council


Natural
Environment
Research
Council

# THE SLAPTON LEY NERC AIRBORNE CAMPAIGN - THE RESULTS OF THE IMAGE ANALYSIS AND THEIR RELEVANCE TO THE HYDROLOGY OF THE CATCHMENT

Institute of Hydrology
Crowmarsh Gifford
Wallingford
Oxon
OX10 8BB
UK

Tel: 0491 838800
Fax: 0491 832256
Telex: 849365 Hydrol G

August 1993

# Executive summary

The analysis of stereo aerial photographs and remotely sensed images acquired during the 1990 NERC airborne campaign over the Slapton wood catchment in Devon is described, and the usefulness of the results for hydrological purposes investigated.

The aerial photographs were analysed under a stereo viewer to provide the exact location of the stream gauging station, difficult on the ground because of trees, and also to delineate the catchment boundary.

The remotely sensed images, recorded on a Daedalus AADS 1268 scanner at a 4.5 m resolution, were analysed to provide the distribution of near surface soil moisture over the grassland areas, and two land cover classifications.

Soil moisture data recorded with a capacitance probe were used as 'ground truths' for the soil moisture distribution though the final result proved disappointing. This was attributed to the very dry conditions and to a lack of variation in soil moisture.

The land use classifications were found to compare well with a field survey and the results of analysing a Landsat image. Evapotranspiration estimates, obtained using neutron probe measurements at three sites under the three dominant land uses, were extrapolated to the catchment scale using the land classification. The resulting catchment evapotranspiration losses compared well with the annual 'water use' of the catchment, given as the difference between rainfall inputs and streamflow outputs.

# Contents

# 1. Introduction

Slapton Ley, located between Plymouth and Torbay in Devon (Fig. 1.1), is the largest freshwater lake in southwest England. Since 1970, four catchments draining into the Ley have been monitored in some detail because of a fear that it was becoming increasingly eutrophic. Much of the work has concentrated on nitrate leaching (Burt *et al.*, 1988) from this mainly agricultural area, but attention has also focused on hillslope runoff processes (Burt *et al.*, 1983). Because of the interest in the area, the Slapton Ley Field Centre was established as a major centre for teaching physical geography and ecology to sixth form students and others. Over 3000 students pass through the field centre every year.

More recently, one of the catchments draining into the Ley (the Slapton Wood catchment, 0.94 sq km in area) has been the location of a study, funded by NIREX, to determine subsurface hillslope runoff processes. This was done using a distributed hydrological model, the Systeme Hydrologique Europeen (SHE; Bathurst, 1986). In order to provide the data requirements of this study, the existing hydrological network has been updated. This will be described later. Also, it was decided to ascertain what remote sensing could provide. Although LANDSAT images of the area are available in the NERC library, and further LANDSAT and SPOT images could have been purchased, it was felt that the ground resolution achieved by satellites is too coarse to provide the information necessary for studying this relatively small area and, ultimately, to provide some of the parameter requirements of SHE. To do this adequately would require images with a pixel resolution of the order of 2 m.

It was decided that the best way of obtaining such images was by putting forward the Slapton Ley area as a 'community site' for the 1990 NERC aircraft campaign. This was particularly so in view of the continued interest expressed in the area by various university departments - distributed hydrological modelling (Universities of Newcastle and Lancaster), nitrate leaching (University of Oxford), and phytoplankton development within the Ley itself (University of Sheffield).

The application proved successful, and the area was earmarked for the spring and summer aircraft campaigns. It was decided to conduct a number of field surveys coincident with the flights and at other times. These included vegetation surveys, soil moisture surveys using capacitance probes, and vegetation reflectances using a hand-held radiometer.

This report describes the results of the various field surveys and the analysis of the visible and infrared images of the Slapton Wood catchment. It also describes how the results were used, in conjunction with data from small plot studies, to calculate a water balance for the catchment.

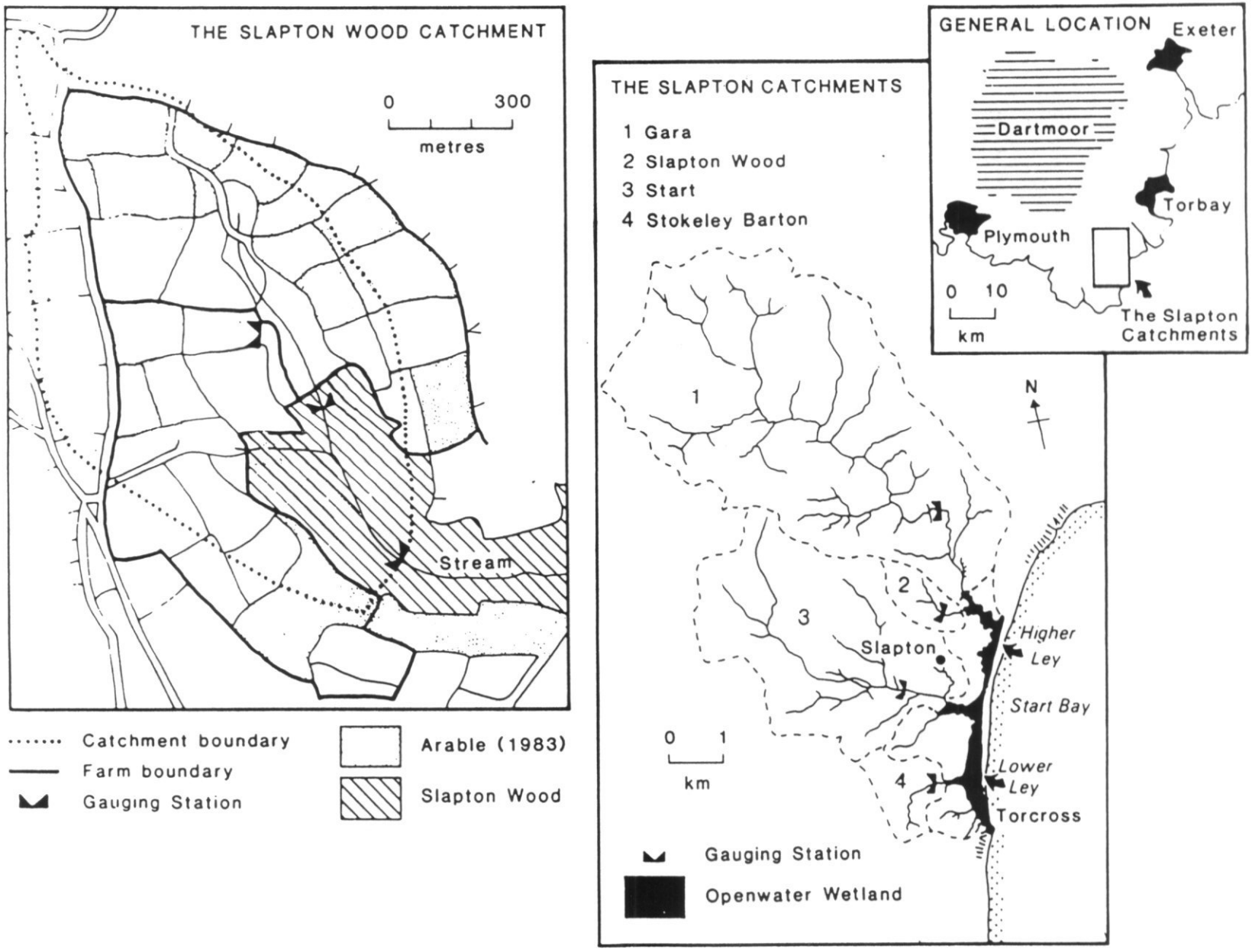


Fig. 1.1 Location of the Slapton Wood catchment

# 2. Study area and instrumentation

A detailed description of the study area and the instrumentation in existence prior to the NIREX study is given in Burt *et al.*, 1988 from which the following brief description has been taken.

The Slapton Wood catchment is 0.94 km$^2$ in area underlain by impermeable Dartmouth slates. The interfluve areas are relatively flat, slopes typically below 5°. The valley sides are much steeper, up to 25°. The soils are freely-draining brown earths of the Manod series, though brown podzolic soils of the Denbigh series are found within the wood (Trudgill, 1983). Only about 15 percent of the catchment is wooded, concentrated towards the bottom of the catchment. The remainder is a mixture of arable land, about 30% confined to the interfluve areas, and permanent pasture.

Initially, rainfall was measured only at the Field Centre, some 800 m below the catchment boundary, using a Cassella 12" natural syphon autographic raingauge and a standard 5" Mark II check gauge. Mean annual rainfall for the period 1961-1985 was 1035 mm. For the NIREX study, four ground-level raingauges were installed within the catchment area (Fig. 2.1). These were read at approximately weekly intervals and their totals time distributed using data from two recording raingauges, one attached to an automatic weather station. Rainfall from the individual gauges were combined to give areal estimates using the Thiessen polygon method (Thiessen, 1911).

Streamflow at the outfall of the catchment has been measured since 1971 as the head of water over a 120° thin plate V-notch weir. Originally, water levels were recorded on an OTT R16 recorder, but more recently a potentiometric water level sensor (Strangeways and Templeman, 1974) attached to a solid state logger has been used. The in-built software of this latter logger allows direct conversion of water level to flow using a theoretical relationship (BSI, 1981). Streamflow is gauged at two other points within the catchment. The first point is approximately 330 m upstream of the V-notch towards the northern edge of Slapton Wood, whilst the second point is an intermittent stream draining Carness hollow (Fig. 2.1). In both instances, a prefabricated Forth River Purification Board (FRPB) short throated trapezoidal flume has been employed. All three flow measuring structures are occasionally calibrated using dilution gauging, flow metering or gravimetric techniques and, if necessary, changes made to the theoretical relationships between water level and flow.

A meteorological station is in operation at the Field Centre. The instruments are read manually at 0900 GMT every day. In addition, an automatic weather station (Strangeways, 1972) has been installed in a grass field within the catchment (Fig. 2.1). Both stations provide the climatological variables required to calculate potential evaporation from grassland (Penman, 1948), at daily intervals.

All data pertaining to the calculation of rainfall, streamflow and evaporation are subject to rigorous quality control procedures as described in Roberts, 1981.

Three sets of six neutron probe access tubes (Bell, 1976) for measuring soil moisture have been installed. They are sited within the forested area, in a barley field (to the right in Fig. 2.1) and in the same grassland field as the automatic weather station. A further two access tubes were subsequently installed at the grassland site. The tubes are read at approximately

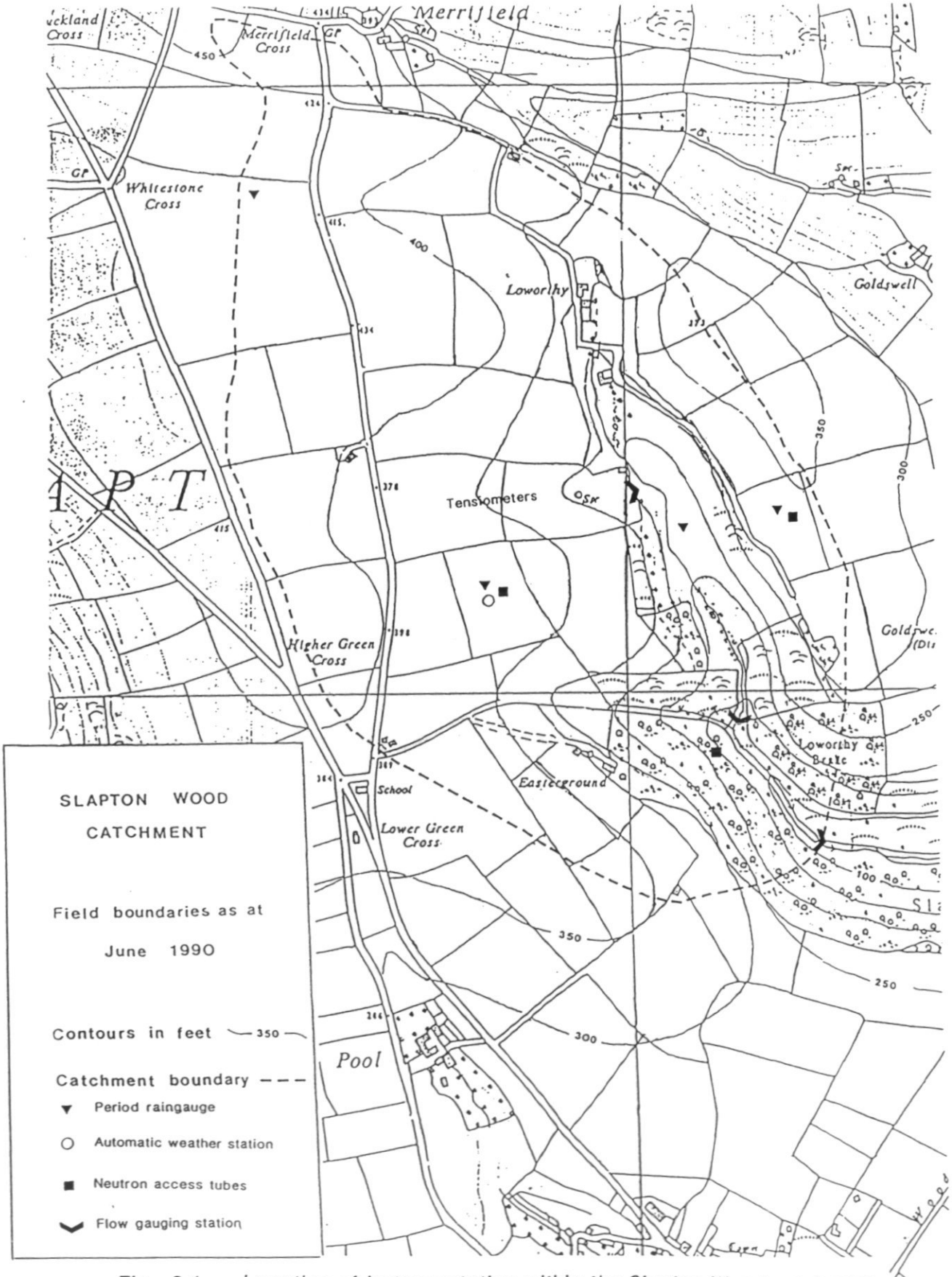


Fig. 2.1 Location of instrumentation within the Slapton Wood catchment

weekly intervals, the data quality controlled and converted into moisture volume fractions at the various reading depths and into profile water contents (Roberts, 1972). A number of tensiometers, designed to give estimates of soil water potential, were also installed next to some of the neutron access tubes. Also, tensiometers were installed along the length of Carness hollow (Fig. 2.1). Two sets of gypsum blocks were installed within the grassland soil moisture site. These are used to give estimates of soil water potential in dry periods, when the potentials are too low to be read with tensiometers (Wellings *et al.*, 1985). A total of over 30 dipwells were installed within the catchment to give estimates of sub-surface water levels. A detailed description of the installation and data collection schedule of all soil moisture measuring instrumentation is given in Boyle, 1991.

# 3. The NERC airborne campaign

A number of NERC aircraft flights were undertaken over the Slapton area in 1990 using various scanners in support of three studies. These studies were:-

(i) The identification of phytoplankton within the Ley itself, conducted by the University of Sheffield.

(ii) Soil moisture monitoring and modelling within the Slapton Wood catchment, conducted by the University of Lancaster.

(iii) The identification of land cover and distribution of soil moisture for hydrological modelling, conducted by the Institute of Hydrology.

The rest of the report will concentrate on the latter study.

Two flights were undertaken, on the 28th April and the 11th July. In both instances, the flying height was specified as 800 m thus ensuring remotely-sensed images with a 2 m ground resolution. Stereo black-and-white aerial photographs using a Wild RC8 camera were obtained simultaneously with a 11-band image using a Daedalus Airborne Thematic Mapper Scanner (AADS 1268). Details of the bands recorded using the AADS 1268 scanner and their Landsat equivalent are given in Table 3.1 below.

*Table 3.1* *The Daedalus 1268 ATM Scanner*

| Channel | Band edges (microns) | Landsat bands |
|---|---|---|
| 1 | 0.42 - 0.45 | |
| 2 | 0.45 - 0.52 | 1 (BLUE) |
| 3 | 0.52 - 0.60 | 2 (GREEN) |
| 4 | 0.605 - 0.625 | |
| 5 | 0.63 - 0.69 | 3 (RED) |
| 6 | 0.695 - 0.75 | |
| 7 | 0.76 - 0.90 | 4 (NEAR INFRARED) |
| 8 | 0.91 - 1.05 | |
| 9 | 1.55 - 1.75 | 5 (MIDDLE INFRARED) |
| 10 | 2.08 - 2.35 | 7 (FAR INFRARED) |
| 11 | 8.5 - 13.0 | 6 (THERMAL) |

A number of field surveys were undertaken to provide 'ground truths' for the analysis of the remotely-sensed images:-

(i) Vegetation surveys were conducted on a number of dates to ascertain what crops were being grown in fields within and immediately outside the catchment area.

(ii) The distribution of soil moisture within the catchment area was assessed on a number of days using a capacitance probe (Dean *et al.*, 1987). These hand-held probes give an integrated value of soil moisture in the top 5 cm and 10 cm of soil. Data have been gathered from under different crop types and along transects within grass fields.

(iii) Radiances of various crop types obtained using a hand-held IRIS spectroradiometer (Rollin and Milton, 1988) taken on the same date (11th July) as the second NERC aircraft flight. This spectroradiometer provides spectra in the wavelength range 0.35 to 2.5 microns, with spectral resolutions varying between 2 nanometres and 5 nanometres.

# 4. Image analysis

## 4.1 BLACK AND WHITE STEREO AERIAL PHOTOGRAPHS

The photographs taken during both flights were used, together with the results of the vegetation surveys, to provide 'ground truths' for, and comparisons with, the image classifications (see below), and also to help identify the position of the catchment boundary.

For the latter, overlapping photographs were viewed under a stereo viewer. This enabled an accurate positioning of the lower flow gauging station, difficult on the ground because of the wood, and the exaggerated vertical scaling generally gave a good indication of the position


Fig. 4.1.1 Slapton Wood Catchment Boundaries

---- Original (1:25K map) —— Current (Aerial Photographs)

of the boundary. The west and east interfluves of the catchment are particularly flat, and it was necessary to conduct ground surveys using levelling equipment to resolve the actual position of the boundary. Figure 4.1.1 shows the 'new' catchment boundary together with the original, simply taken from a 1:25,000 topographic map.

As shown in Fig. 4.1.1, the actual catchment areas are very similar, though the aerial photographs suggest that there are additional areas within the catchment at the top end, together with a similar reduction in area at the lower end. The current catchment area in use is 0.94 sq km.

## 4.2 THE IRIS SPECTRORADIOMETER

A hand-held IRIS spectroradiometer was used on July 11th, coincident with the second aircraft flight, to obtain reflectance spectra of a number of land cover types within the Slapton Wood catchment. Details of the IRIS spectroradiometer are given in Rollin and Milton, 1988. The locations of the sampling sites and the land covers sampled are given in Fig. 4.2.1.

In total, 16 sites were sampled, covering 9 different land cover types. At each site, a radiance spectrum from a barium sulphate plate was taken as well as a radiance spectrum from the vegetation type. The two spectra were combined to give the percentage of the incoming solar radiation reflected by the crop. The individual reflectance spectra are shown in Figs 1 to 16 of Appendix I. Values in the two wavelength bands where strong water vapour absorption takes place have been set to zero.

Those vegetation types - temporary grass, winter barley, spring barley, bare earth, and permanent grass - where more than one spectrum was obtained, have been plotted in Figures 1 to 5 in Appendix II. These show that, although differences do exist at various wavelengths, general patterns are consistent for individual vegetation types. This is particularly so for temporary grass where differences between the two spectra rarely exceed 5% reflectance. In contrast, substantial differences occurred in the individual spectra for both winter and spring barley throughout the spectral range. This, presumably, is a reflection of the incomplete and varied vegetation cover within these fields, in contrast to the temporary grass field where the cover was more even and complete. Differences between the four individual bare soil spectra were small but consistent. Two of the sites (the spectra shown in Figs 11 and 12 of Appendix I) had recently been irrigated. This resulted in slightly lower reflectances than those obtained from the drier soils. The two individual permanent grass spectra differ appreciably, probably as a result of reflectances from different broad-leaved species.

The biggest differences between the spectra of the individual vegetation types is a reflection of the amount of bare soil that is covered by vegetation i.e. the equivalent of a leaf area index. This is best illustrated by taking average reflectance values of selected parts of the spectra for each vegetation type. The regions of the electromagnetic spectrum chosen are:-

| | | |
|---|---|---|
| (i) | The visible bands | (0.45 - 0.70 microns) |
| (ii) | The near infrared | (0.70 - 1.30 microns) |
| (iii) | The middle infrared | (1.50 - 1.75 microns) |
| (iv) | The far infrared | (2.00 - 2.40 microns) |

Average, minimum and maximum reflectances in each of the above regions of the electromagnetic spectrum for each vegetation type are given in Table 4.2.1. The results

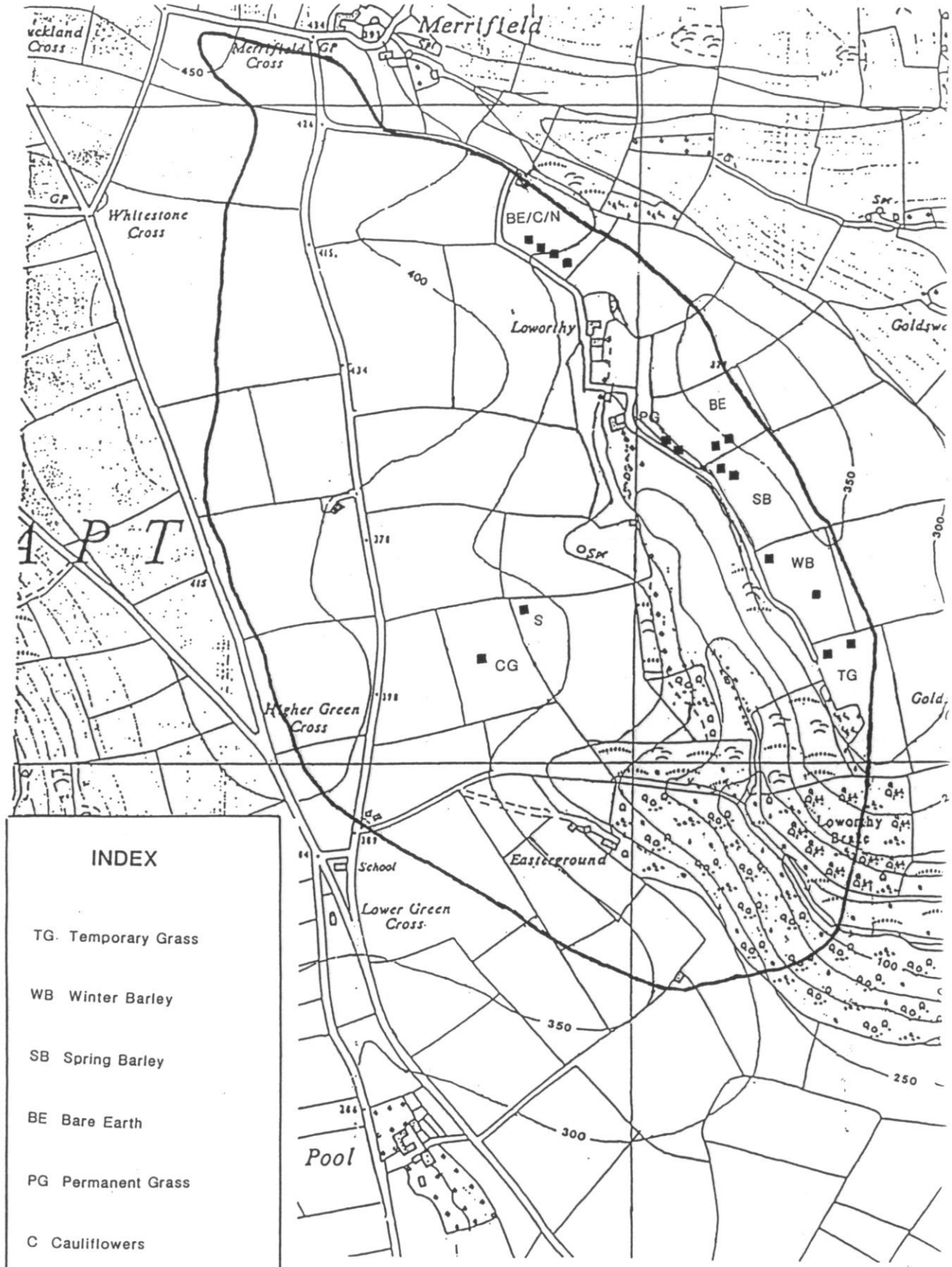


Fig. 4.2.1 Location of sampling points for the IRIS spectroradiometer

generally agree with past observations and are a consequence of the reflectance properties of growing vegetation (see, for example, pages 23-28 of Curran, 1985).

Visible radiation (0.45 → 0.70 microns), particularly in the blue and red regions, is highly absorbed by growing vegetation. This results in the type of pattern shown in Table 4.2.1, where the highest reflectance value is given by bare earth, and the lowest by the more vigorously growing vegetation, temporary grass and spring sown barley. Sparse crops and less vigorous green vegetation show intermediate values. Winter sown barley and cut grass give relatively high reflectances. At the time when the spectra were taken, the winter sown barley was a pale yellow colour and well into the ripening stage, whilst the grass had been cut some weeks previously. In both cases, plant pigments would be breaking down, accompanied by a rise in reflection of blue and red wavelengths.

In contrast, a vegetation cover reflects radiation in the near infrared regions. This is confirmed by the results in Table 4.2.1, where the lowest reflectances are shown by the winter sown barley and bare earth. For the former, not only was the crop senescing, but it was also very sparse, and most of the area viewed by the IRIS would in fact have been bare earth. The rest of the vegetation types, in particular the broad-leaved varieties, gave high reflectance values. Of interest are the relatively low values given by the spring sown barley and the high values for the cut grass. For the former, the vegetation cover would not be as complete as, for example, the temporary grass, whilst, for the latter, the ground cover was very dense, comprising of the uncut growing vegetation and the mat of dead grass.

A much-used measure of vegetation status is the ratio of red to near infrared radiances (Tucker *et al.*, 1980). This combines the effects of the near infrared band, positively correlated to green biomass, with the red band, negatively correlated to chlorophyll content. This is shown in Fig. 4.2.2. using reflectances from the near infrared (0.76 → 0.90 microns) and the red (0.63 → 0.69 microns) bands of the IRIS spectra. This suggests that the vegetation types can be split into three groups:-

(i) Those having a low reflectance in the red band and a high reflectance in the infrared, the vigorously growing vegetation. This includes temporary grass, cauliflowers, and swedes.

(ii) Those having a high reflectance in the red band and a low reflectance in the infrared. This includes bare earth and winter barley ie. dying or no vegetative growth.

(iii) A less vigorously growing class than (i), having a low reflectance in the red and intermediate reflectance in the infrared. This includes nettles, permanent grass, and spring barley.

Cut grass, with a high reflectance in both the red and near infrared seems to be a combination of (i) and (iii) ie. vigorously growing uncut grass and dead grass. Such a vegetation distinction will be used later when classifying the aircraft images.

The middle infrared bands (1.50 → 1.75 microns) and (2.00 → 2.40 microns) are negatively related to both the amount of water in the leaves of the vegetation and the thickness of the leaves. The results from both bands of the IRIS confirm these observations, with the more vigorously growing vegetation, temporary grass and spring barley, having the lowest values, whilst bare earth and cut grass have the highest.

**Table 4.2.1** *IRIS spectroradiometer. Average (minimum → maximum) reflectances in four regions of the electromagnetic spectrum*

| Vegetation/band | Visible (0.45 → 0.70 microns) | Near infrared (0.70 → 1.30 microns) | Middle infrared (1.50 → 1.75 Microns) | Middle infrared (2.00 → 2.40 Microns) |
|---|---|---|---|---|
| TEMPORARY GRASS | 3.3 (1.7 → 9.3) | 48.6 (9.4 → 58.7) | 15.7 (9.7 → 18.7) | 13.6 (8.5 → 22.2) |
| WINTER BARLEY | 8.3 (4.0 → 13.7) | 24.1 (12.0 → 35.9) | 26.6 (21.0 → 31.7) | 23.8 (19.7 → 33.7) |
| SPRING BARLEY | 3.1 (1.4 → 6.9) | 32.5 (4.7 → 43.0) | 14.0 (7.3 → 18.8) | 12.7 (6.5 → 20.6) |
| BARE EARTH | 12.4 (6.0 → 19.8) | 27.5 (17.4 → 35.9) | 36.2 (33.8 → 40.4) | 39.7 (35.7 → 47.8) |
| PERMANENT GRASS | 5.3 (2.7 → 9.8) | 42.8 (10.3 → 57.2) | 26.6 (16.6 → 33.6) | 18.4 (12.9 → 23.9) |
| CAULIFLOWERS | 6.0 (3.8 → 9.8) | 51.8 (10.7 → 60.7) | 16.9 (10.2 → 20.2) | 13.6 (8.7 → 13.6) |
| NETTLES | 4.2 (2.9 → 7.0) | 40.4 (7.8 → 49.3) | 22.5 (15.7 → 25.6) | 16.3 (10.3 → 20.8) |
| SWEDES | 5.4 (3.1 → 10.2) | 57.0 (11.5 → 65.9) | 18.6 (9.9 → 22.7) | 12.8 (7.1 → 19.4) |
| CUT GRASS | 9.3 (5.6 → 15.7) | 60.5 (16.9 → 74.3) | 45.4 (37.5 → 49.7) | 32.2 (29.0 → 37.1) |

Fig. 4.2.2 Near Infrared and Red Reflectances from the IRIS Spectroradiometer

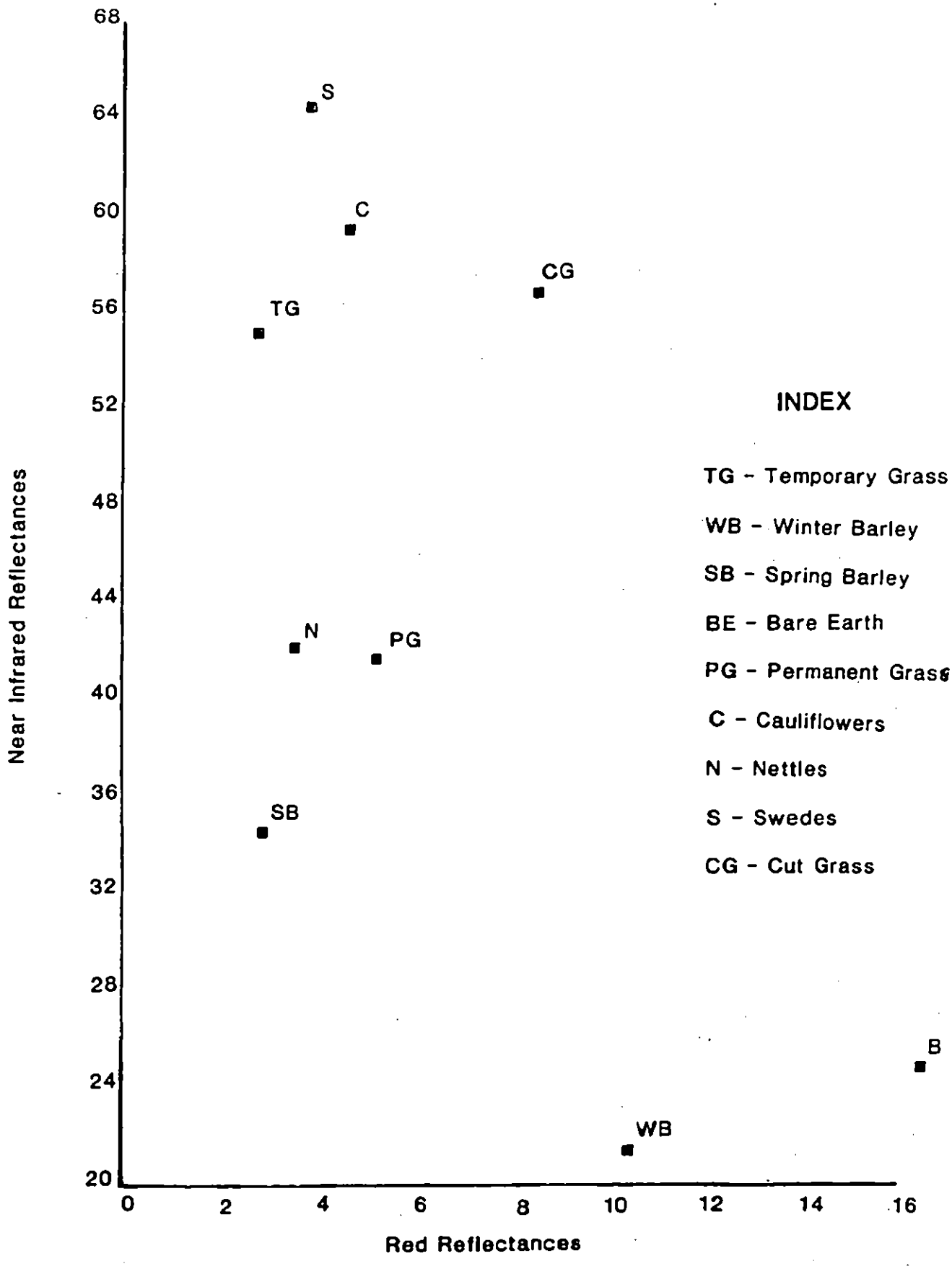

## 4.3 THE DETERMINATION OF ATMOSPHERIC EFFECTS

Simultaneous measurements of radiance spectra using the IRIS spectroradiometer and the Daedalus scanner on board the NERC aircraft, enable an estimate to be made of the effect of the atmosphere on images recorded by the Daedalus (Wilson, 1988). These effects are caused by absorption and scattering of radiation by particulate matter or gases within the layer of atmosphere between the reflecting surface and the sensor. Put in its simplest form, the radiance measured by the Daedalus, R(ATM) can be given as:-

$$R(ATM) = a.\ R + b$$

where
- R is the reflected radiance from the land surface, in this case as measured by the IRIS,
- a is a constant associated with absorption within the atmosphere,
- b is a constant associated with scattering in the atmosphere.

By plotting radiances from the same area, though with very different sensor footprints, measured by the Daedalus and the IRIS, some estimates of these atmospheric effects may be obtained. These effects will vary depending on wavelength and on atmospheric conditions.

A comparison was made between the data acquired by the Daedalus scanner on board the NERC aircraft and those obtained using the IRIS spectroradiometer on the 11th July. The latter were obtained between 1035 and 1530 GMT at the sites indicated in Fig. 4.2.1. The time of overflight of the NERC aircraft was 1150 GMT. Prior to this comparison, the IRIS data were corrected to what would have been measured at 1150 GMT using the ratios of the reflectances from the barium sulphate panel.

Figure 4.3.1 shows a plot of hourly solar radiation recorded by a Kipp solarimeter on the automatic weather station on the day of the overflight. Also shown are the maximum expected solar radiation, based on the latitude, day number and hour angle, as described on page 19 of Roberts, 1981, and the net radiation recorded by a Dirmhirn type net radiometer on the weather station (Strangeways, 1972). The closeness of the measured to the maximum expected solar radiation testifies to the ideal conditions on the day of the overflight.

Figure 4.3.2 shows a plot of hourly specific humidity and dry bulb temperature measured by the automatic weather station. Again, the values obtained suggest that the atmospheric conditions at the time of overpass were conducive to the recording of remotely sensed images.

The data recorded by the Daedalus and the IRIS were converted to a common unit (watts x $10^{-7}$ $cm^{-2}$ $sr^{-1}$ $nm^{-1}$) prior to comparison. For the former, a relationship of the form

$$\text{Radiance} = \text{Gain} \times (\text{DN} - \text{Base})$$

was used, where

Radiance = radiance in watts x $10^{-7}$ $cm^{-2}$ $sr^{-1}$ $nm^{-1}$,
DN = the digital number recorded by the Daedalus,
Gain, Base = constants determined by laboratory calibrations on the 5th July 1990.

Both constants vary with waveband, and also with the gain-setting of the Daedalus. For this particular flight, the values used were as follows:-

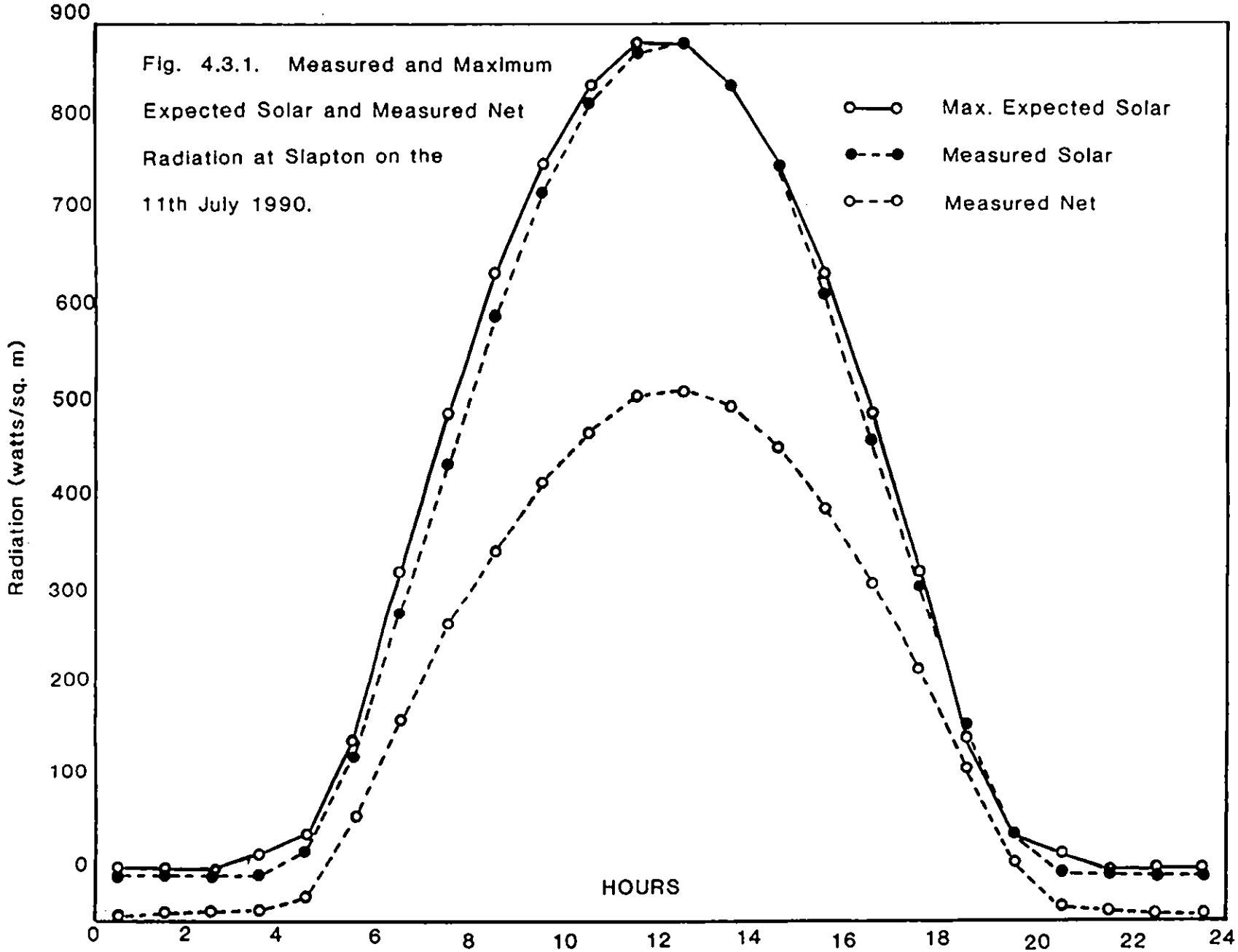
Fig. 4.3.1. Measured and Maximum Expected Solar and Measured Net Radiation at Slapton on the 11th July 1990.
Max. Expected Solar
Measured Solar
Measured Net
Radiation (watts/sq. m)
900
800
700
600
500
400
300
200
100
0
HOURS
0
2
4
6
8
10
12
14
16
18
20
22
24

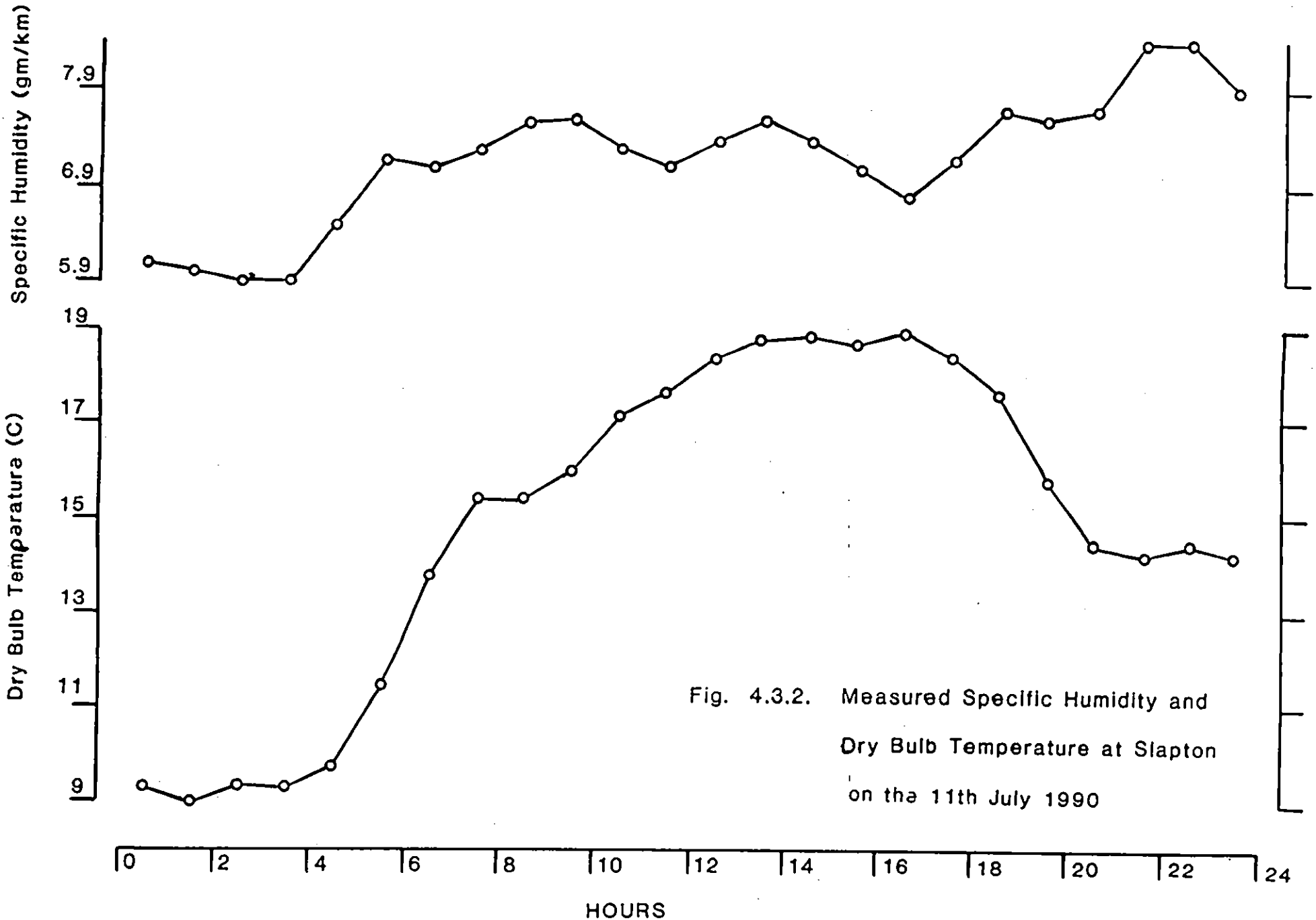


Fig. 4.3.2. Measured Specific Humidity and Dry Bulb Temperature at Slapton on the 11th July 1990

| Channel | Gain-setting | Gain | Base |
|---|---|---|---|
| 1 | 8 | 0.437 | 16.64 |
| 2 | 8 | 0.301 | 31.68 |
| 3 | 8 | 0.372 | 29.55 |
| 4 | 8 | 0.694 | 33.54 |
| 5 | 4 | 0.693 | 19.26 |
| 6 | 4 | 0.731 | 19.33 |
| 7 | 2 | 0.799 | 10.50 |
| 8 | 4 | 0.575 | 19.14 |
| 9 | 4 | 0.129 | 15.17 |
| 10 | 4 | 0.0284 | 20.00 |

Because of saturation problems, the calibration for channel 10 for gain setting 4 could not be done. Instead, the above Gain and Base values were obtained by extrapolations from the average for Gain 2 values for 19.4.90, 8.5.90, and 5.7.90. The method (Wilson, 1986) involves obtaining nearest gain setting values for the same calibration date and double or half the gain/base to create new gain/base values at the higher gain setting.

For the IRIS, the recorded values were converted into radiances for the ATM wavebands using software written at the NERC Equipment Pool for Field Spectroscopy, University of Southampton following calibration using a uniform light source (Rollin and Milton, 1988).

Regressions of ATM Radiances against IRIS Radiances for the ATM Bands over the various land covers (Fig. 4.2.1) are given in Appendix III. For some of the sites, the precise location at which the IRIS spectra were obtained could not be ascertained; in these cases Daedalus values over a larger area were used. The values from two of the sampling sites had to be ignored; these were over strips of cauliflowers and nettles found in one field. The width of the strip was too narrow to ensure 'pure' pixels from the ATM sensor. There is a great deal of scatter in the points for each of the regressions. This may largely be attributed to the different areas sampled by the Daedalus scanner and the IRIS, and to the fact that the precise location at which the IRIS spectra were obtained could not be determined. This is particularly so for those fields having an incomplete crop cover. In spite of this, similar trends were found for the regressions of individual ATM bands.

Slopes and intercepts obtained by least squares for each of the ATM bands are shown in Table 4.3.1 and graphically in Fig. 4.3.3. Put simply, the slopes shown are a measure of the atmospheric transmission ie. the amount of radiation absorbed between the ground surface and the Daedalus sensor. Similarly, the intercepts are a measure of the path radiance ie. the amount of radiation that the atmosphere contributes by reflection from the sun to the sensor.

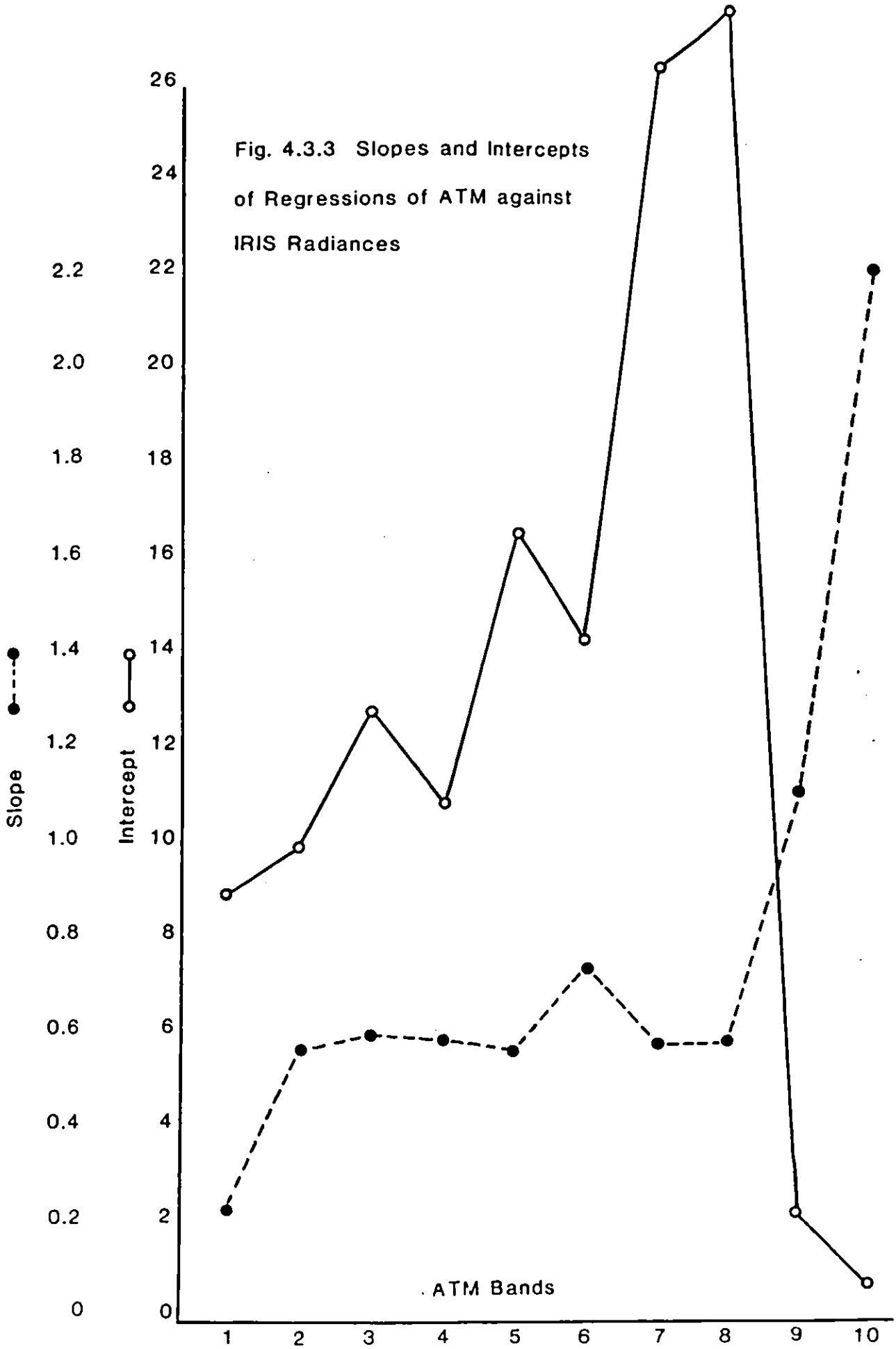


Fig. 4.3.3 Slopes and Intercepts of Regressions of ATM against IRIS Radiances

*Table 4.3.1* *Slopes and intercepts of regressions of ATM against IRIS radiances for the ATM bands*

| ATM band | Slope | Intercept | $r^2$ |
|---|---|---|---|
| 1 | 0.23 | 9.0 | 0.50 |
| 2 | 0.57 (0.63) | 10.0 (5.7) | 0.49 |
| 3 | 0.60 (0.43) | 12.8 (9.2) | 0.85 |
| 4 | 0.59 | 10.9 | 0.94 |
| 5 | 0.57 (0.31) | 16.6 (11.7) | 0.94 |
| 6 | 0.74 | 14.3 | 0.86 |
| 7 | 0.58 (0.45) | 26.1(4.9) | 0.93 |
| 8 | 0.59 | 27.5 | 0.81 |
| 9 | 1.11 | 2.3 | 0.93 |
| 10 | 2.21 | 0.8 | 0.76 |

Both particulate matter and gases absorb radiation. Whereas absorption by the former is a continuous function of the wavelength, absorption of radiation by gases is a selective process, and is a function of the energy required to promote a transition between one energy state and another. For low altitudes, as is the case for aircraft imagery, diatomic oxygen is the main absorber in the visible region of the electromagnetic spectrum; in the infrared regions water vapour, carbon dioxide, and oxygen are the main absorbers.

Path radiance, or scattering of radiation by the atmosphere, can be caused by air molecules (Rayleigh scattering), and by water droplets and dust particles (Mie scattering). Rayleigh scattering is greatest at shorter wavelengths and is insignificant at wavelengths longer than visible. Mie scattering is less sensitive to wavelength, because of the variability in the form, size, and distribution of dust particles, and the effects of the condensation of water droplets.

A more detailed description of the effects of the atmosphere on radiation is given in Iqbal (1983; Chapter 6). In theory, it is possible to estimate the magnitude of the various contributing components. Normally, this is done to correct satellite images, though Singh (1988) describes an algorithm for the correction of atmospheric effects in remotely sensed data collected from any altitude of the sensor. However in the absence of data sets relating to the atmospheric conditions pertaining at the time of image acquisition, a number of assumptions and generalisations have to be made for applying this, and other, algorithms. This has not been attempted in this case.

Instead, the estimates of atmospheric transmission and path radiance for the various ATM bands, shown in Table 4.3.1, have been compared with values obtained during the NERC 1989 airborne campaign over Conington airport, Peterborough (Wilson, 1990). These are shown in brackets for ATM bands 2, 3, 5 and 7 in Table 4.3.1. There are two unexpected values in Table 4.3.1; these are the intercepts of the ATM against IRIS radiances for channels 7 and 8, two of the near-infrared bands. As indicated previously, it would have been expected that these intercepts, a measure of the path radiance, would have decreased with longer wavelengths. Whilst this is the case for the other infrared band, it is not so for Band 7 and 8. One possible explanation is that this apparently enhanced contribution to the radiance measured in Band 7 and 8 is due to scattering by dust particles, as the atmosphere on the 11th July 1990 was relatively dry (Fig. 4.3.2), whereas the ground surface was extremely dry (see Section 4.4) and conducive to wind erosion.

The values shown in Table 4.3.1 will be used to correct the Daedalus radiances prior to further analysis.

## 4.4 SOIL MOISTURE DISTRIBUTIONS

A number of field measurements of soil moisture distribution over the Slapton Wood catchment were made to coincide with the two aircraft flights and at intermediate dates between the flights. The instrument used for these surveys was a portable capacitance probe, a detailed description of which is given in Dean *et al.*, 1987. Basically, the capacitance probe produces an estimate of soil moisture in terms of its dielectric constant, utilizing the large difference in dielectric constant of free water and typical dry soil at frequencies of less than 1000 Mhz. Because of this, it is necessary to calibrate the results obtained from the capacitance probe against known estimates of actual soil moisture. Normally, this is done by simultaneously obtaining soil cores and determining their water content by oven drying at 105°C. In our case, soil samples were not collected; instead, the capacitance probe estimates, integrated over 5 cm and 10 cm depth below ground level, were calibrated using neutron probe measurements (Bell, 1976) at 10 cm depths at each of the three sites within the catchment (Fig. 2.1). Since the main interest of the study was the distribution of soil moisture over the catchment, any loss in accuracy using such a calibration would be minimized.

Capacitance probe readings were mainly taken in a transect across the valley on either side of the main stream. Figure 4.4.1 shows the location of the transect. The transect on the east side of the stream between the farm track and the stream is steep (approx. 30%). On the other side of the stream is a shallow slope leading to a line of trees. Above the trees on the west side of the stream up to the fence surrounding Field no. 3 the slope increases to approx. 30%, before levelling out in Field no. 3. All the transect was under permanent grass except for Field no. 3 which was sown to various agricultural crops. In addition, a number of fields, under various crops, were sampled, either at single points or as additional transects. The locations of these fields are indicated in Fig. 4.4.1, and the dates of the surveys and the fields sampled given in Table 4.4.1.

*Table 4.4.1* *Capacitance probe surveys*

| Date | Type of survey | |
|---|---|---|
| 28.4.90 | VALLEY TRANSECT<br>POINT VALUES | FARM TRACK → STREAM<br>FIELDS 1 → 15 |
| 10.5.90 | VALLEY TRANSECT | FARM TRACK → TREES |
| 21.5.90 | VALLEY TRANSECT | FARM TRACK → FIELD 2 |
| 14.6.90 | POINT VALUES<br>TRANSECTS | FIELDS 13, 14, 15, 18, 11, 19<br>FIELDS 16, 3, 12, 10 , 8, 7, WOODLAND |
| 10/11.7.90 | VALLEY TRANSECT<br>POINT VALUES | FARM TRACK → FIELD 2<br>FIELDS 38, 15, 14, 13, 24, 11, 3, 2 |

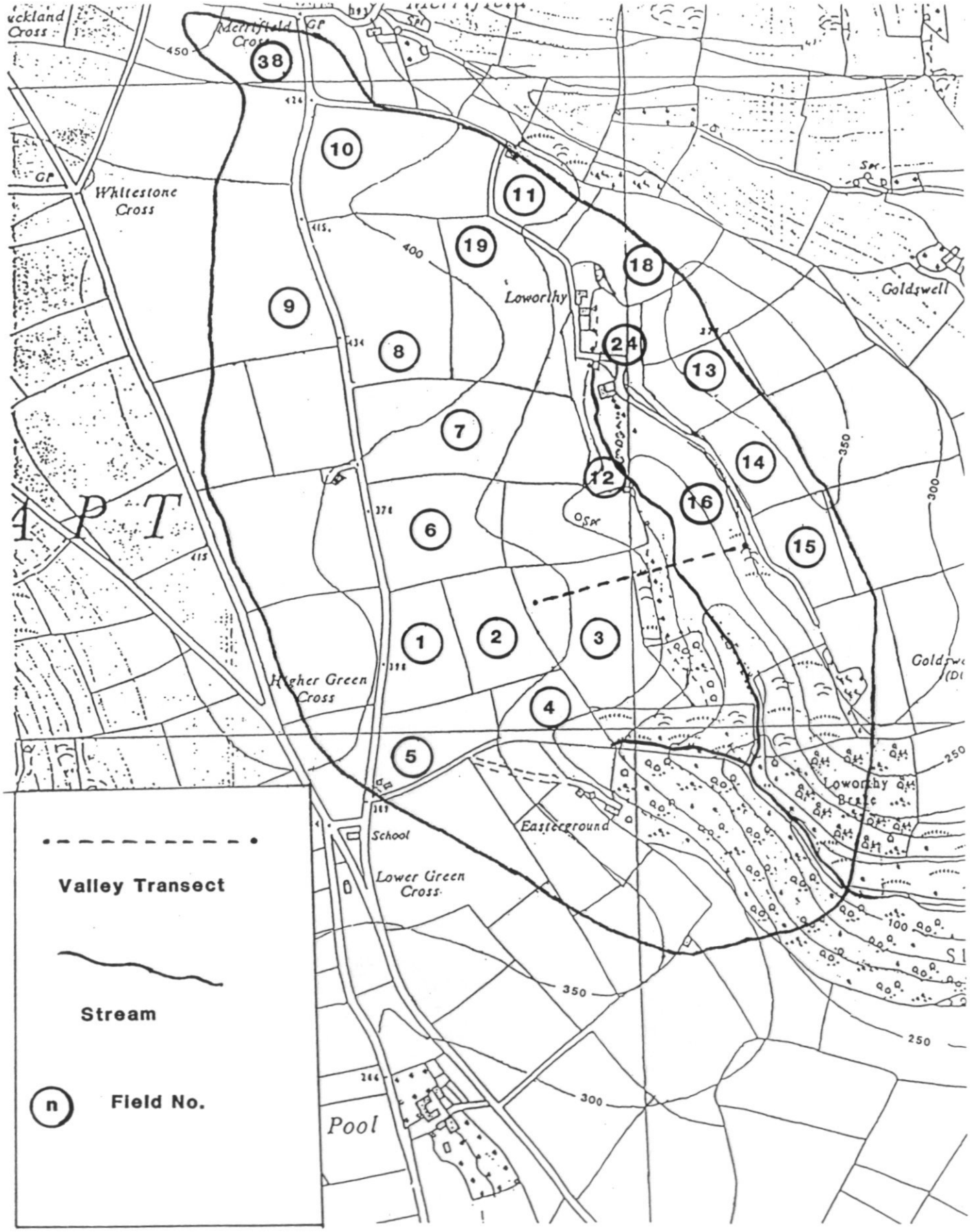


Fig. 4.4.1 Location of Capacitance Probe Surveys

As well as being of general interest for an understanding of the hydrological processes within the catchment the capacitance probe readings taken on the 28th April and on the 11th July can be used as 'ground truths' in an attempt to distribute near surface soil moisture using the Daedalus images. Data from all the wavebands recorded by the Daedalus can provide information on the distribution of soil moisture.

In the visible and near infrared regions, the albedo of bare soil varies with its moisture content, with wet soil albedo being half that of the same dry soil (Idso *et al.*, 1975). However, this technique is limited because of variations in soil type and roughness, and is a measure of the soil surface, subject to rapid wetting and drying, and not of the moisture within the soil matrix itself. For this, the condition of the vegetation can be used as a surrogate, as this reflects the water availability within the whole of the root zone. Water stress in green vegetation is manifest as a lowering of near infrared reflectance as leaf turgor reduces, followed by an increase in red reflectance as leaf chlorophyll is lost (Richardson and Everitt, 1987). Also, vegetation indices based on the ratio between red and infrared reflectances give an indication of crop vigour which, in turn, is subject to the availability of soil moisture. However, such effects are also dependent on the availability of nutrients (Blakeman, 1990). For unmanaged grasslands, the distribution of indigenous species is an indicator of soil moisture availability. Gurnell *et al.*, 1985 used this fact to determine the extent of waterlogged or runoff contributing areas in the Highland water catchment, Hampshire. For this technique to be employed in UK situations, aircraft imagery must be employed as the ground resolution of satellite imagery is too coarse to map small-scale changes in indigenous vegetation, and hence in soil water availability.

Images in the thermal infrared regions of the electromagnetic spectrum provide the distribution of surface temperature which, in turn, can be related to soil moisture using the thermal inertia method. This utilises the fact that wet soil, because of its higher thermal capacity, has a smaller diurnal range of temperature than dry soil. An analysis of thermal infrared images obtained using the warmer and colder periods of the day should give some indication of the distribution in soil moisture. This is the subject of a separate study at Slapton using images obtained during the NERC 1990 aircraft campaign, and will not be considered further in this report.

Middle infrared radiation is strongly absorbed by the presence of moisture in soil and vegetation. Laboratory measurements done on bare soil by Musick and Pelletier, 1986 showed that the ratio of Landsat bands 5 and 7 (ATM bands 9 and 10) gave a good relationship with soil moisture over a wide range of moisture conditions, though different relationships were obtained for different soils. As with the visible and near infrared techniques, only the thin surface soil layer is observed, and its relevance for determining the distribution of soil moisture is limited. For vegetated surfaces, the mid-infrared reflectance is governed by leaf moisture content (Ripple, 1986), which can be taken as a surrogate for the amount of soil moisture within the rooting zone.

For hydrological purposes, the spatial distribution of soil moisture within the rooting zone is much more useful than is the condition of the ground surface which is subject to rapid wetting and drying cycles. For this reason, it was decided to concentrate capacitance probe surveys and image analysis on vegetated surfaces. This was further restricted to grassland areas, because the incomplete canopy coverage associated with arable crops would result in significant soil reflectance being associated with that from the vegetation canopy.

Most of the analysis has been done on results from the valley transect as this was likely to

provide the greatest range of soil moisture, though the point values are also considered, particularly when data from the IRIS spectroradiometer are available.
For this particular study, two indices related to vegetation have been used. These are:-

(i) The normalized difference vegetation index, NDVI, given by:-

$$NDVI = (Near\ Infrared - Red)/ (Near\ Infrared + Red)$$

(ii) The moisture stress index, MSI, given by:-

$$MSI = (Middle\ Infrared) / (Near\ Infrared)$$

The ratio of the middle infrared bands (ATM9/ATM10) was also considered but it was found that this ratio fluctuated wildly and, if anything, increased with moisture volume fraction. A similar effect was observed by Musick and Pelletier (1986) for dry bare soils.

In each case, reflectance values have been converted to radiance and, where possible, corrected for atmospheric effects. Also, the use of two bands for each index will minimize differences in radiance across the areas of interest.

The results are not presented in chronological order but rather in the order of the dates of greatest data availability. The object of the analysis is to try to develop relationships between the soil moisture as given by the capacitance probe and radiances in various ATM bands. These relationships can then be applied to all of the grassland areas within the Slapton Wood catchment and the resulting soil moisture distribution compared with the topography.

**(i) 11th July 1990**

Table 4.4.2 gives estimated moisture volume fractions at 5 cm and 10 cm depths across the valley transect from the farm track to the edge of Field 3. Table 4.4.3 gives radiance values, corrected for atmospheric effects using the relationships given in Table 4.3.1, for ATM Band 5 (Red), ATM Band 7 (Near Infrared), and ATM Band 9 (Middle Infrared). Also shown are the Normalized Difference Vegetation Index (NDVI) and the Moisture Stress Index (MSI).

Figure 4.4.2 shows the variations in moisture volume fractions and the two vegetation indices over the valley transect. Also shown is the general topography of the transect. As expected, the moisture content at both depths increases downslope from the farm track to the stream. This increase continues to the line of trees. Borehole studies showed that the trees are growing on a spring line. Unfortunately, no capacitance probe data could be obtained within the spring line. Above the line of trees, lower moisture volume fractions were obtained, with the values, if anything, increasing up slope.

The patterns in the two vegetation indices generally reflect the soil moisture distributions for the main transect (Track → Line of Trees). The Normalized Difference Vegetation Index increases downslope reflecting healthier vegetation in the valley bottom whilst the Moisture Stress Index decreases, reflecting higher leaf water contents in the valley bottom. Above the line of trees, the NDVI decreases upslope whilst the MSI increases. Both of these trends are as expected but are at variance with the pattern in the moisture volume fractions. A comparison of capacitance probe values and vegetation indices from the IRIS spectroradiometer for the two grassland sites (Fig.4.2.1) confirm the patterns shown for the main valley transect:-

*Table 4.4.2* *Moisture Volume Fractions for the Valley Transect 11th July*

| Distance from track (m) | 5 cm MVF | 10 cm MVF |
|---|---|---|
| TRACK | | |
| 10 | 0.096 | 0.111 |
| 15 | 0.137 | 0.145 |
| 20 | 0.125 | 0.147 |
| 25 | 0.124 | 0.143 |
| 30 | 0.120 | 0.138 |
| 35 | 0.131 | 0.139 |
| 40 | 0.125 | 0.133 |
| 45 | 0.111 | 0.127 |
| 50 | 0.143 | 0.151 |
| 55 | 0.154 | 0.161 |
| 60 | 0.140 | 0.151 |
| 65 | 0.130 | 0.158 |
| 70 | 0.137 | 0.156 |
| 75 | 0.140 | 0.155 |
| 80 | 0.157 | 0.178 |
| 85 | 0.134 | 0.162 |
| 90 | 0.153 | 0.168 |
| 92 | 0.152 | 0.166 |
| STREAM | | |
| 94 | 0.130 | 0.158 |
| 99 | 0.161 | 0.174 |
| 104 | 0.143 | 0.158 |
| 109 | 0.162 | 0.176 |
| 114 | 0.164 | 0.174 |
| 118 | 0.161 | 0.182 |
| TREES | | |
| 144 | 0.145 | 0.162 |
| 149 | 0.127 | 0.150 |
| 154 | 0.130 | 0.163 |
| 156 | 0.118 | 0.156 |
| 159 | 0.141 | 0.160 |
| 164 | 0.139 | 0.168 |
| 165 | 0.134 | 0.157 |
| 169 | 0.136 | 0.154 |
| 174 | 0.130 | 0.161 |
| 176 | 0.150 | 0.162 |
| 179 | 0.145 | 0.158 |
| 184 | 0.148 | 0.173 |
| 189 | 0.136 | 0.154 |
| 194 | 0.133 | 0.137 |

*Table 4.4.3* *Corrected Radiances (w x $10^{-7}$ $cm^{-2}$ $sr^{-1}$ $nm^{-1}$) and Vegetation Indices for the Valley Transect 11th July*

| Distance from track | ATM5 | ATM7 | ATM9 | NDVI | MSI |
|---|---|---|---|---|---|
| TRACK | | | | | |
| 8 | 25.0 | 57.4 | 6.5 | 0.39 | 0.113 |
| 12 | 22.4 | 66.7 | 6.4 | 0.50 | 0.096 |
| 16 | 23.7 | 65.5 | 7.2 | 0.47 | 0.110 |
| 20 | 19.7 | 66.7 | 5.4 | 0.54 | 0.081 |
| 24 | 19.7 | 64.3 | 6.5 | 0.53 | 0.101 |
| 28 | 19.7 | 69.0 | 5.7 | 0.56 | 0.083 |
| 32 | 17.0 | 66.7 | 5.7 | 0.59 | 0.085 |
| 36 | 17.0 | 71.3 | 6.3 | 0.61 | 0.088 |
| 40 | 18.4 | 71.3 | 5.4 | 0.59 | 0.076 |
| 44 | 19.7 | 73.6 | 6.0 | 0.58 | 0.082 |
| 48 | 23.7 | 77.1 | 6.3 | 0.53 | 0.082 |
| 52 | 19.7 | 76 0 | 5.8 | 0.59 | 0.076 |
| 56 | 15.7 | 69.0 | 5.8 | 0.63 | 0.084 |
| 60 | 19.7 | 71.3 | 6.0 | 0.57 | 0.084 |
| 64 | 18.4 | 73.6 | 5.4 | 0.60 | 0.073 |
| 68 | 19.7 | 71.3 | 6.1 | 0.57 | 0.086 |
| 72 | 19.7 | 78.2 | 5.5 | 0.60 | 0.070 |
| 76 | 22.4 | 80.6 | 5.5 | 0.57 | 0.068 |
| 80 | 22.4 | 82.9 | 5.3 | 0 57 | 0.064 |
| 84 | 22.4 | 80.6 | 6.4 | 0.57 | 0.079 |
| 88 | 23.7 | 84.1 | 6.0 | 0.56 | 0.071 |
| 92 | 21.0 | 79.4 | 6.0 | 0.58 | 0.076 |
| STREAM | | | | | |
| 96 | 22.4 | 72.5 | 5.7 | 0.53 | 0.079 |
| 100 | 21.0 | 101.5 | 7.0 | 0.66 | 0.069 |
| 104 | 18.4 | 98.0 | 6.3 | 0.68 | 0.064 |
| 108 | 15.7 | 107.2 | 6.4 | 0.74 | 0.060 |
| 112 | 19.7 | 103.8 | 7.7 | 0.68 | 0.074 |
| 116 | 21.0 | 107.2 | 5.4 | 0.67 | 0.050 |
| TREES | | | | | |
| 144 | 31.7 | 94.5 | 6.4 | 0.50 | 0.068 |
| 148 | 26.4 | 91.0 | 7.2 | 0.55 | 0.080 |
| 152 | 27.7 | 94.5 | 6.8 | 0.55 | 0.072 |
| 156 | 26.4 | 94.5 | 7.0 | 0.56 | 0.074 |
| 160 | 23.7 | 99.1 | 6.4 | 0.61 | 0.065 |
| 164 | 29.0 | 87.6 | 6.3 | 0.50 | 0.072 |
| 168 | 29.0 | 82.9 | 7.4 | 0.48 | 0.089 |
| 172 | 33.0 | 92.2 | 8.0 | 0.47 | 0.087 |
| 176 | 30.4 | 93.3 | 7.2 | 0.51 | 0.078 |
| 180 | 34.3 | 100.3 | 7.1 | 0.49 | 0.071 |
| 184 | 33.0 | 94.5 | 7.1 | 0.48 | 0.075 |
| 188 | 35.7 | 92.2 | 7.4 | 0.44 | 0.080 |
| 192 | 31.7 | 79.4 | 7.0 | 0.43 | 0.088 |
| 196 | 43.7 | 86.4 | 7.0 | 0.33 | 0.081 |

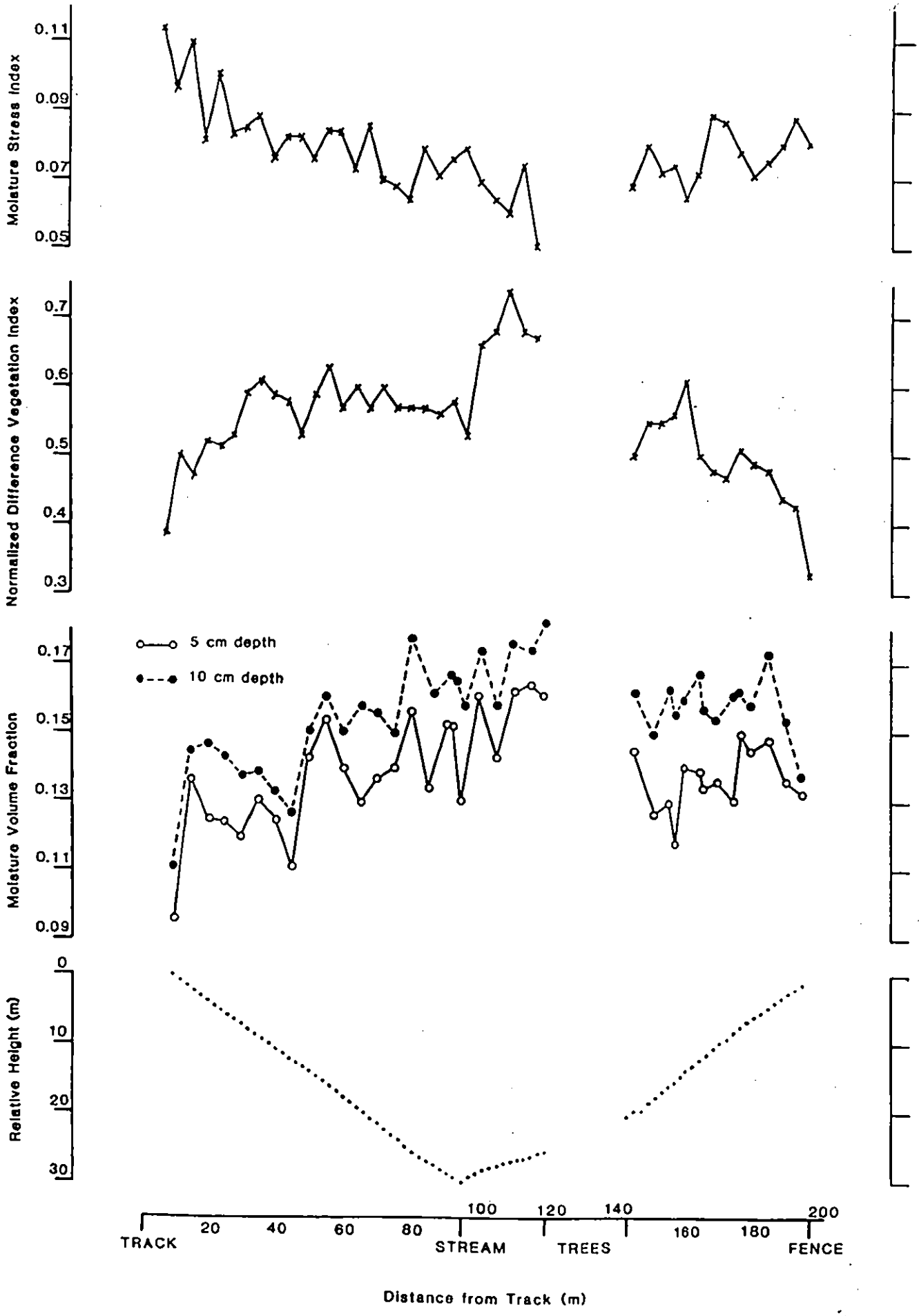


Fig. 4.4.2 Moisture Volume Fractions and Vegetation Indices for the valley transect on the 11th July 1990

| | MOISTURE VOLUME FRACTIONS | | NDVI | MSI |
|---|---|---|---|---|
| | 5 CM DEPTH | 10 CM DEPTH | | |
| TEMPORARY GRASS | 0.130 | 0.148 | 0.86 | 0.028 |
| PERMANENT GRASS | 0.119 | 0.129 | 0.67 | 0.059 |

There is a great deal of scatter in all of the trends. Also, the point values of moisture volume fractions do not necessarily correspond to the position of the pixels of vegetation indices. Another problem concerns the representivity of the various data values. Whilst the moisture volume fractions represent a very small sphere of influence around the capacitance probe (a few square centimetres in area), each value of the vegetation indices represents an area of 16 sq metres. For these reasons, it was found necessary to smooth the data sets before direct comparisons could be made.

Figure 4.4.3 shows these smoothed patterns (running means of 3 values). The dashed line for each data set was obtained by least squares. The slopes of these regressions highlight the patterns found in the original data sets. For the main transect (track to the line of trees), the trends are as expected and agree with the two point values taken with the IRIS spectroradiometer. Above the line of trees, the trends in the vegetation indices are as expected, whilst the trends in the soil moisture are opposite to what would have been expected. The soil moisture at 5 cm depth, in particular, increases upslope, though this may be a reflection of the scatter in the data set; the water content at the bottom of the slope is, in fact, higher than that at the top of the slope. The same is true for the water content at 10 cm depth. For this reason, the trends in this transect have not been used for distributing soil moisture over the grassland areas of the catchment.

To do this, the regressions of moisture volume fraction against distance have been combined with regressions of vegetation indices against distance for the main transect to produce regressions of moisture volume fractions against vegetation indices. The relevant relationships are:-

| | | | |
|---|---|---|---|
| Moisture volume fraction | 5 cm depth | MVF = | 0.00037 DIST + 0.1146 |
| | 10 cm depth | MVF = | 0.00040 DIST + 0.1290 |
| Normalized Difference Vegetation Index | | NDVI = | 0.0013 DIST + 0.499 |
| Moisture Stress Index | | MSI = | -0.000317 DIST + 0.0987 |

Combining these various regressions gives:-

| | | | |
|---|---|---|---|
| 5 cm depth | MVF | = | 0.300 NDVI - 0.036 |
| | MVF | = | -1.273 MSI + 0.239 |
| 10 cm depth | MVF | = | 0.307 NDVI - 0.025 |
| | MVF | = | -1.303 MSI + 0.257 |

These are the relationships that have been used in an attempt to determine the distribution of

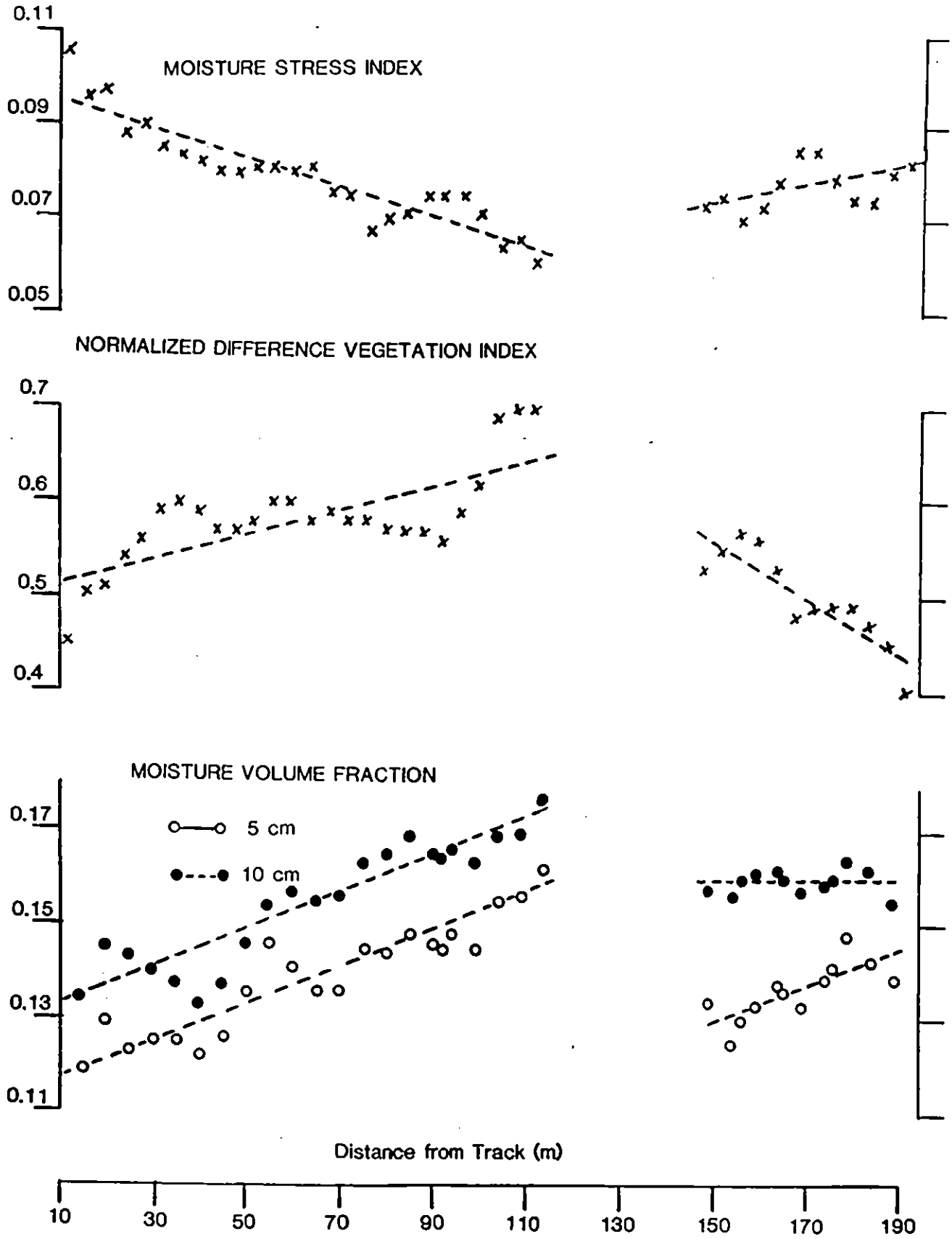


Fig. 4.4.3. Smoothed Moisture Volume Fractions and Vegetation Indices for the Valley Transect July 1990

near surface moisture content over the grassland areas of the Slapton Wood catchment. The derived distribution using the Normalized Difference Vegetation Index is shown in Fig. 4.4.4 whilst that using the Moisture Stress Index is shown in Fig. 4.4.5. The distributions, particularly for 5 cm depth, are similar, though this is not altogether surprising in view of the fact that most of the distribution is caused by variations in ATM Band 7 (Near Infrared), used in both indices. However, there are differences, particularly at 10 cm.

In terms of type of grass, the catchment can be divided by a line drawn through its centre from south west to north east. To the north west of this line, temporary grass is dominant, whereas to the south east, permanent grass predominates. The major exception to this is a temporary grass field immediately below Field no. 15 in Fig. 4.4.1. This is shown at the extreme south east in Figs. 4.4.4 and 4.4.5.

Inspection of the derived distributions suggests that both the Normalized Difference Vegetation Index and the Moisture Stress Index are actually differentiating between temporary and permanent grass. Whilst this is hardly surprising for the former, it is disappointing for the latter, although it could be argued that the radiance in ATM Band 9 (middle infrared) is governed by the leaf water content and the amount of vegetation.

Assuming that the distributions do in fact reflect, to some extent, near surface soil moisture, it is interesting to note that the NDVI suggests that moisture volume fractions are lower at 10 cm depth than at 5 cm, whereas the MSI suggests the opposite. This alone suggests that the distribution given by the MSI is closer to the true soil moisture distribution than is the one given by the NDVI. Unfortunately, no time was available for an intensive capacitance probe survey of the grassland areas apart from the valley transect. For the two grassland sites used for the atmospheric corrections (Fig. 4.2.1), the following was found:-

| | | | | |
|---|---|---|---|---|
| TEMPORARY GRASS | MEASURED MVF 5 cm | 0.13 | 10 cm | 0.15 |
| | ESTIMATED (NDVI) | 0.24 | | 0.26 |
| | ESTIMATED (MSI) | 0.21 | | 0.23 |
| PERMANENT GRASS | MEASURED MVF 5 cm | 0.12 | 10 cm | 0.13 |
| | ESTIMATED (NDVI) | 0.14 | | 0.15 |
| | ESTIMATED (MSI) | 0.15 | | 0.16 |

The above figures show that, whereas the moisture volume fractions under the permanent grass site were well predicted, with the NDVI being slightly better than the MSI, the MVFs under the temporary grass site were substantially overestimated. This again suggests that the indices are not really a reflection of the soil moisture, certainly not in the case of temporary grass. On reflection, it would have been useful to have derived separate moisture regressions for temporary and permanent grass.

**(ii) 28th April 1990**

The capacitance probe survey of the valley transect on the 28th April was confined to the area

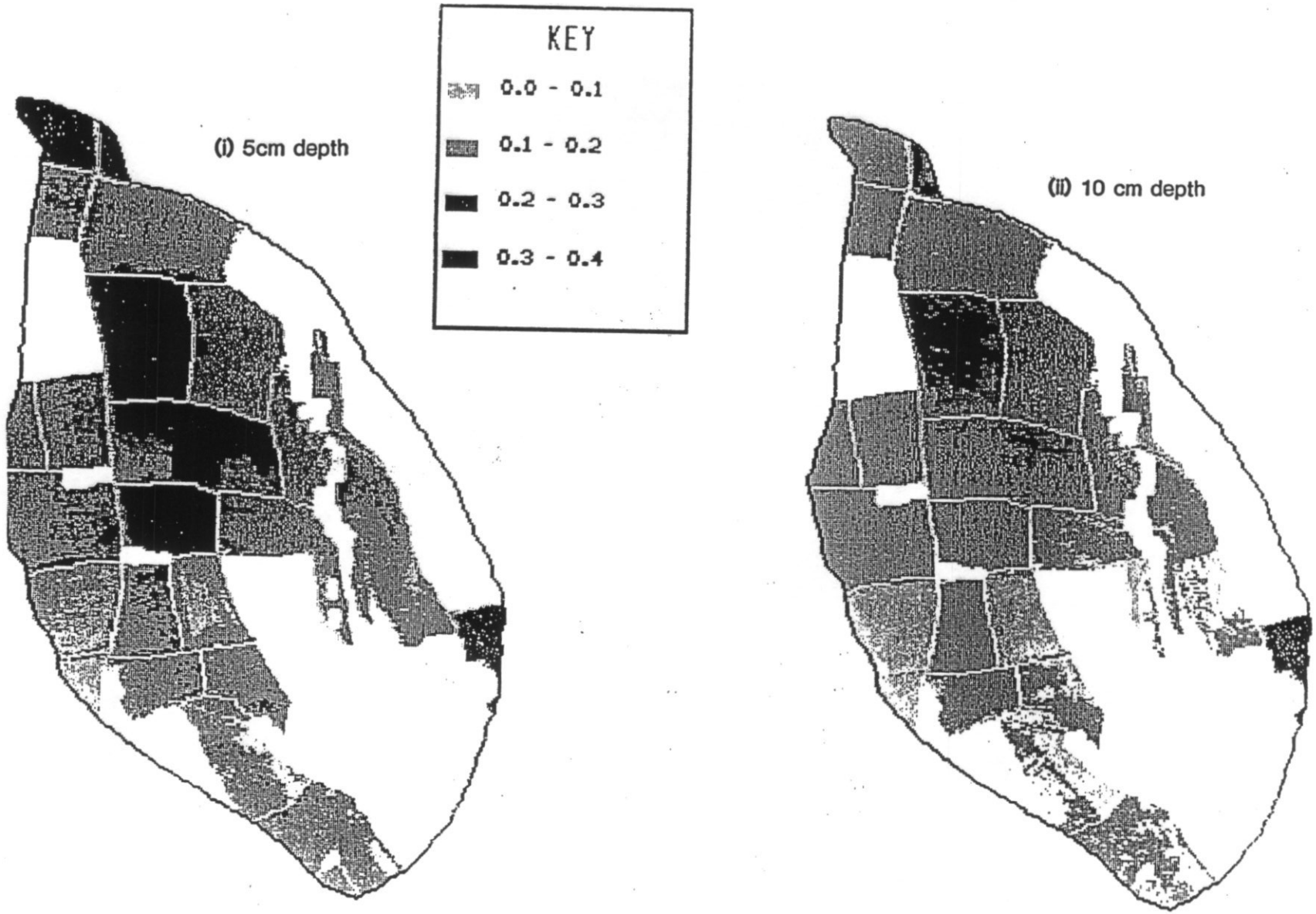


Fig. 4.4.4. The distribution of Moisture Volume Fraction over the Grassland Areas of Slapton Wood catchment 11th July 1990 – NDVI Method

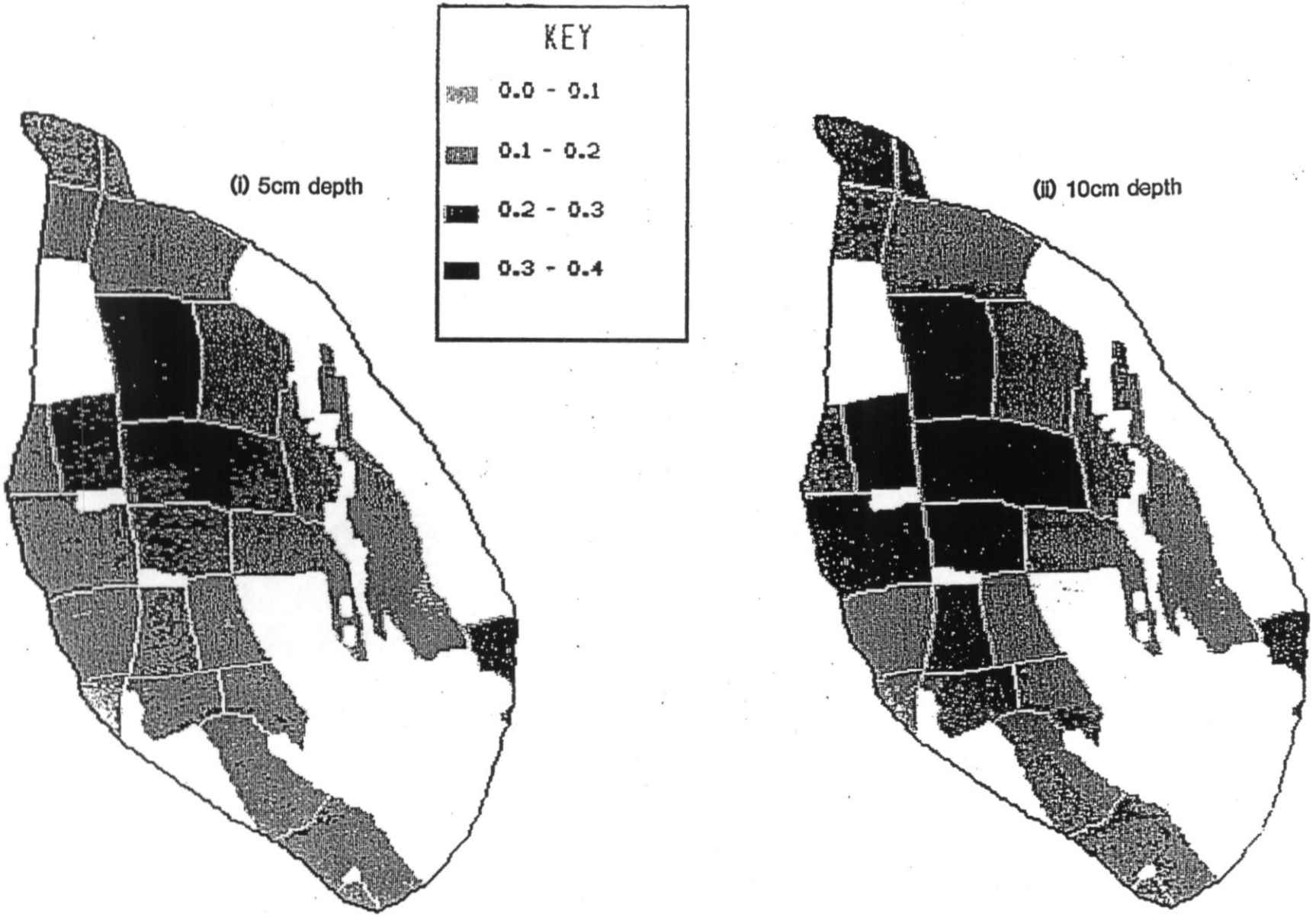


Fig. 4.4.5 The distribution of Moisture Volume Fraction over the Grassland Areas of Slapton Wood catchment 11th July 1990 – MSI Method

between the farm track and the stream. Table 4.4.4 lists the moisture volume fractions at 5 cm and 10 cm depth, whilst Table 4.4.5 lists radiances for ATM5, ATM7 and ATM9, the Normalized Difference Vegetation Index and the Moisture Stress Index. In the absence of spectra from the IRIS spectroradiometer, no atmospheric correction could be applied to the Daedalus images.

Variations in moisture volume fractions and the vegetation indices are shown in Fig. 4.4.6. The trends are generally as expected with the moisture volume fractions and normalized difference vegetation index increasing downslope, whilst the moisture stress index decreases downslope. However, the rates of change are rather different. For the moisture volume fractions, the greatest increases occur within about 6 m of the stream, whilst the vegetation indices change most rapidly just below the farm track. As a result, realistic relationships between moisture volume fractions and vegetation indices could not be obtained. It is unlikely that the situation could be improved even if atmospheric corrections could be applied, and the attempt to map near surface soil moisture over the grassland area of the catchment using these data sets was abandoned.

Capacitance probe values were obtained from Fields 1 to 15 (Fig. 4.4.1) on the 28th April 1990. Of these, 6 fields (nos. 1, 2, 6, 7, 8 and 10) were under temporary grass, whilst 3 (nos. 4, 5 and 12) were under permanent grass. Fig. 4.4.7 shows plots of moisture volume fraction against NDVI for 5 and 10 cm depth, whilst Fig. 4.4.8 shows the same for MSI. For the temporary grass sites, the patterns are as expected with NDVI increasing and MSI decreasing with increasing moisture volume fractions. At 5 cm depth, the moisture volume fraction at one site (Field 8) is substantially higher than expected. In fact, the moisture volume fraction, as measured by the capacitance probe, is greater at 5 cm depth than at 10 cm depth. Only one value was taken at each depth, so it was not possible to establish whether the measured values were correct. Moisture volume fractions obtained by capacitance probe along a transect of this field on the 14th June 1990 gave consistently higher values at 10 cm depth. This suggests that the 28th April 5 cm depth moisture volume fraction was in error.

The situation is less clear for the permanent grass sites. This is partly due to the small number of sites sampled and to the results from one site (Field 12, Fig. 4.4.1) in particular. This field was on a very steep slope and gave, not surprisingly, low values of moisture volume fraction at both the 5 cm and 10 cm depths. This was not reflected in either the NDVI or the MSI. In fact, the graphs shown in Figs. 4.4.7 and 4.4.8 suggest that the vegetation in this field could be regarded as temporary as opposed to permanent pasture. Visual inspection of the vegetation suggested that this is not the case, and it is the low moisture volume fractions, as a result of the severe slope, that caused the discrepancy.

The results given in Figs. 4.4.7 and 4.4.8 show that, as suggested for the 11th July distributions, it is necessary to obtain separate regressions for permanent and temporary grass. However, the biggest problem in attempting to distribute near surface soil moisture over the Slapton Wood catchment using the aircraft images is the very dry conditions and the small variation in moisture conditions. This problem was also experienced by Musick and Pelletier, 1986 for bare soil. Perhaps a fairer test of these techniques would be in an area experiencing wetter conditions and a wider variation in soil moisture. A survey of a valley transect under rough pasture at Plynlimon, mid Wales on the 4th June 1992 gave a range of moisture volume fractions of 0.30 to 0.90. The range for the 11th July 1990 Slapton transect was 0.09 to 0.17. It is proposed that an area such as Plynlimon would be more appropriate to test these techniques.

*Table 4.4.4* *Moisture Volume Fractions for the Valley Transect 28th April*

| Distance from track (m) | 5 cm MVF | 10 cm MVF |
|---|---|---|
| TRACK | | |
| 6 | 0.115 | 0.139 |
| 12 | 0.125 | 0.149 |
| 18 | 0.125 | 0.145 |
| 24 | 0.126 | 0.141 |
| 30 | 0.123 | 0.156 |
| 36 | 0.130 | 0.150 |
| 42 | 0.129 | 0.143 |
| 48 | 0.134 | 0.155 |
| 54 | 0.140 | 0.168 |
| 60 | 0.136 | 0.155 |
| 66 | 0.135 | 0.157 |
| 72 | 0.140 | 0.163 |
| 78 | 0.136 | 0.160 |
| 80 | 0.133 | 0.147 |
| 82 | 0.143 | 0.160 |
| 84 | 0.134 | 0.158 |
| 86 | 0.148 | 0.158 |
| 88 | 0.153 | 0.168 |
| 90 | 0.162 | 0.174 |
| 92 | 0.184 | 0.196 |
| STREAM | | |

*Table 4.4.5* *Radiances (w x $10^{-7}$ $cm^{-2}$ $sr^{-1}$ $nm^{-1}$) and Vegetation Indices for the Valley Transect 28th April*

| Distance from track | ATM5 | ATM7 | ATM9 | NDVI | MSI |
|---|---|---|---|---|---|
| TRACK | | | | | |
| 8 | 49.7 | 86.3 | 11.7 | 0.27 | 0.136 |
| 12 | 40.6 | 104.9 | 11.6 | 0.44 | 0.111 |
| 16 | 36.4 | 108.2 | 11.4 | 0.50 | 0.105 |
| 20 | 33.6 | 108.2 | 10.1 | 0.53 | 0.093 |
| 24 | 32.2 | 113.0 | 9.6 | 0.56 | 0.085 |
| 28 | 35.0 | 105.7 | 10.5 | 0.50 | 0.099 |
| 32 | 32.9 | 108.2 | 10.1 | 0.53 | 0.093 |
| 36 | 30.8 | 112.2 | 9.7 | 0.57 | 0.086 |
| 40 | 34.3 | 105.7 | 10.5 | 0.51 | 0.099 |
| 44 | 32.9 | 110.6 | 10.1 | 0.54 | 0.091 |
| 48 | 28.7 | 113.0 | 9.2 | 0.59 | 0.081 |
| 52 | 28.7 | 110.6 | 9.6 | 0.59 | 0.087 |
| 56 | 29.4 | 115.4 | 9.0 | 0.59 | 0.078 |
| 60 | 28.7 | 113.0 | 8.5 | 0.59 | 0.075 |
| 64 | 28.7 | 117.1 | 8.5 | 0.61 | 0.073 |
| 68 | 28.7 | 116.3 | 9.4 | 0.60 | 0.080 |
| 72 | 28.7 | 115.4 | 8.5 | 0.60 | 0.074 |
| 76 | 29.4 | 117.9 | 8.8 | 0.60 | 0.075 |
| 80 | 29.4 | 117.1 | 8.9 | 0.60 | 0.076 |
| 84 | 28.7 | 116.3 | 8.9 | 0.60 | 0.077 |
| 88 | 28.7 | 113.8 | 9.0 | 0.60 | 0.079 |
| 92 | 28.7 | 116.3 | 8.6 | 0.60 | 0.074 |
| STREAM | | | | | |

Fig. 4.4.6 Moisture Volume Fractions and Vegetation Indices for the Valley Transect on the 28th April

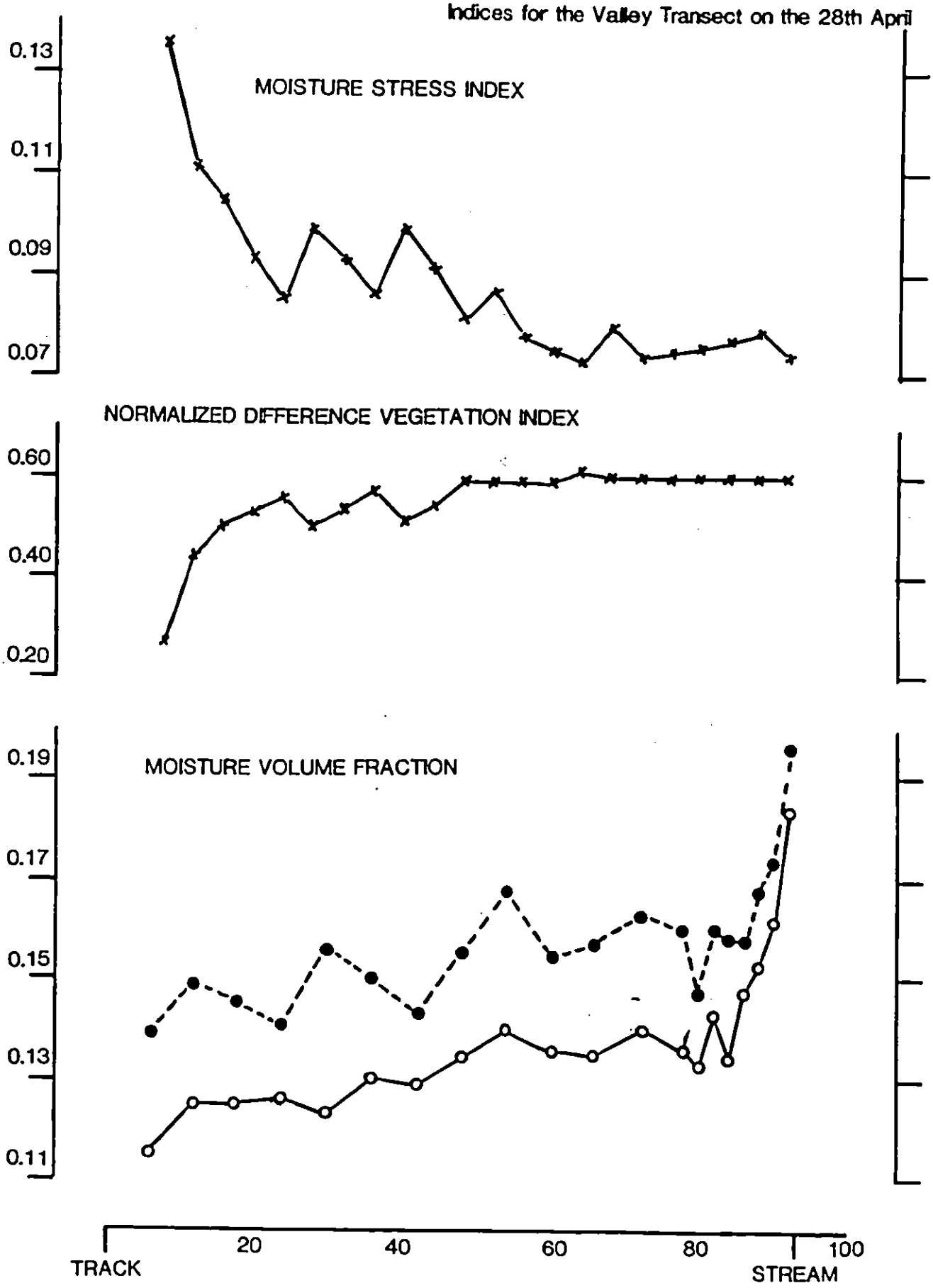

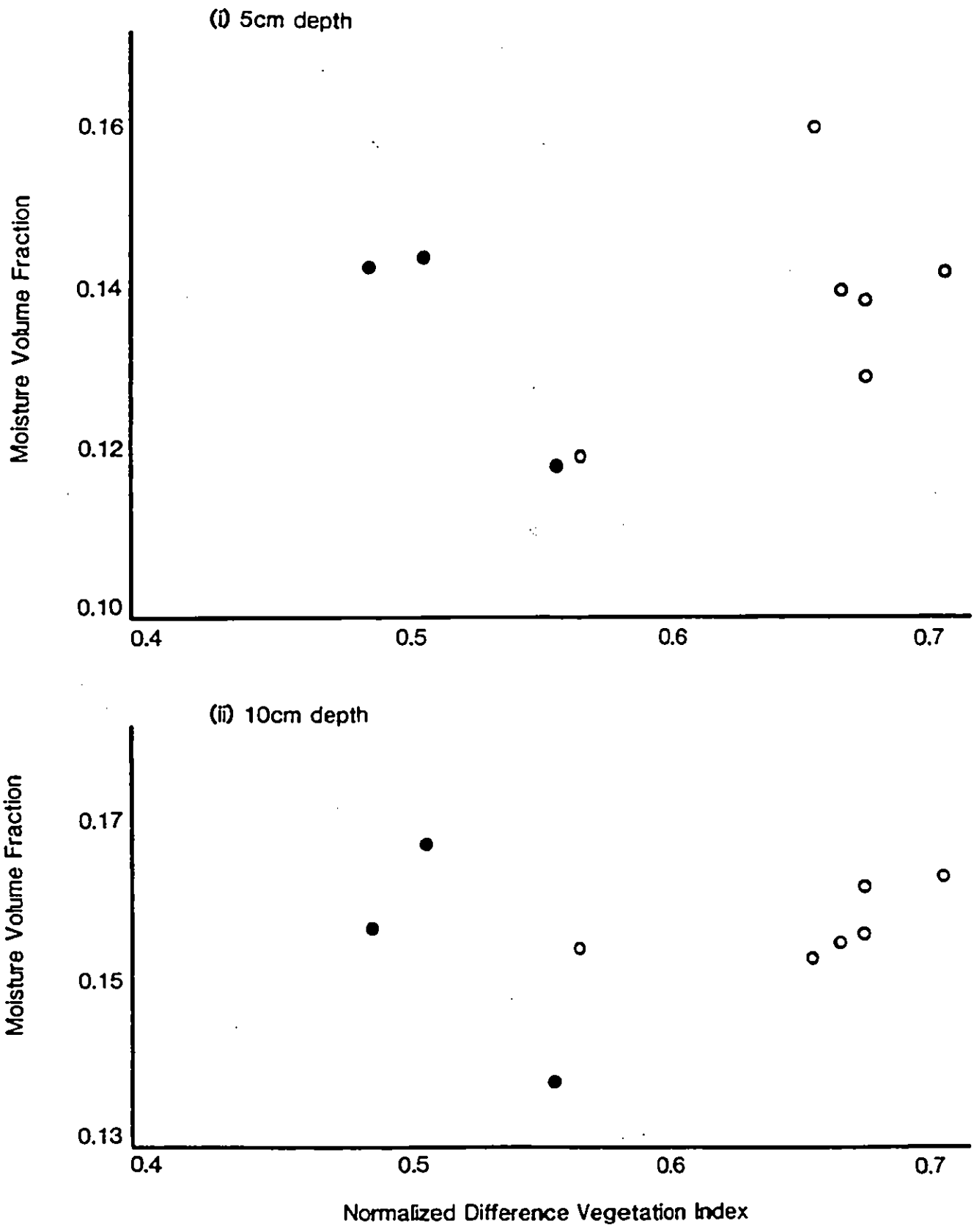


Fig. 4.4.7 Point values of Moisture Volume Fraction against Normalized Difference Vegetation Index 28th April 1990

o Temporary Grass ● Permanent Grass

## 4.5 LAND USE CLASSIFICATIONS

The land cover within the catchment was determined in three ways:-

(i) Ground surveys
(ii) The analysis of the aircraft remotely sensed images
(iii) The analysis of a Landsat image.

The methods used and the results obtained for all three will be described individually. Following this, a comparison will be made of the land cover distributions obtained.

### (i) Ground surveys

For the non-forested areas, the ground surveys were simply done by superimposing field numbers on a map of the area (Fig. 4.5.1), and asking people involved in the study to make a note of the land cover in each field during visits to the area. Also, a questionnaire was sent to all the farmers with land in the area. The results obtained were collated with the ground surveys to produce a time series of cover for each parcel of land within the area. This is shown in Table 4.5.1. It was found that, in terms of percentages of grassland to arable land, there was little change during the period of study. There were, however, changes in the arable cropping cycles, and occasional conversions of arable land to temporary grassland and vice versa.

The forested area was obtained by digitizing a 1: 10K scale map. It was a reverted mixed natural forest with no cropping. There had been a great deal of windthrow in recent years, and an extensive understorey vegetation had been established.

The percentages of each vegetation type found within the catchment boundary from ground surveys undertaken on the 28th April and on the 11th July, coincident with the aircraft overpasses, is given in Table 4.5.2.

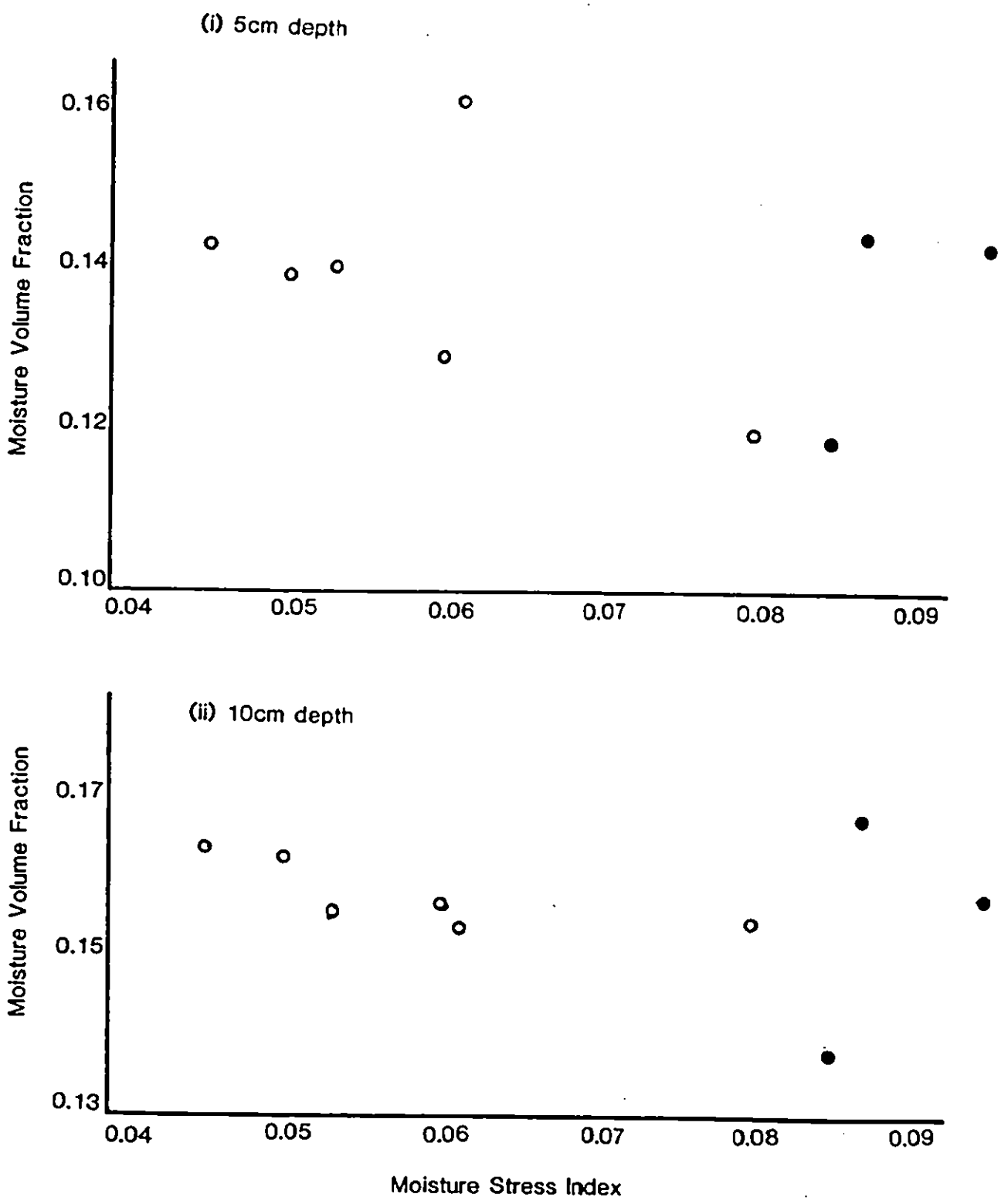


Fig. 4.4.8 Point values of Moisture Volume Fraction against Moisture Stress Index 28th April 1990

● Permanent Grass ○ Temporary Grass

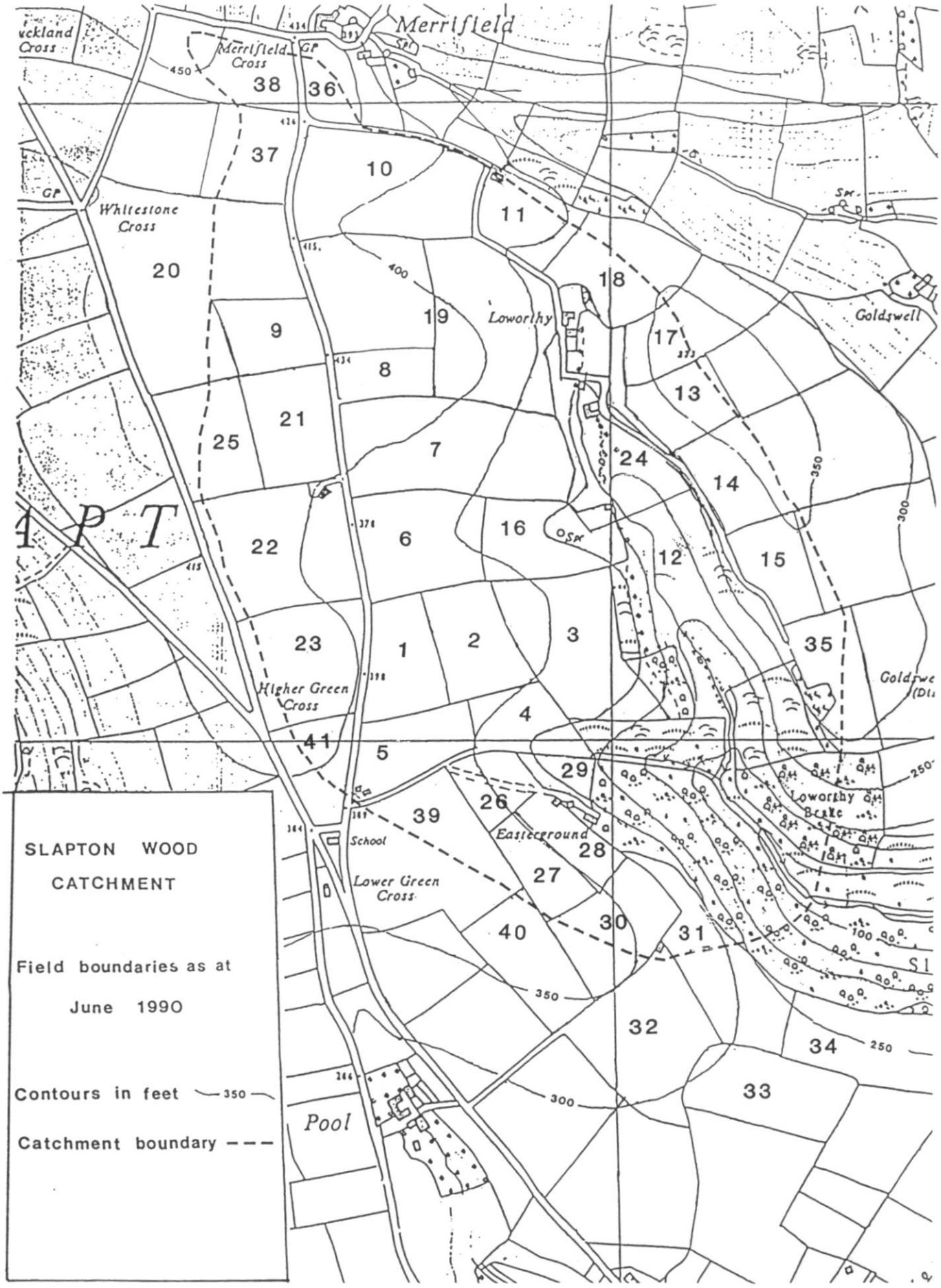


Fig. 4.5.1 Field Numbers used at Slapton for the Ground Surveys

*Table 4.5.1* *Land cover at Slapton from the field surveys*

| Field | 28.4.90 | 10.5.90 | 14.6.90 | 11.7.90 | 25.3.91 | 11.11.91 |
|---|---|---|---|---|---|---|
| 1 | T.G. | | T.G. | | T.G. | T |
| 2 | T.G. | | T.G. | T.G. | T.G. | T |
| 3 | R | B.E. | S | S | T.G. | T.G. |
| 4 | P.G. | | P.G. | | P.G. | P.G. |
| 5 | P.G. | | P.G. | | P.G. | P.G. |
| 6 | T.G. | | T.G. | T.G. | T.G. | T.G. |
| 7 | T.G. | | T.G. | | T.G. | T.G. |
| 8 | T.G | | T.G. | | T.G. | B |
| 9 | B.E./P | | P | P | W.B. | B.E. |
| 10 | T.G. | | T.G. | | B.E. | B.E. |
| 11 | B.E./B | | P/B.E./B | B.E./B/N | W.B. | T.G. |
| 12 | P.G. | | P.G. | | P.G. | P.G. |
| 13 | B/B.E. | | B.E./S.B. | B.E./S.B | B | W.B. |
| 14 | B.E. | | S.B./P | S.B./P | W.B. | W.B. |
| 15 | W.B. | W.B. | W.B. | W.B. | T.G. | T.G. |
| 16 | P.G. | P.G. | P.G. | | P.G. | P.G./K |
| 17 | B.E. | | S.B./P | B.E./B | B | B |
| 18 | B.E. | | P | P | B.E. | B.E. |
| 19 | T.G. | | T.G. | | B.E. | B/B.E. |
| 20 | | | | P | W.B. | B.E. |
| 21 | P.G. | | P.G. | P.G. | P.G. | P.G. |
| 22 | T.G. | | T.G. | | T.G. | T.G. |
| 23 | T.G. | | T.G. | | T.G. | T.G. |
| 24 | | | P.G. | P.G. | P.G. | P.G. |
| 25 | T.G. | | | | T.G. | T.G. |
| 26 | P.G. | | | P.G. | P.G. | P.G. |
| 27 | P.G. | | | P.G. | P.G. | P.G. |
| 28 | P.G. | | | P.G. | P.G. | P.G. |
| 29 | | | | P.G. | P.G. | P.G. |
| 30 | P.G. | | | P.G. | P.G. | P.G. |
| 31 | P.G. | | | P.G. | P.G. | P.G. |
| 32 | P.G. | | | P.G. | P.G. | |
| 33 | P.G. | | | | P.G. | |
| 34 | W.B. | | | W.B. | B.E. | |
| 35 | P.G. | | | T.G. | T.G. | T.G. |
| 36 | T.G. | | | T.G. | T.G. | T.G |
| 37 | T.G. | | | T.G. | T.G. | T.G. |
| 38 | T.G. | | | T.G. | T.G. | B.E. |
| 39 | S.B. | | | S.B. | S.B. | B.E. |
| 40 | S.B. | | | S.B. | T.G. | T.G. |
| 41 | T.G. | | | | T.G. | T.G. |

**ABBREVIATIONS**

| | | | | | |
|---|---|---|---|---|---|
| T.G. | = | TEMPORARY GRASS | P | = | POTATOES |
| P.G. | = | PERMANENT GRASS | W.B. | = | WINTER BARLEY |
| T | = | TURNIPS | N | = | NETTLES |
| R | = | RAPE | S.B. | = | SPRING BARLEY |
| B.E. | = | BARE EARTH | K | = | KALE |
| S | = | SWEDES | | | |
| B | = | BRASSICAS | | | |

*Table 4.5.2* *Percentages of each vegetation type within the Slapton Wood catchment obtained from ground surveys on the 28th April and 11th July 1990*

| | 28th April | 11th July |
|---|---|---|
| GRASSLAND | 64.9 | 64.9 |
| TEMPORARY | 39.3 | 40.5 |
| PERMANENT | 25.6 | 24.4 |
| ARABLE | 18.5 | 18.2 |
| RAPE | 4.0 | - |
| POTATOES | 3.8 | 4.9 |
| BARE EARTH | 6.0 | 2.7 |
| WINTER BARLEY | 2.0 | 2.1 |
| BRASSICAS | 0.8 | 0.8 |
| SPRING BARLEY | 1.9 | 3.7 |
| SWEDES | - | 4.0 |
| FOREST | 14.3 | 14.3 |
| OTHER | 2.2 | 2.4 |

### (ii) The aircraft remotely sensed images

As indicated previously, two sets of airborne images of the Slapton Wood catchment were obtained; details of these are given in Chapter 3. These images were analysed on an International Imaging Systems ($I^2S$) Model 75 processor at the Institute of Hydrology.

The first step in the processing involved registering the images to a 1: 10K base map. This was done by noting the map and pixel (picture element) coordinates of a number, approximately 20, easily identifiable points, and using these as input to a warping routine written specifically for aircraft imagery (Devereaux *et al.*, 1990). At the same time, the images were re-sampled to provide a pixel resolution of 4.5 m. This was done to simplify further analysis. As a result of the warping and resampling, a mean error of registration of less than one pixel ($< 4.5$ m) was found between the final images and the base map.

Early inspection of the aircraft images showed that it was not possible to generate a land cover classification based on a fixed number of bands using conventional software written mainly for satellite imagery. The higher spatial resolution of the aircraft imagery resulted in a wider range of radiances than obtained from lower resolution satellite imagery. This was particularly so over the forest, where areas affected by windthrow, in particular, resulted in widely varying radiance values. Also, the availability of eleven bands from the Daedalus

scanner (Table 3.1) meant that a greater number of combinations could be used compared with, for instance, the seven bands of Landsat imagery.

The technique adopted was to analyse and compare radiance values in each band for selected areas of the catchment and to develop algorithms, based on threshold values, that would identify individual vegetation types or differentiate between two similar types. Many of these algorithms were developed as a result of analysing the IRIS spectra (section 4.2). Some were based on single bands whereas others were based on combinations of bands. For the latter, the resulting combination often had to be scaled, and no Digital Number (DN) threshold is quoted in the accompanying tables. When more than one algorithm was used for an individual identification, it was decided to adopt the policy that more than a half of the criteria had to be satisfied before a vegetation identification could be justified.

A process of elimination was adopted, ie. those vegetation already identified were not subject to successive algorithms. By doing this, complications due to similar spectral responses of already classified vegetation were eliminated. Using this technique, each vegetation type was eliminated in turn. This resulted in a non-classified residual area that, in some cases, had to be subjected to additional algorithms before it could be predicted with any accuracy that the residual was composed of only one vegetation type.

Because of small changes in vegetation type, and different spectral responses at different times, the algorithms used and the order in which the different vegetation types were eliminated were different for the two sets of aircraft imagery.

**28th April 1990**

Table 4.5.3 outlines the sequence of algorithms that had to be applied to the aircraft images of the 28th April 1990. In this case, three iterations were needed to provide the final classifications. The algorithms employed reflect, to a great extent, the amount of green vegetation within each picture element, as suggested in section 4.2

Table 4.5.4 shows the percentages of crop types within the Slapton Wood catchment as given by the Field Survey and the classification of the aircraft images.

*Table 4.5.3* *Bands and threshold digital numbers (DN) used for classifying the vegetation using the aircraft images of the 28th April 1990*

| | | |
|---|---|---|
| WHOLE AREA | TREES | BAND 5 (DN < 41), BAND 6 (DN < 80)<br>BAND 7 (DN < 58), BAND 9 (DN < 43)<br>BAND 11 (DN < 102) |
| | BARE EARTH | BAND 2 (DN > 148), BAND 3 (DN > 180)<br>BAND 4 (DN > 114), BAND 5 (DN > 105)<br>BAND 9 (DN > 120), BAND 10 (DN > 130) |
| | POTATOES | BAND 7 (DN < 70), BAND 8 (DN < 81) |
| | T.GRASS | BANDS (6+7+8) - BANDS (2+4+5) HIGH |
| | S.BARLEY | BAND 9 (DN < 54), BAND 10 (DN < 43) |
| | BRASSICAS | BAND 2 (DN > 132), BAND 3 (DN > 170)<br>BAND 4 (DN > 104), BAND 5 (DN > 95)<br>BAND 10 (DN > 126) |
| | RAPE | BANDS (3+4+5) - BANDS (7+8+9)<br>MEDIUM |
| | W.BARLEY | BAND 7 (132 < DN < 142) |
| RESIDUE 1 | BRASSICAS | BAND 1 (DN > 61), BAND 2 (DN > 132)<br>BAND 3 (DN > 158), BAND 4 (DN > 94)<br>BAND 5 (DN > 84), BAND 10 (DN > 104) |
| | S.BARLEY | BAND 9 (DN < 56), BAND 10 (DN < 43)<br>BAND 11 (DN < 113) |
| | W.BARLEY/T.GRASS | BAND 8 W.B. (DN > 147) T.G. (DN < 147)<br>BAND 10 W.B. (DN > 48) T.G. (DN < 48) |
| | S.BARLEY/P.GRASS | BAND 7 S.B. (DN < 128) P.G. (DN > 128)<br>BAND 8 S.B. (DN < 155) P.G. (DN > 155) |
| RESIDUE 2 | T.GRASS/P.GRASS | BANDS (7-3) T.G. (DN > 158)<br>P.G. (DN < 158) |
| | P.GRASS/RAPE | BANDS (8-3) P.G. (DN > 100)<br>RAPE (DN < 100) |
| | T.GRASS/W.BARLEY | BANDS (3+5+12) T.G. (DN < 220)<br>W.B. (DN > 220) |
| | P.GRASS/S.BARLEY | BANDS (6+7+9+11) P.G. (DN > 196)<br>S.B. (DN < 196) |
| RESIDUE 3 | TREES | |

*Table 4.5.4* *Percentages of crops within the Slapton Wood catchment - 28th April 1990*

| Crop | Field survey | ATM classification |
|---|---|---|
| T.GRASS | 39.3 | 39.3 |
| P.GRASS | 25.6 | 26.4 |
| RAPE | 4.0 | 5.4 |
| POTS | 3.8 | 3.7 |
| BARE EARTH | 6.0 | 6.1 |
| W.BARLEY | 2.0 | 2.2 |
| BRASSICAS | 0.8 | 1.2 |
| S.BARLEY | 1.9 | 3.9 |
| FOREST | 14.3 | 11.8 |
| OTHER | 2.2 | - |

In terms of percentage areas, the agreement is very good, the only significant differences being underestimation of the forested area and overestimation of oil seed rape and spring barley. This is confirmed in Table 4.5.5 which shows a pixel by pixel comparison of the field survey and the ATM classification. The figures in the brackets indicate number of pixels for each vegetation type in the ATM classification as a percentage of the total in the ground survey. These values show that the ATM classification correctly identified the vegetation types in the range 91.6% (temporary grass) to 35.8% (winter barley). The biggest mis-classifications occurred for permanent grass (temporary grass), rape (permanent grass); winter barley (temporary grass and permanent grass), brassicas (permanent grass), spring barley (permanent grass), and forest (permanent grass and spring barley). These mis-classifications are as suggested by the need to use multiple algorithms (Table 4.5.3), and are hardly surprising bearing in mind that various cereal crops and grass look very similar during the spring months.

The results in Table 4.5.5 also show that the good agreement shown between the ground survey and the ATM classification, Table 4.5.4, is somewhat fortuitous for permanent grass and the cereal crops, errors of omission being generally balanced by errors of inclusion. In contrast, the forested area has been underestimated, windthrow areas having been classified either as permanent grass or spring barley.

When the land classification is degraded into grassland, arable land, and forest, the classes required for hydrological modelling purposes, the patterns shown in Fig. 4.5.2 are obtained. Percentage areas and a pixel by pixel comparison of the results of the Field survey and the ATM classification are shown in Table 4.5.6 and Table 4.5.7, respectively.

*Table 4.5.5 Pixel by pixel comparison of the field survey and ATM classification - 28th April 1990*

| Ground/ATM | 1 | | 2 | | 3 | | 4 | | 5 | | 6 | | 7 | | 8 | | 9 | | 10 |
|---|---|---|---|---|---|---|---|---|---|---|---|---|---|---|---|---|---|---|---|
| 1. TEMPORARY GRASS | 18949 | (91.6) | 1096 | (5.3) | 63 | (0.3) | 54 | (0.3) | 13 | (0.1) | 86 | (0.4) | 10 | (-) | 258 | (1.2) | 154 | (0.7) | - |
| 2. PERMANENT GRASS | 2025 | (15.0) | 8848 | (65.6) | 474 | (3.5) | 18 | (0.1) | 123 | (0.9) | 553 | (4.1) | 57 | (0.4) | 1220 | (9.0) | 164 | (1.2) | - |
| 3. RAPE | - | | 472 | (22.3) | 1625 | (76.8) | - | | 3 | (0.1) | 1 | (-) | 2 | (0.1) | 9 | (0.4) | 3 | (0.1) | - |
| 4. POTATOES | - | | 7 | (0.4) | 32 | (1.6) | 1808 | (91.0) | 31 | (1.6) | - | | 70 | (3.5) | 6 | (0.3) | 31 | (1.6) | - |
| 5. BARE EARTH | 4 | (0.1) | 36 | (1.1) | 65 | (2.1) | 3 | (0.1) | 2860 | (91.2) | 3 | (0.1) | 117 | (3.7) | 28 | (0.9) | 21 | (0.7) | - |
| 6. WINTER BARLEY | 339 | (32.0) | 321 | (30.3) | 4 | (0.4) | - | | 2 | (0.2) | 380 | (35.8) | 13 | (1.2) | 2 | (0.2) | - | | - |
| 7. BRASSICAS | - | | 132 | (29.9) | 33 | (7.5) | - | | 49 | (11.1) | 24 | (5.4) | 200 | (45.4) | 3 | (0.7) | - | | - |
| 8. SPRING BARLEY | 17 | (1.7) | 367 | (37.1) | 6 | (0.6) | 3 | (0.3) | - | | - | | - | | 579 | (58.6) | 16 | (1.6) | - |
| 9. FOREST | 112 | (1.5) | 776 | (10.3) | 218 | (2.9) | 3 | (-) | 8 | (0.1) | 18 | (0.2) | 16 | (0.2) | 1070 | (14.2) | 5316 | (70.5) | - |
| 10. OTHER | 2 | | 199 | | 185 | | 88 | | 149 | | 56 | | 40 | | 81 | | 252 | | - |

Land Survey

ATM Classification

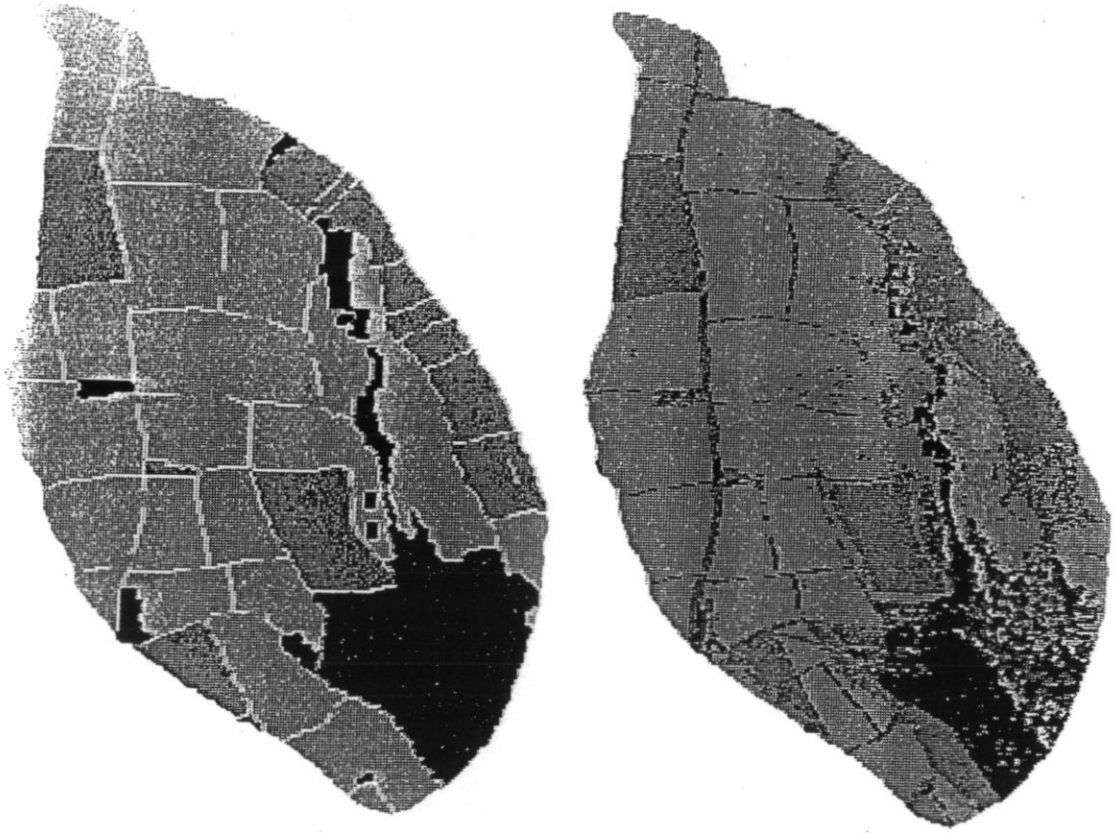

KEY

Grass

Arable

Forest

Other

Slapton Wood Catchment - April 1990

Fig. 4.5.2

*Table 4.5.6* *Percentage land use within the Slapton Wood catchment - 28th April 1990*

| Land use | Field survey | ATM classification |
|---|---|---|
| GRASSLAND | 64.9 | 65.7 |
| ARABLE LAND | 18.5 | 22.5 |
| FORESTRY | 14.3 | 11.8 |
| OTHER | 2.2 | - |

*Table 4.5.7* *Pixel by pixel comparison of land use within the Slapton Wood catchment - 28th April 1990*

| Ground/ATM | Grassland | Arable land | Forest |
|---|---|---|---|
| GRASSLAND | 30918 (90.5) | 2929 (8.3) | 318 (0.9) |
| ARABLE LAND | 1695 (17.4) | 7961 (81.8) | 71 (0.7) |
| FOREST | 888 (11.8) | 1333 (17.7) | 5316 (70.5) |

These results show that, for grassland areas, the comparison between the Field survey and ATM classification is excellent, and well within the agreement expected in lowland Britain for grassland areas (Atkinson *et al.*, 1985; Fuller *et al.*, 1989). The main misclassification was in heavily used areas within grass fields, where the grass had virtually disappeared, and was classified as bare earth. In this case, the misclassification was 'correct'.

The arable land classification was less good, but within the error expected (Atkinson *et al.*, 1985). As indicated previously, most of the misclassification was caused by similar responses from cereal crops and grassland. The underestimate in the forested area is realistic because, as indicated earlier, there were a number of areas affected by windthrow. Whether these should be classified as grassland or arable (bare earth/sparse vegetation) is uncertain.

**11th July 1990**

Table 4.5.8 outlines the sequence of algorithms that had to be applied to the aircraft images of the 11th July 1990. In this case only one iteration was used. The reason for this was not that this classification was simpler than the April one; on the contrary, it was very difficult to separate some vegetation types having complete ground cover. In fact the residual following the one iteration consisted of part of a potato field and part of a field of swedes. It proved impossible to separate these satisfactorily. In the event, this residual was classified as potatoes. This will obviously distort the classification based on individual vegetation types, but not the land use classification.

The percentage of vegetation types within the Slapton Wood catchment as given by the Field Survey and the classification of the aircraft imagery is given in Table 4.5.9.

*Table 4.5.8* *Bands and threshold digital numbers used for classifying the vegetation using the aircraft images of the 11th July 1990*

| | | |
|---|---|---|
| WHOLE AREA | TREES | BAND 2 (DN<65), BAND 3 (DN<83)<br>BAND 4 (DN<52), BAND 9 (DN<42)<br>BAND 10 (DN<36), BAND 11 (DN<52) |
| | BARE EARTH | BAND 4 (DN>103), BAND 5 (DN>94)<br>BAND 10 (DN>110), BAND 11 (DN>110) |
| | S.BARLEY/W.BARLEY | BAND (6+7+8) LOW<br>BAND 6 S.B. (DN>90) W.B. (DN<90)<br>BAND 7 S.B. (DN>75) W.B. (DN<75) |
| | BRASSICAS | BAND 2 (DN>125), BAND 3 (DN>150)<br>BAND 4 (DN>90), BAND 5 (DN>80) |
| | T.GRASS/P.GRASS | BAND 5 T.G. (DN<63) P.G. (DN>63) |
| | POTATOES | BAND (6-5) HIGH |
| | S.BARLEY | BAND 6 (DN<102) |
| | T.GRASS | BAND (6+7-9-10) LOW |
| RESIDUAL | POTATOES/SWEDES | not resolvable |

*Table 4.5.9* *Percentages of crops within the Slapton Wood catchment - 11th July 1990*

| Crop | Field survey | ATM classification |
|---|---|---|
| T.GRASS | 40.5 | 58.1 |
| P.GRASS | 24.4 | 16.2 |
| POTS | 4.9 | 4.6 |
| BARE EARTH | 2.7 | 4.4 |
| BRASSICAS | 0.8 | 0.1 |
| S.BARLEY | 3.7 | 5.2 |
| FOREST | 14.3 | 9.2 |
| W.BARLEY | 2.1 | 2.2 |
| SWEDES | 4.0 | - |
| OTHER | 2.4 | - |

As expected, the agreement between the Field Survey and ATM classification is poor with temporary grass being substantially overestimated, with smaller underestimations of permanent grass, the forested areas, and as indicated earlier, swedes. This is confirmed by the pixel by pixel comparison shown in Table 4.5.10. These values show that the ATM classification correctly identified the vegetation types in the range 90.0% (spring barley) to 1.8% (brassicas). A number of gross mis-classifications occurred including temporary grass (permanent grass), permanent grass (temporary grass), potatoes (permanent grass), brassicas (temporary grass and permanent grass), forest (temporary grass), and winter barley (permanent grass).

*Table 4.5.10 Pixel by pixel comparison of the field survey and ATM classification - 11th July 1990*

| Ground/ATM | 1 | | 2 | | 3 | | 4 | | 5 | | 6 | | 7 | | 8 | | 9 | 10 |
|---|---|---|---|---|---|---|---|---|---|---|---|---|---|---|---|---|---|---|
| 1. TEMPORARY GRASS | 17248 | (80.9) | 3118 | (14.6) | 590 | (2.8) | 145 | (0.7) | 7 | (-) | 98 | (0.5) | 105 | (0.5) | 9 | (-) | - | - |
| 2. PERMANENT GRASS | 8277 | (64.5) | 3823 | (30.0) | 6 | (-) | 234 | (18.2) | 4 | (-) | 340 | (2.7) | 121 | (0.9) | 24 | (0.2) | - | - |
| 3. POTATOES | 752 | (29.1) | 44 | (1.7) | 1580 | (61.1) | 49 | (1.9) | - | | 157 | (6.1) | 5 | (0.2) | 1 | (-) | - | - |
| 4. BARE EARTH | 114 | (7.9) | 77 | (5.3) | - | | 1195 | (82.9) | 13 | (0.9) | 18 | (1.2) | 10 | (0.7) | 15 | (1.0) | - | - |
| 5. BRASSICAS | 279 | (62.6) | 150 | (33.6) | - | | 8 | (1.8) | 8 | (1.8) | 1 | (0.2) | - | | - | | - | - |
| 6. SPRING BARLEY | 76 | (3.9) | 42 | (2.1) | - | | 5 | (0.3) | 1 | (0.1) | 1764 | (90.0) | 7 | (0.4) | 66 | (3.4) | - | - |
| 7. FOREST | 2440 | (32.4) | 139 | (1.8) | 4 | (0.1) | 82 | (1.1) | - | | 265 | (3.5) | 4541 | (60.4) | 53 | (0.7) | - | - |
| 8. WINTER BARLEY | 45 | (4.1) | 135 | (12.3) | - | | 14 | (1.3) | - | | 13 | (1.2) | - | | 889 | (81.1) | - | - |
| 9. SWEDES | 1218 | (52.6) | 531 | (25.1) | 336 | (15.9) | 23 | (1.1) | - | | 2 | (0.1) | 5 | (0.2) | - | | - | - |
| 10. OTHER | 286 | | 292 | | - | | 351 | | 14 | | 112 | | 27 | | 85 | | - | - |

A degraded classification - grassland, arable land, and forest is given in Fig. 4.5.3. Percentage areas and a pixel by pixel comparison of the results of the Field Survey and the ATM classification are shown in Table 4.5.11 and Table 4.5.12, respectively.

*Table 4.5.11 Percentage land use within the Slapton Wood catchment - 11th July 1990*

| Land use | Field survey | ATM classification |
|---|---|---|
| GRASSLAND | 64.9 | 74.3 |
| ARABLE LAND | 18.2 | 16.5 |
| FORESTRY | 14.3 | 9.2 |
| OTHER | 2.4 | - |

*Table 4.5.12 Pixel by pixel comparison of land use within the Slapton Wood catchment - 11th July 1990*

| Ground/ATM | Grassland | Arable land | Forest |
|---|---|---|---|
| GRASSLAND | 32466 (95.1) | 1457 (4.3) | 226 (0.7) |
| ARABLE LAND | 3463 (35.9) | 6158 (63.8) | 27 (0.3) |
| FOREST | 2579 (34.3) | 404 (5.4) | 4541 (60.4) |

These show that, whilst 95.1% of the grassland pixels were correctly classified, substantial areas of arable land and forest were also classified as grassland. Whilst this is acceptable for windthrow areas within the forest, it is unreasonable for the arable areas, and results in an unacceptable overestimation of the grassland areas within the catchment.

### (iii) The Landsat image

The Landsat image was acquired on the 4th May 1990. It was recorded in seven bands - three visible, three infrared, and one thermal (Table 3.1) - at a ground resolution of 28.5 m.

The image was analysed on the International Imaging System ($I^2S$) Model 75 processor at IH. The first step involved registering the image to a base map. This was done by identifying a number of readily recognisable points on the image and on a 1:25K base map, and warping the coordinates of the points on the image to those on the base map using a bilinear routine available on the processor. This resulted in a root mean square error of one pixel (picture element) ie. approximately 28.5 m.

An initial visual analysis of the resulting image suggested that a detailed analysis of the radiances in the various bands would not achieve the kind of differentiation obtained using the aircraft images. This being the case, an unsupervised classification was attempted. In this routine, six bands of the image - the maximum permissable - are used to generate a classification based on the different radiances in the bands. Of the seven Landsat bands, the thermal band was omitted, as this band provided the least information.

Land Survey

ATM Classification

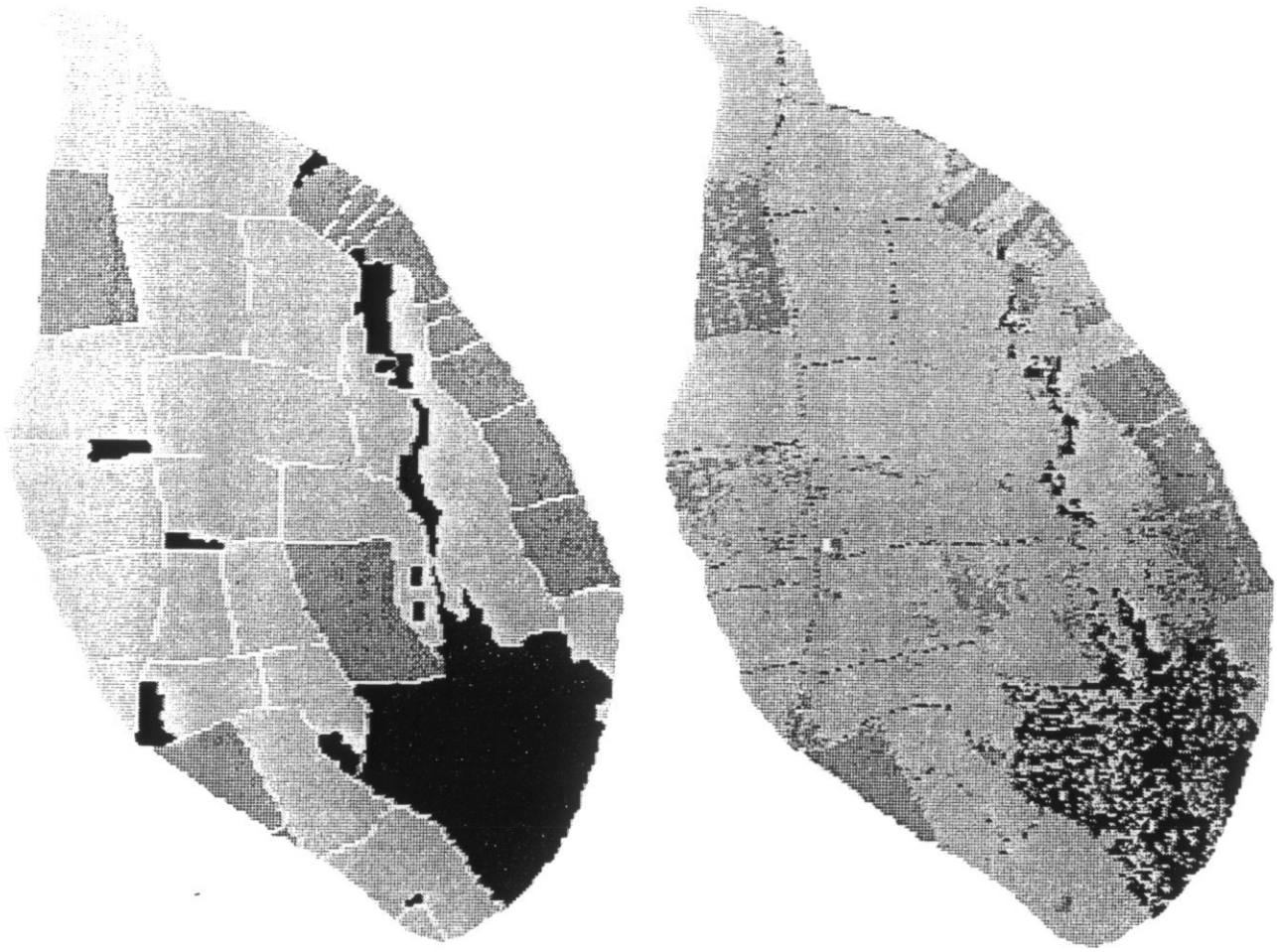

KEY

Grass

Arable

Forest

Other

Slapton Wood Catchment - July 1990

Fig. 4.5.3

A total of sixteen separate classes were identified. There was also a residual class which, in this case, could be regarded as a single class. Figure 4.5.4 shows average near infrared against red reflectances for all of the classes. The various classes were assigned to vegetation types by comparison with the land survey of the 28th April. The resulting pattern is as expected and very similar to the one given by the data from the IRIS spectroradiometer (Fig. 4.2.2). In terms of the Normalized Difference Vegetation Index, NDVI ((band 4-band 3)/(band 4 + band 3)), the average values were:-

| Vegetation type | NDVI |
|---|---|
| Temp. Grass | 0.68 |
| Perm. Grass | 0.57 |
| Forest | 0.52 |
| Rape | 0.48 |
| Arable | 0.25 |
| Bare Earth | 0.22 |
| Water | -0.27 |

When this classification was reduced to grassland, arable, forest, and other, and applied to the Slapton Wood catchment, the pattern in Figure 4.5.5 is obtained. Percentage land covers are given in Table 4.5.13 whilst a pixel-by-pixel comparison with the land survey of the 28th April given in Table 4.5.14.

*Table 4.5.13 Percentage land use within the Slapton Wood catchment - Landsat image*

| Land use | Field survey | Landsat classification |
|---|---|---|
| GRASSLAND | 64.9 | 71.5 |
| ARABLE LAND | 18.2 | 17.5 |
| FORESTRY | 14.3 | 10.9 |
| OTHER | 2.4 | - |

Fig. 4.5.4 Near Infrared and Red Reflectances for the Landsat classes

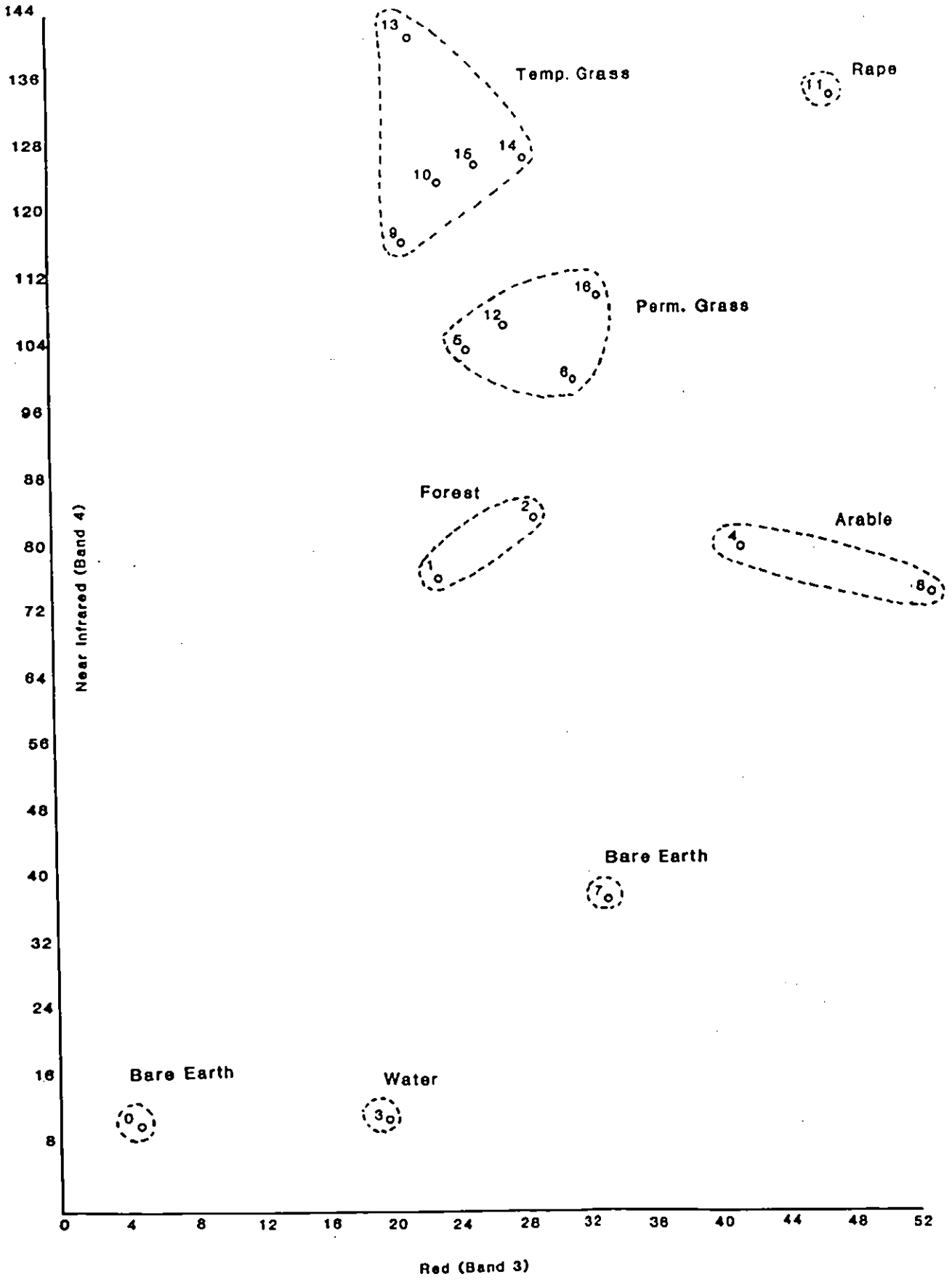

Land Survey

Landsat

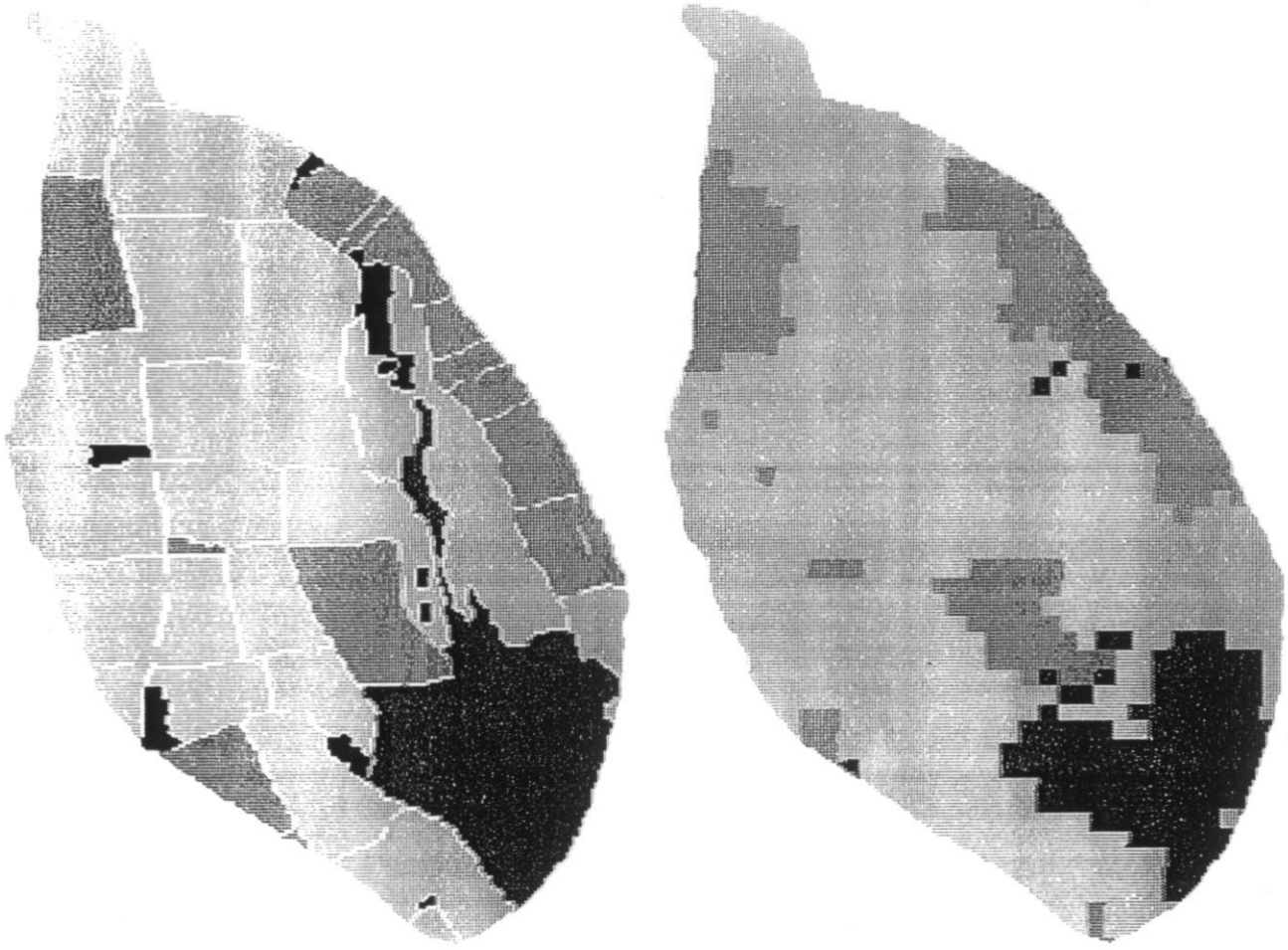

KEY

Grass

Arable

Forest

Other

**Fig. 4.5.5**

Slapton Wood Catchment - May 1990

*Table 4.5.14* *Pixel by pixel comparison of land use within the Slapton Wood catchment - Landsat image*

| Ground/Landsat | Grassland | | Arable land | | Forest | |
|---|---|---|---|---|---|---|
| GRASSLAND | 32168 | (94.1) | 1782 | (5.2) | 219 | (0.6) |
| ARABLE LAND | 2748 | (28.2) | 6866 | (70.6) | 114 | (1.2) |
| FOREST | 1910 | (25.3) | 73 | (1.0) | 5555 | (73.7) |

The results in these two tables show that a satisfactory agreement has been obtained between the land survey and the Landsat classification. In this case, the windthrow areas within the catchment have been classed exclusively as grassland. Some areas of arable land, notably a field of spring barley at the bottom left hand corner of the catchment, have also been classified as grassland. As a result, the grassland areas have been overestimated in the Landsat classification by about 10%, with smaller underestimations in the forested and arable areas.

**(iv) Comparison of the various classifications**

Table 4.5.15 shows the percentages of land use within the Slapton Wood catchment based on the field surveys, the two aircraft images, and the Landsat image.

*Table 4.5.15* *Comparisons of the percentage land cover within the Slapton Wood catchment*

| Land use | Field survey | ATM 28th April | ATM 11th July | Landsat |
|---|---|---|---|---|
| GRASSLAND | 64.9 | 65.7 | 74.3 | 71.5 |
| ARABLE LAND | 18.5 | 22.5 | 16.5 | 17.5 |
| FORESTRY | 14.3 | 11.8 | 9.2 | 10.9 |
| OTHER | 2.2 | - | - | - |
| TOTAL ERROR | | 9.5 | 18.7 | 13.2 |

Assuming that the field survey is correct, then summing the 'errors' in the classifications suggests that the classification based on the aircraft image of the 28th April is the best and the aircraft image of the 11th July is the worst. A similar conclusion is reached when comparing the percentages of pixels correctly identified for each land use classification (Table 4.5.16).

*Table 4.5.16* *Percentage of pixels correctly identified for each land use classification*

| Land use | ATM 28th April | ATM 11th July | Landsat |
|---|---|---|---|
| GRASSLAND | 90.5 | 95.1 | 94.1 |
| ARABLE LAND | 81.8 | 63.8 | 70.6 |
| FORESTRY | 70.5 | 60.4 | 73.7 |
| TOTAL ERROR | 58.2 | 80.7 | 61.6 |

These comparisons are slightly misleading in the sense that, as indicated earlier, the extent of forestry given by the field survey is almost certainly on overestimation because of the areas of windthrow. Of importance is what these areas are classified as. In the case of the 28th April aircraft image, they are classified as arable whereas, for the other two images, they are classified as grassland. For modelling purposes, it is uncertain which of these is correct. Because of this uncertainty, and bearing in mind the relatively small differences between the errors in the classifications from the aircraft 28th April and Landsat images it is concluded that the Landsat classification is adequate if, as in this application, percentages of different arable crops are not required.

# 5. Estimating actual evapotranspiration from the different vegetation types

In order to utilize the results from the land cover classification (Section 4.5) for catchment water balance purposes (Section 6), it is necessary to have some estimate of actual evapotranspiration from the different vegetation types. As indicated previously (Section 1.4), soil moisture data are available under three vegetation types - grass, barley, and the forested area - and these data have been used to estimate actual evapotranspiration. For water balance purposes, it has been assumed that the barley field represents all the arable areas in the catchment, whilst the results from the temporary grass field are applicable also to permanent grassland.

The techniques involved in estimating actual evapotranspiration losses from each vegetation type were:-

(i) calculate the field capacity of each neutron access site as the mean water content for all reading dates in the months December to March (inc.) when there was little or no rain for the preceding five days,

(ii) identify periods between soil moisture measuring dates when no rain fell,

(iii) for the grass field, include low rainfall periods, when it could be predicted with some confidence, that no losses to streamflow occurred. For the barley field and the forested area, these latter periods were used to calculate interception losses,

(iv) calculate actual transpiration losses for all the periods considered as the mean change in water content for all the neutron access tubes read, correcting for rainfall where necessary for the grass field,

(v) if the calculated actual transpiration is greater than potential, the difference is assumed to be drainage,

(vi) compute the ratio of actual to potential evapotranspiration as given from the automatic weather station data for grass for each of these periods,

(vii) calculate an average soil moisture deficit over each period considered as the mean of the neutron access sites,

(viii) obtain relationships between the ratio of actual to potential evapotranspiration and soil moisture deficit,

(ix) obtain relationships between drainage and soil moisture deficit,

(x) use these relationships to calculate soil moisture deficit and actual evapotranspiration on a daily basis using the following techniques (Calder *et al.*, 1983).

$$SMD(i+1) = SMD(i) + ETa(i) - P(i) + INT(i) + DRAIN(i) \quad SMD(i) > 0$$

$$SMD(i+1) = ETa(i) - P(i) + INT(i) + DRAIN(i) \quad SMD(i) < 0$$

ETa(i)/ETp(i) = f(SMD(i))

where SMD(i) = soil moisture deficit on day i,

ETa(i) = actual evapotranspiration on day i,

ETp(i) = potential evapotranspiration on day i,

P(i) = precipitation on day i,

INT(i) = canopy interception on day i,

DRAIN(i) = drainage from the soil profile on day i.

All values are in mm per day. The results obtained for the three neutron access networks were as follows.

## 5.1 GRASSLAND SITE

Six neutron access tubes were installed in the grassland site during September 1989. The depth of installation varied between 80 and 120 cm below ground level. Two additional tubes were installed to depths of 300 cm and 550 cm during July 1990.

For the sake of uniformity, 80 cm below ground level has been adopted as the depth to which soil moisture changes, and hence actual evapotranspiration, have been calculated, though changes over greater depths have been estimated to ensure that significant deep seepage was not occurring. Again, for the sake of consistency, only those dates during the winter months 1989/1990 when data from all six original tubes were deemed 'correct' have been used to calculate field capacity. Only one date, 7.3.90, satisfied this criterion; the soil moisture totals to 80 cm depth have been taken as the field capacities for the individual tubes. These are as follows:-

***Tables 5.1.1*** *Field capacity values for the grassland site*

| TUBE | 1 | 2 | 3 | 4 | 5 | 6 | MEAN |
|---|---|---|---|---|---|---|---|
| | 234.8 | 223.2 | 209.6 | 246.5 | 235.8 | 196.9 | 224.5 |

This particular day was, in fact, one of the wettest experienced in terms of soil moisture. No field capacity values have been calculated for Tubes 7 and 8.

A total of 23 periods were identified which satisfied the criteria given in (ii) and (iii) above, and which could be used to provide estimates of actual evapotranspiration from the grass field. These periods are listed in Table 5.1.2, together with the period rainfall, the ratio of actual to potential evapotranspiration, and the average soil moisture deficit over the period

*Table 5.1.2* *Periods used for estimating actual evapotranspiration from the grassland field showing Total Precipitation (P), Actual/Potential Daily Evapotranspiration (ETa/ETp), and Average Soil Moisture Deficit (SMD)*

| Period | P | Tube | 1 | 2 | 3 | 4 | 5 | 6 |
|---|---|---|---|---|---|---|---|---|
| 29.09-10.10.89 | 5.7 | ETa/ETp | 0.88 | 1.03 | 1.01 | 1.11 | | |
| | | SMD | 25.5 | 41.0 | 27.7 | 36.7 | | |
| 10.10-18.10.89 | 0.0 | ETa/ETp | 0.87 | 0.92 | 0.58 | 0.82 | 0.65 | 0.71 |
| | | SMD | 35.7 | 52.3 | 37.1 | 46.9 | 38.0 | 31.5 |
| 21.11-06.12.89 | 3.5 | ETa/ETp | 1.08 | 1.43 | | 1.06 | | |
| | | SMD | 0.7 | 15.8 | | 2.5 | | |
| 01.03-07.03.90 | 2.0 | ETa/ETp | 2.81 | 2.44 | | 3.77 | 3.23 | 1.60 |
| | | SMD | -5.8 | -4.9 | | -8.0 | -6.8 | -2.9 |
| 07.03-15.03.90 | 6.0 | ETa/ETp | 1.67 | 2.10 | 1.66 | 1.80 | | |
| | | SMD | 3.4 | 5.0 | 3.3 | 3.9 | | |
| 15.03-23.03.90 | 5.5 | ETa/ETp | 0.52 | 1.24 | 0.61 | 0.90 | | |
| | | SMD | 6.0 | 12.0 | 6.2 | 8.4 | | |
| 23.03-28.03.90 | 0.5 | ETa/ETp | 0.85 | 1.10 | 0.91 | 0.69 | | 0.68 |
| | | SMD | 9.6 | 19.8 | 10.6 | 12.7 | | 13.0 |
| 28.03-04.04.90 | 7.5 | ETa/ETp | 1.00 | 1.05 | 1.13 | 1.09 | 1.06 | 0.80 |
| | | SMD | 17.0 | 28.5 | 18.9 | 19.8 | 18.5 | 18.1 |
| 04.04-11.04.90 | 0.5 | ETa/ETp | 0.53 | 0.60 | 0.49 | 0.45 | 0.42 | 0.48 |
| | | SMD | 25.4 | 38.3 | 27.5 | 27.9 | 26.2 | 24.6 |
| 18.04-25.04.90 | 7.0 | ETa/ETp | 0.87 | 0.83 | 0.66 | 0.66 | 0.57 | 0.68 |
| | | SMD | 35.1 | 47.6 | 37.1 | 39.2 | 33.4 | 34.7 |
| 25.04-02.05.90 | 0.5 | ETa/ETp | 0.78 | 1.03 | 0.78 | 0.86 | 0.62 | 0.83 |
| | | SMD | 50.6 | 65.7 | 50.2 | 53.3 | 43.5 | 48.7 |
| 02.05-11.05.90 | 5.5 | ETa/ETp | 0.78 | 0.89 | 0.60 | 0.93 | 0.79 | 0.74 |
| | | SMD | 70.3 | 90.6 | 66.8 | 76.5 | 61.4 | 68.4 |
| 13.06-19.06.90 | 7.0 | ETa/ETp | | | | 0.78 | 0.77 | |
| | | SMD | | | | 100.0 | 89.9 | |
| 12.07-01.08.90 | 9.5 | ETa/ETp | 0.42 | | | 0.42 | 0.37 | |
| | | SMD | 106.2 | | | 107.1 | 91.3 | |
| 01.08-08.08.90 | 0.0 | ETa/ETp | 0.12 | | | 0.10 | 0.17 | |
| | | SMD | 123.1 | | | 124.0 | 107.1 | |
| 08.08-13.08.90 | 0.0 | ETa/ETp | 0.06 | | | 0.02 | 0.03 | |
| | | SMD | 125.8 | | | 125.8 | 110.3 | |
| 22.08-29.08.90 | 0.0 | ETa/ETp | 0.42 | 0.53 | | 0.48 | 0.18 | |
| | | SMD | 103.7 | 104.9 | | 101.3 | 100.1 | |
| 29.08-05.09.90 | 11.5 | ETa/ETp | 0.43 | 0.44 | | 0.73 | 0.41 | 0.49 |
| | | SMD | 106.0 | 109.0 | | 107.9 | 100.5 | 100.0 |
| 05.09-12.09.90 | 4.0 | ETa/ETp | 0.43 | 0.48 | | 0.33 | 0.31 | 0.15 |
| | | SMD | 108.1 | 111.0 | | 111.5 | 100.5 | 99.1 |
| 12.09-26.09.90 | 9.0 | ETa/ETp | 0.48 | 0.41 | | 0.52 | 0.48 | 0.47 |
| | | SMD | 112.9 | 112.7 | | 116.5 | 102.1 | 98.7 |
| 03.10-17.10.90 | 14.0 | ETa/ETp | 0.63 | 0.82 | | 0.71 | 0.62 | 0.44 |
| | | SMD | 103.9 | 98.7 | | 104.9 | 95.5 | 88.2 |
| 15.11-21.11.90 | 12.5 | ETa/ETp | 1.25 | 1.43 | 0.91 | 1.27 | 0.56 | 1.11 |
| | | SMD | 32.2 | 35.2 | 32.7 | 39.4 | 48.0 | 13.0 |
| 28.11-08.12.90 | 4.0 | ETa/ETp | 1.41 | 0.90 | 1.57 | | 0.94 | 0.87 |
| | | SMD | 8.4 | 20.3 | 16.4 | | 21.9 | 8.9 |

for each access tube. In order to determine whether in fact the adoption of 80 cm depth below ground level for the calculation of evapotranspiration losses is reasonable, mean soil moisture changes to a depth of 80 cm for Tubes 1-6 were compared to those for Tube 7 (300 cm depth) and Tube 8 (550 cm depth) for the accounting periods later than July 1990 shown in Table 5.1.2. This comparison shows that, whilst differences did occur, they were random rather than systematic, and generally within the variation exhibited in Tubes 1 to 6. An overall $r^2$ value of 0.73 was obtained, and it has been assumed that the data shown in Table 5.1.2 are sufficient for this purpose.

As far as possible, each period relates to the time between consecutive neutron probe readings, normally one week. In some cases, however, it was found necessary to combine two periods in order to produce 'sensible' values. The gaps in Table 5.1.2 were caused by a number of factors apart from data rejected following quality control. In some cases, the neutron access tubes were not read to 80 cm depth, or readings were taken at the incorrect depths. Also, the grass was cut for silage on the 14th June 1990, some of the access tubes could not be read after this.

Inspection of Table 5.1.2 shows that for some periods, particularly at the beginning of the monitoring, actual evapotranspiration at some sites was greater than potential evapotranspiration. This could be caused by a number of factors. In the first place, the original six access tubes were installed during September 1989, and may have taken time to "settle down" ie. the actual moisture volume fraction measurements may have been in error as a result of soil disturbance during installation. Also, the soil profile could have been draining during these periods, and the reduction in soil moisture would have been greater than actual evapotranspiration. It is possible that the estimate of potential evapotranspiration as given by the automatic weather station may have been in error. Whatever the cause it has been assumed that, for those times when actual evapotranspiration was greater than potential, the grass was transpiring at potential, and the difference assumed to be drainage from the soil profile.

Also, there were some periods, notably 4.4 - 11.4.90, when the ratio of actual to potential evapotranspiration was much lower than would have been expected considering the soil moisture deficit pertaining at the time. This suggests an additional constraint on actual evapotranspiration, apart from soil moisture deficit. One obvious possibility is temperature, as it is well known that growth is curtailed when the air temperature is below about 6°C. Investigating whether temperature is having an effect and correcting for this effect is difficult because, potentially, the following processes may be occurring simultaneously in each of the periods considered in Table 5.1.2:-

(a) the profile may be draining,
(b) actual evapotranspiration may be reduced as a result of soil moisture deficit,
(c) actual evapotranspiration may be reduced as a result of low temperatures,

and separating the effects of each process may be rather subjective. This will be considered later.

Values from individual tubes have been averaged for each period. These are shown in Table 5.1.3 together with standard deviations. Point values for some individual sites were deemed

*Table 5.1.3* *Mean and standard deviation of actual/potential daily evapotranspiration, daily drainage and average soil moisture deficit for the temporary grass field*

| Period | Actual/Potential evapotranspiration | | Drainage (mm/day) | | Soil moisture deficit (mm) | |
|---|---|---|---|---|---|---|
| 29.09-10.10.89 | 0.97 | (0.06) | 0.07 | (0.09) | 32.7 | (7.3) |
| 10.10-18.10.89 | 0.76 | (0.13) | 0.0 | | 40.3 | (7.8) |
| 21.11-06.12.89 | 1.00 | | 0.15 | (0.16) | 6.3 | (8.2) |
| 07.03-15.03.90 | 1.00 | | 0.77 | (0.20) | 3.9 | (0.8) |
| 23.03-28.03.90 | 0.99 | (0.01) | 0.04 | (0.09) | 13.1 | (4.0) |
| 28.03-04.04.90 | 1.00 | | 0.11 | (0.10) | 20.1 | (4.2) |
| 18.04-25.04.90 | 0.85 | (0.11) | 0.0 | | 37.9 | (4.7) |
| 25.04-02.05.90 | 0.81 | (0.12) | 0.0 | | 52.0 | (7.5) |
| 02.05-11.05.90 | 0.79 | (0.12) | 0.0 | | 72.3 | (10.2) |
| 13.06-19.06.90 | 0.78 | (0.01) | 0.0 | | 95.0 | (7.1) |
| 12.07-01.08.90 | 0.40 | (0.03) | 0.0 | | 101.5 | (8.9) |
| 01.08-08.08.90 | 0.13 | (0.04) | 0.0 | | 118.1 | (9.5) |
| 08.08-13.08.90 | 0.04 | (0.02) | 0.0 | | 120.6 | (8.9) |
| 22.08-29.08.90 | 0.40 | (0.16) | 0.0 | | 102.5 | (2.2) |
| 29.08-05.09.90 | 0.50 | (0.13) | 0.0 | | 104.8 | (4.2) |
| 05.09-12.09.90 | 0.34 | (0.13) | 0.0 | | 106.0 | (5.9) |
| 12.09-26.09.90 | 0.47 | (0.04) | 0.0 | | 108.6 | (7.7) |
| 03.10-17.10.90 | 0.64 | (0.14) | 0.0 | | 98.2 | (6.8) |
| 28.11-08.12.90 | 1.00 | | 0.12 | (0.17) | 15.2 | (6.3) |

'suspect', and were not used to calculate those averages. Also, periods when no soil moisture deficit was evident have been omitted. For these periods, it is assumed that rapid runoff occurs, and the drainage values are not relevant.

The values given in Table 5.1.3 are shown graphically in Fig. 5.1.1. The regression of actual/potential evapotranspiration against soil moisture deficit is represented by two straight lines, in this case the transition point is at a deficit of 95 mm. The drainage decreases exponentially with deficit. There is some degree of scatter in the relationships. In particular, at lower soil moisture deficits, the relationship between actual/potential evapotranspiration to deficit is not particularly good. As indicated previously, this could be due to a number of factors, including low temperatures, for which some correction will be made. It is gratifying to note however, that, at higher deficits, where ETa/ETp changes most rapidly against deficit, the agreement is very good indeed. The relationship between drainage and deficit is also not particularly good, being influenced by one high drainage value. In spite of these reservations, these were the regressions used to estimate actual evapotranspiration from the grass field.

Continuous hydrological data from the Slapton Wood catchment were available for the period October 1989 to July 1991 (inclusive). Ideally, it would have been better to start the analysis during a period when the soil was at or close to field capacity. The relative shortness of the data records meant that this could not be done, and it was decided to carry out the analysis on the whole data set. The first 15 months (Oct 1989 - Dec 1990) can be regarded as the calibration period (Table 5.1.3), though only a third of the available data were used for calibration purposes. The analysis was conducted using rainfall and potential evapotranspiration estimates from the automatic weather station. Average soil moisture values from the grassland sites were used. The initial soil moisture deficit was calculated as the difference between the water content in the top 80 cm of soil on the 29th September 1989 and the field capacity value (Table 5.1.1). A time step of one day was employed; the calculations employed were as follows:-

(i) Calculate the actual evapotranspiration (ETa) from the potential evapotranspiration (ETp) and soil moisture deficit (SMD).

$$ETa = ETp\ (a.SMD + b)$$

where a and b, dependent on SMD, are as given in Fig. 5.1.1.

(ii) Modify the estimated actual evapotranspiration according to the mean daily air temperature (T) as follows:

| | |
|---|---|
| $T > 8.0°C$ | $ETa = ETa$ |
| $0°C \leq T \leq 8.0°C$ | $ETa = ETa * 0.125 * T$ |
| $0°C > T$ | $ETa = 0$ |

A number of relationships of the type suggested by Andersson and Harding (1991) were attempted. It was found that the above gave the best 'fit' for those periods, particularly during April 1990 (Table 5.1.2), when actual evapotranspiration, uncorrected for temperature, was lower than expected.

(iii) Calculate the drainage from the soil profile (Fig. 5.1.1).

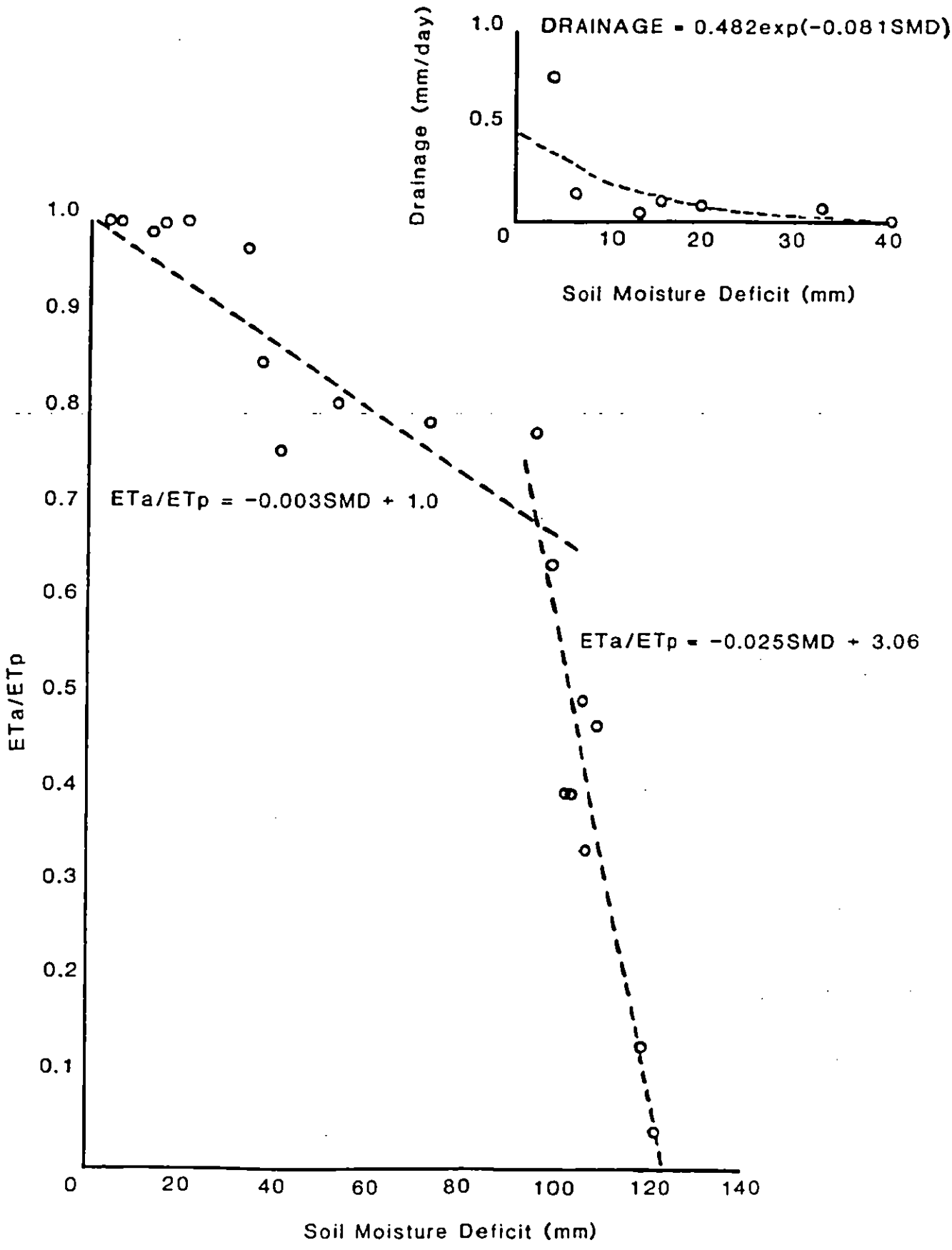


Fig. 5.1.1 Regressions of Actual/Potential Evapotranspiration against Soil Moisture Deficit for the Temporary Grass Field

$$DRAINAGE = 0.482 \exp(-0.081\ SMD)$$

(iv) Update the soil moisture deficit.

$$SMD(i+1) = SMD(i) - RAIN(i+1) + ETa(i+1) + DRAINAGE(i+1)$$

(v) Calculate the amount of rapid runoff (RUNOFF)

| | |
|---|---|
| SMD > 0 | RUNOFF = 0.0 |
| SMD < 0 | RUNOFF = ABS (SMD) |
| | SMD = 0.0 |

ie. it is assumed that if the soil moisture is above field capacity, then this 'excess' becomes rapid runoff and the new soil moisture is put to zero.

(vi) Continue to next day

Figure 5.1.2 shows the estimated and measured soil moisture deficits for the grassland site at Slapton. The agreement is generally very good (normally within ± 5 mm), though there are some periods where significant differences occur. For instance, the soil moisture deficit is underestimated for most of the winter 1990/91. The differences between estimated and measured deficits shown in Fig. 5.1.2 are exaggerated because an 'error' in one accounting period will result in a difference that will be manifest in succeeding periods until the soil moisture deficit becomes zero. This particular 'error' occurred in the period 17.9 - 26.9.90 when the estimated soil moisture deficit fell by 12.9 mm whilst the measured SMD fell by 3.4 mm. There were no low temperatures during this particular period nor was it likely that the soil profile was draining. Therefore, the discrepancy is likely to be due to the calculation of actual evapotranspiration; the regression used suggested a ETa/ETp ratio of 0.38; measured soil moisture measurements suggested a value of 0.68.

Another discrepancy occurred in the period 6.2 - 13.2.91. Again, estimated SMD was underestimated. The measured soil moisture values suggested an increase in SMD of 8.8 mm whilst the estimated value fell by 0.1 mm. This period was characterized by very low temperatures (mean daily air temperatures between -5.8°C and +1.5°C), and the estimated actual evapotranspiration over the whole period was only 0.1 mm. Even if no temperature correction was applied, and the evapotranspiration assumed to be at potential rate, then the estimated drop in SMD would have been only half of that measured.

In contrast, soil moisture deficit was overestimated at the end of May 1991. During the period 22nd May to the 29th May the estimated SMD increased by 18.8 mm whilst the measured SMD increased by 12.3 mm. In this case it would appear that ETa/ETp is an overestimation, in contrast to the situation during September 1990.

Table 5.1.4 shows the monthly totals (mm) of measured rainfall, potential evapotranspiration, and flow, and estimated actual evapotranspiration, drainage, rapid runoff, and total flow. Also shown are annual totals (January to January) for 1990. For the latter, the difference between measured rainfall and flow (the SMD was insignificant at the beginning and end of the year) gives an annual 'water use' of 477.1 mm.

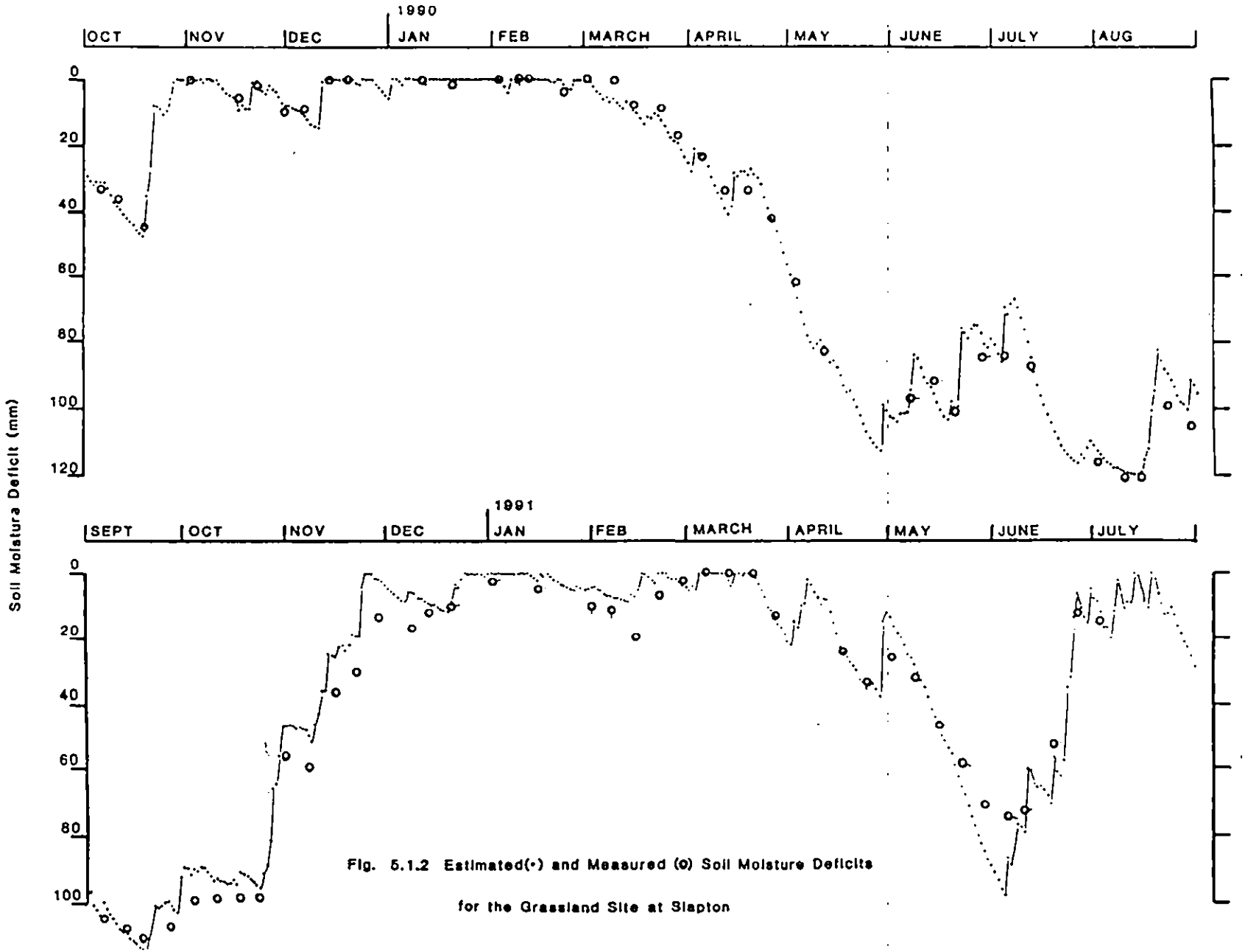


Fig. 5.1.2 Estimated(•) and Measured (o) Soil Moisture Deficits for the Grassland Site at Slapton

*Table 5.1.4* *Measured and estimated monthly totals (mm) of hydrological variables for the temporary grass field at Slapton*

| Month | Measured | | | Estimated | | | |
|---|---|---|---|---|---|---|---|
| | Rain | ETp | Flow | ETa | Drainage | Rapid Runoff | Total flow |
| 1989 | | | | | | | |
| OCT | 105.5 | 44.3 | 15.0 | 39.7 | 3.5 | 35.7 | 39.2 |
| NOV | 70.9 | 26.4 | 50.8 | 23.4 | 11.6 | 42.1 | 53.7 |
| DEC | 191.5 | 25.6 | 155.9 | 22.4 | 11.5 | 156.2 | 167.7 |
| 1990 | | | | | | | |
| JAN | 191.0 | 5.6 | 107.3 | 5.3 | 14.9 | 165.4 | 180.3 |
| FEB | 287.5 | 18.9 | 274.5 | 17.1 | 13.5 | 257.2 | 270.7 |
| MARCH | 15.5 | 37.6 | 57.8 | 31.7 | 7.8 | 1.3 | 9.1 |
| APRIL | 36.0 | 87.0 | 21.2 | 66.1 | 1.1 | 0.0 | 1.1 |
| MAY | 23.5 | 110.1 | 14.1 | 69.3 | 0.0 | 0.0 | 0.0 |
| JUNE | 78.5 | 85.8 | 11.5 | 55.3 | 0.0 | 0.0 | 0.0 |
| JULY | 38.0 | 133.6 | 10.0 | 69.9 | 0.0 | 0.0 | 0.0 |
| AUG | 53.0 | 109.5 | 8.0 | 37.6 | 0.0 | 0.0 | 0.0 |
| SEPT | 43.5 | 83.5 | 6.7 | 36.9 | 0.0 | 0.0 | 0.0 |
| OCT | 76.5 | 48.3 | 8.9 | 34.3 | 0.0 | 0.0 | 0.0 |
| NOV | 87.0 | 30.7 | 9.5 | 22.8 | 4.0 | 17.6 | 21.6 |
| DEC | 89.5 | 27.8 | 12.9 | 19.5 | 9.8 | 57.5 | 67.5 |
| TOTAL | 1019.5 | 778.4 | 542.4 | 465.8 | 51.1 | 499.2 | 550.3 |
| 1991 | | | | | | | |
| JAN | 136.5 | 27.4 | 90.1 | 17.8 | 13.4 | 110.2 | 123.6 |
| FEB | 69.5 | 24.0 | 41.1 | 10.5 | 10.1 | 48.6 | 58.7 |
| MARCH | 136.0 | 45.4 | 129.8 | 37.7 | 11.8 | 104.0 | 115.8 |
| APRIL | 67.0 | 68.4 | 38.6 | 53.3 | 4.0 | 0.0 | 4.0 |
| MAY | 3.5 | 96.8 | 19.8 | 79.2 | 1.0 | 0.0 | 1.0 |
| JUNE | 150.0 | 82.8 | 17.1 | 64.9 | 1.0 | 0.0 | 1.0 |
| JULY | 88.0 | 94.4 | 24.6 | 88.6 | 7.1 | 16.7 | 23.8 |

The yearly estimate of evapotranspiration , 465.8 mm, is similar to, but slightly greater than, other values reported in the literature. Roberts and Roberts (1992), in their study at Grendon Underwood reported a 22-year mean annual estimate of 422 mm (363-460 mm). McGowan and Williams (1980), in their study at Kingston Brook, Nottinghamshire reported values of 435 and 390 mm for May 1969 to April 1970 and April 1970 to March 1971, respectively. Finally, Kristensen (1974), in his study in Denmark, reported annual evapotranspiration totals in the range 358 to 409 mm (mean 394 mm). The enhanced value at Slapton presumably reflects better growing conditions in 1990, and the fact that potential evaporation was exceptionally high. This was caused by windspeeds and net radiation that are higher than those experienced at inland sites.

## 5.2 ARABLE SITE

Six neutron access tubes were also installed in the arable field during September 1989. At the time of installation the land was fallow, having been prepared for the sowing of winter barley. The depth of installation varied between 60 and 130 cm below ground level.

As with the grassland site, 80 cm below ground level has been adopted as the depth to which soil moisture changes, and hence actual evapotranspiration, have been calculated. This being the case, the data from one site (Tube no. 1) have not been used. Again, for the sake of consistency with the grassland site, the water contents measured to 80 cm depth on the 7.3.90 have been adopted as the field capacity values.

*Table 5.2.1 Field capacity values for the arable site*

| TUBE | 2 | 3 | 4 | 5 | 6 | MEAN |
|---|---|---|---|---|---|---|
| | 169.6 | 199.0 | 198.7 | 182.7 | 231.2 | 196.2 |

Obtaining relationships between the ratio of actual to potential evapotranspiration and soil moisture deficit for an arable crop is more difficult than for grassland because of the different phases of the growth cycle. Doorenbos and Pruit, 1984 identified five typical stages for an arable crop cycle. These are:-

Stage 1 Germination → 10% cover,
2 10% cover → 75% cover,
3 75% cover → start of maturing,
4 Start of maturing → harvesting,
5 Harvesting → Re-germination,

and it is necessary to consider each stage separately, as their evapotranspiration losses may differ appreciably. For the arable field at Slapton, winter barley was grown in the year 1989/90, whilst the field was sown to temporary grass in the autumn 1990. Table 5.2.2 shows the different stages of the crop cycle within the arable field. The duration of each stage has been ascertained following discussions with the farmer.

*Table 5.2.2* *Growing cycle of the winter barley and temporary grass at Slapton*

| | | | |
|---|---|---|---|
| Stage | 1 | Bare Earth | 13.9.89 → 1.11.89 |
| | 2 | Germination → 10% cover | 1.11.89 → 28.2.90 |
| | 3 | 10% → 75% cover (70 cm high) | 1.3.90 → 11.5.90 |
| | 4 | 75% cover → start of maturing | 11.5.90 → 30.6.90 |
| | 5 | Start of maturing → harvest | 1.7.90 → 20.7.90 |
| | 6 | Stubble | 20.7.90 → 10.9.90 |
| | 7 | Bare Earth | 10.9.90 → 30.9.90 |
| | 8 | Germination → 10% cover | 1.10.90 → 28.2.91 |
| | 9 | 10% cover → 75% cover (23 cm high) | 1.3.91 → 8.5.91 |
| | 10 | Established sward | 9.5.91 → 31.7.91 |

*Table 5.2.3* *Processes and Factors likely to be significant during the various stages of the Arable Crop Cycle*

| Stage | Drainage | B.S. Evap. | Crop Trans. | Interception | Low Temps. | SMD |
|---|---|---|---|---|---|---|
| 1 | Y | Y | | | | |
| 2 | Y | Y | Y | | Y | |
| 3 | Y | Y | Y | Y | Y | Y |
| 4 | | Y | Y | Y | | Y |
| 5 | | | Y | Y | | Y |
| 6, 7 | | Y | | | | Y |
| 8 | Y | Y | Y | | Y | Y |
| 9 | Y | Y | Y | | Y | |
| 10 | Y | | Y | | | Y |

It is appreciated that some of these stages merge into one another. Also, in terms of evapotranspiration losses, some of the stages may be considered as similar and combined.

A number of different processes are likely to be occurring during the individual stages of the arable crop cycle (Table 5.2.3). These include drainage from the soil profile, bare soil evaporation, crop transpiration, and crop interception. Bare soil evaporation and crop transpiration will occur simultaneously during the growing phases (less than 100% cover) of the crop. Bare soil evaporation will be limited by the amount of water in the profile; crop transpiration will be limited by soil moisture and temperature. These parameters will vary significantly during the cycle.

To illustrate this point, Figure 5.2.1 shows how the percentage crop cover and the soil

Fig. 5.2.1 Percentage Crop Cover and Soil Moisture Deficit (mm) during the various stages of the Arable Crop Cycle

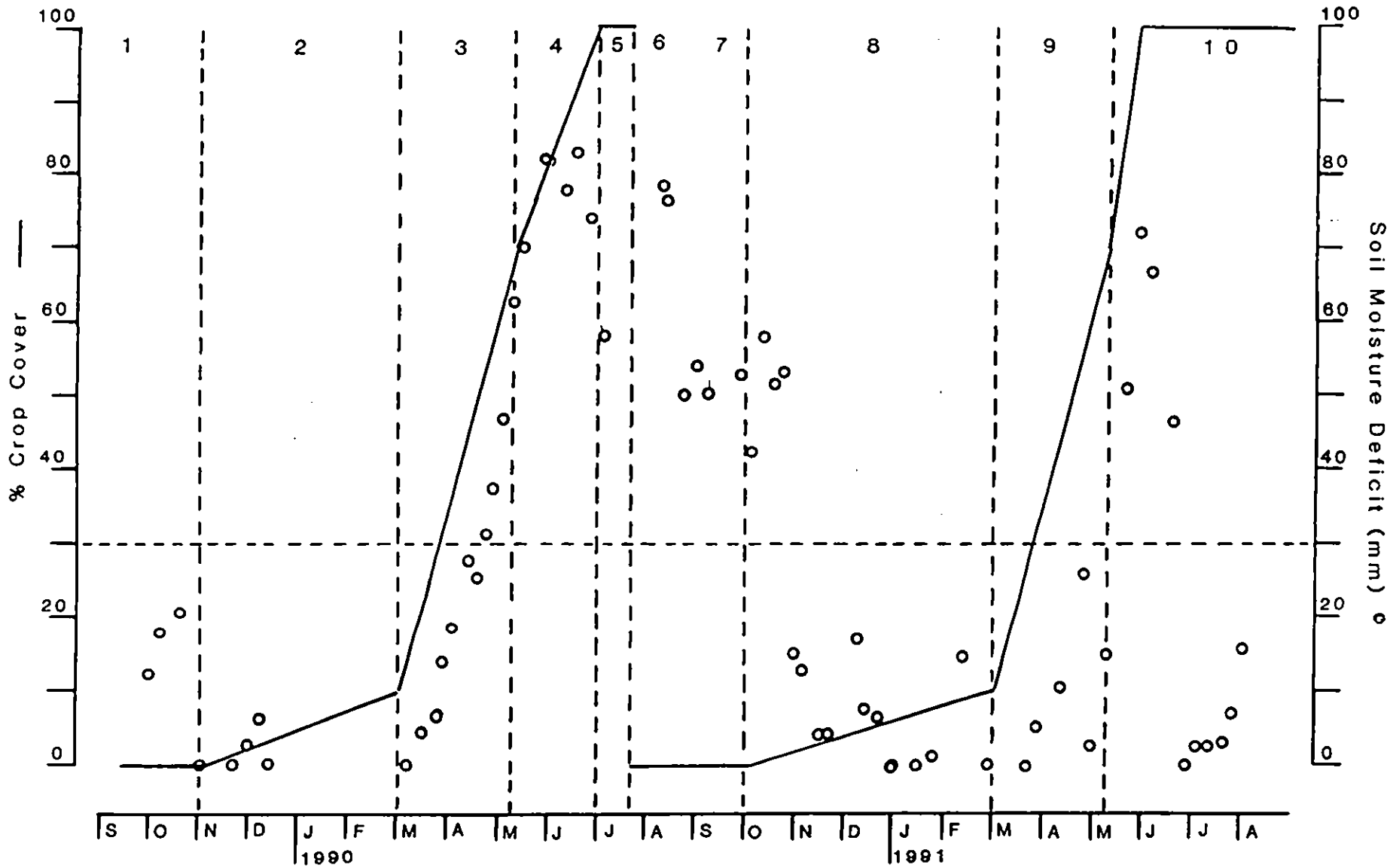

moisture deficit, as given by the neutron probe readings, varied over the measurement period. The vertical dashed lines show the duration of each stage, with the stage no. (Table 5.2.2) denoted. The horizontal dashed line is a 'first guess' estimate of soil moisture deficit (30 mm) below which profile drainage occurs, and above which evaporative losses will be limited by the amount of soil moisture. Assuming that this soil moisture 'cut off' point is sensible, Table 5.2.3 indicates what processes are likely to be significant during each stage. This shows the problems involved in obtaining estimates of the rates of soil moisture losses by the various processes.

The approach adopted was to start with the 'simpler' stages i.e. those in which only a small number of processes were likely to occur, and to derive estimates of the rates of losses as a result of these processes. These rates of losses are assumed to be similar when considering the more complicated stages. In this way, it is hoped to obtain estimates of all the processes during each stage, though it is recognised that a number of assumptions are involved, some of which are rather tenuous.

Inspection of Table 5.2.3 shows that stages 1, 6 and 7 are the simplest. These relate to those periods when no crop was actually growing, and it is with these stages that the analysis begins.

(i) Bare earth and stubble

These two stages in the crop cycle represent those periods when crop transpiration losses are zero and only evaporation from the surface layers of the soil need be considered. It could be argued that there is a difference between the two stages, in the sense that, strictly speaking, the barley stubble will intercept some of the rainfall and lose it subsequently by evaporation without it entering the soil store. However, since this process is considered insignificant for grassland, it is unlikely to be significant for barley stubble, a less dense vegetation cover than grass.

Two situations need be considered; one in which zero or little rain fell in the period considered, and the other in which significant rainfall occurred. Past experience suggests that evaporation from bare earth during periods of rainfall are much greater than for dry periods (Doorenbos and Pruit, 1984).

Table 5.2.4 gives the ratio of actual/potential evaporation to soil moisture deficit for zero or low rainfall periods during the bare earth and stubble stages of the winter barley growth cycle. Of the five periods, four have low actual/potential evaporation ratios whilst the other, the first considered, has substantially higher ratios. These high ratios are consistent. In two cases, tubes 4 and 6, the data suggest that the profiles were still draining at significant rates. This period was the first from which soil moisture data were collected following ploughing a few weeks previously. It is possible that the soil profile had not yet settled following the ploughing, and the evaporation rate was greater than would have been under a consolidated soil. In addition, the soil moisture deficit (15.9 mm) was such that some drainage would have been expected, judging by what was found under the grass field. This also applies, to a lesser extent, to the other two periods in 1989. Unfortunately, the data from these two periods are required to give some estimate of the change in bare soil evaporation with soil moisture deficit. This being the case, it has been assumed that drainage from the soil profile is negligible at a soil moisture deficit of 20 mm, and that the changes in soil moisture for the last four periods in Table 5.2.4 are due solely to evaporation losses. This will be discussed later.

Mean values of the ratio of actual to potential evaporation are plotted against soil moisture deficit in Fig. 5.2.2. Although only four points are available, the data do suggest an inverse linear relationship, and the regression obtained by least squares is used to calculate actual evaporation from bare soil/stubble during no rainfall periods. However, it is possible that other inverse relationships e.g. exponential, would be more appropriate outside the range of soil moisture deficit experienced.

Calculating evaporation losses from bare soil during rainfall periods is rather more difficult. To do this, simple models were applied on a daily basis to the bare earth/ stubble period for the 1990/91 growing cycle. The reason why only the 1990/91 bare earth period was considered was as a result of the soil moisture deficits prevalent during the two years. In contrast to the bare earth period of 1989/90, the deficits in 1990/91 were sufficiently high that it was highly unlikely that any profile drainage was occurring (stages 6 and 7 in Fig. 5.2.1). This means that, during this period, only bare earth evaporation is significant. Knowing the relationship between bare earth evaporation and soil moisture deficit during non-rainy days, then evaporation losses during rainy days could be optimised by comparing estimated and measured soil moisture deficits at the beginning and end of each period. Evaporation during no rainfall days was given by the relationship in Fig. 5.2.2. For rainy days, the best formulation tested was the assumption that any rainfall during the day would be lost as evaporation up to the rate of Penman open water evaporation (given as 1.17 ETp from the annual totals from Slapton for 1990) for that particular day. If the rainfall total for the day was less than open water evaporation, it was further assumed that evaporation from the soil profile, given by Fig. 5.2.2, also occurred. Any excess rainfall over open water evaporation would act to reduce the soil moisture deficit within the soil profile, or, if of sufficient intensity, would run off the soil surface.

Having obtained estimates of evaporation losses from bare earth during rainy and non-rainy periods, it is now possible to estimate drainage losses. This can only be done using data for the 1989/90 season because, for the 1990/91 season, the soil moisture deficit was approximately 50 mm when the grass seed was sown, and did not reduce to levels at which drainage would be significant until mid-November, at which time the grass sward was well established and transpiration losses would be significant. In contrast, the winter barley was sown approximately a month later than the temporary grass, at which time the deficit had fallen to 12 mm and drainage likely to be significant. Unfortunately, this restriction reduces the number of suitable periods to three; these are given in Table 5.2.5.

A straight line regression was fitted to these points and the following relationship obtained:-

$$\text{DRAINAGE} = -0.05\ \text{SMD} + 1.015$$

This gave a surprisingly good fit considering the assumptions involved. In particular, it is gratifying to note that drainage becomes insignificant at about 20 mm; this being the basic assumption used for calculating evaporation losses from bare soil.

In brief, the steps employed for calculating soil moisture losses during the bare soil/stubble periods were as follows:-

(i) Calculate the drainage from the soil profile as

$$\text{DRAINAGE} = -0.05\ \text{SMD} + 1.015$$

*Table 5.2.4* *Actual/Potential Evaporation (ETa/ETp) and Soil Moisture Deficit (mm) for the bare soil and stubble*

| Period | | Tube 2 | Tube 3 | Tube 4 | Tube 5 | Tube 6 | Mean |
|---|---|---|---|---|---|---|---|
| 29.09-05.10.89 | ETa/ETp | 0.83 | 0.87 | 1.00 | | 1.00 | |
| | SMD | 12.9 | 15.2 | 17.8 | | 17.5 | |
| 05.10-10.10.89 | ETa/ETp | 0.07 | 0.13 | 0.20 | 0.33 | 0.09 | 0.16 |
| | SMD | 15.0 | 17.8 | 22.9 | 12.4 | 28.9 | 19.4 |
| 10.10-19.10.89 | ETa/ETp | 0.10 | 0.23 | 0.24 | | 0.19 | 0.19 |
| | SMD | 15.0 | 18.9 | 24.4 | | 21.7 | 20.0 |
| 01.08-08.08.90 | ETa/ETp | 0.09 | 0.09 | | | | 0.09 |
| | SMD | 52.3 | 61.8 | | | | 57.1 |
| 08.08-13.08.90 | ETa/ETp | 0.06 | 0.03 | | 0.07 | 0.06 | 0.06 |
| | SMD | 54.5 | 63.6 | | 68.1 | 107.8 | 73.5 |

*Table 5.2.5* *Periods used for estimating drainage losses from bare soil*

| Period | Drainage rate (mm/day) | Deficit (mm) |
|---|---|---|
| 29.9 - 10.10.89 | 0.24 | 16.4 |
| 10.10 - 19.10.89 | 0.01 | 19.4 |
| 15.11 - 21.11.89 | 1.02 | 0.0 |

(ii) Calculate the actual evaporation,

(a) For non-rainy days:-

$$ETa = ETp\ (-0.0022\ SMD + 0.219)$$

(b) For rainy days (daily rainfall = P):-

$$ETa = ETp * 1.17 \text{ (open water evaporation)}$$

If $P < ETa$, $ETa = P + ETp\ (-0.0022\ SMD + 0.219)$ up to a limit of $ETp * 1.17$

When these formulations were applied to the appropriate periods, allowing for rapid runoff when the soil moisture deficit became negative, the agreement between measured and estimated soil moisture deficit was acceptable, generally within $\pm 5$ mm.

(ii) Established Temporary Grass Sward

This stage in the arable crop cycle (stage 10 in Fig. 5.2.1 and Table 5.2.3) is the next considered as it involves the least unknowns. Of three significant factors (Table 5.2.3), the rate of change of drainage with soil moisture deficit has already been estimated, and it only remains to consider changes in grass transpiration with deficit. Bare soil evaporation is not likely to be significant because, using a degree day value of 303°C from March 1st 1991, as

Fig. 5.2.2 Ratio of Actual to Potential Evaporation vs. Soil Moisture Defict (mm) for bare earth/stubble during low rainfall periods

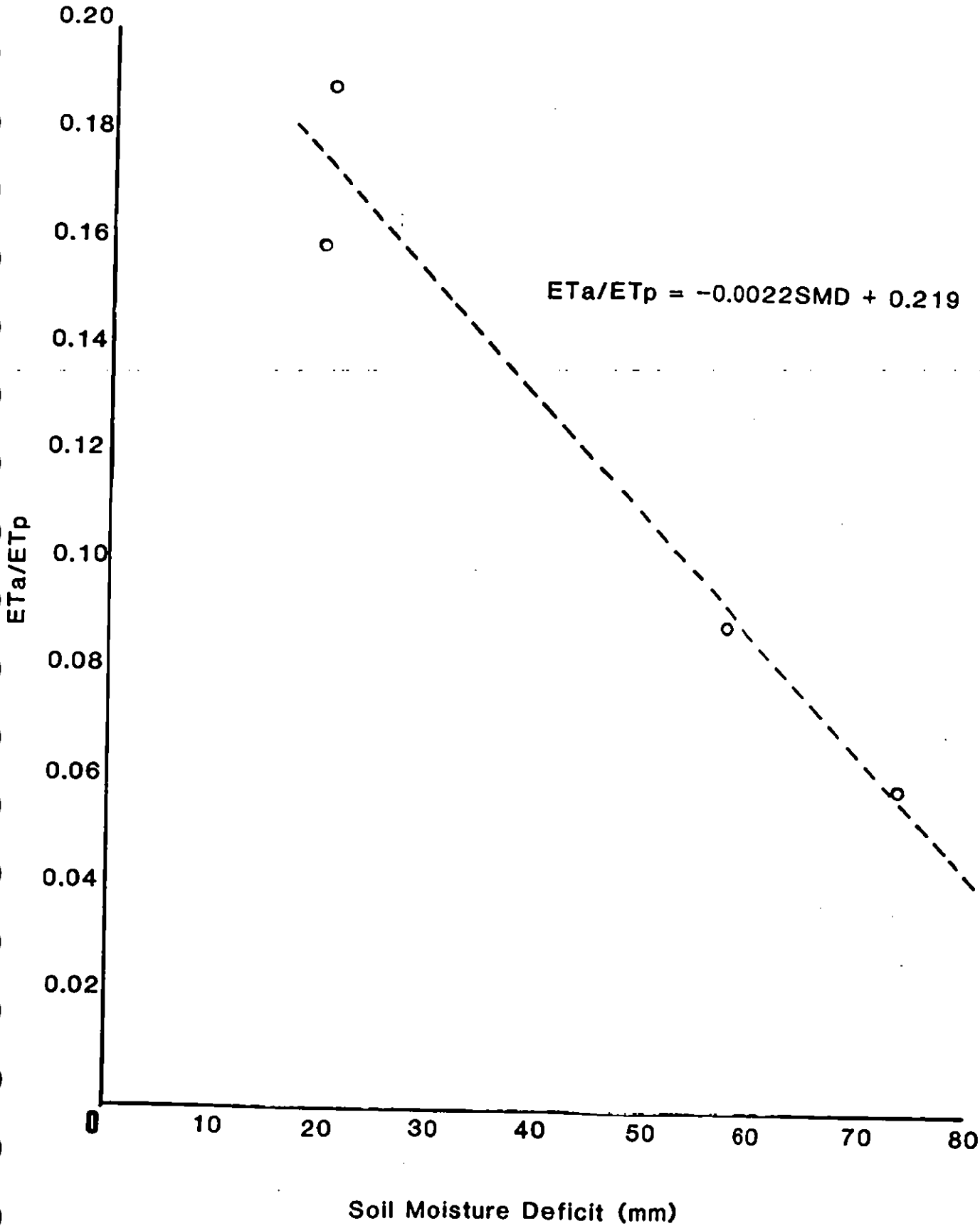

suggested by Olesen (1992), the maximum leaf area index would have been achieved on the 10th April, using mean daily air temperatures recorded by the automatic weather station. Although this degree day value was derived for a 'normal' year in Denmark, the adoption of alternative values would not significantly change the date at which a low value of leaf area index would restrict transpiration. In brief, an analysis of the data obtained during this stage will provide information on transpiration losses from a complete grass canopy cover. These losses should, in theory, be similar to those obtained for the grass field (Section 5.1) under similar conditions.

A total of six periods were suitable from which soil moisture data were available for calculating actual transpiration losses for this stage. The ratio of actual (corrected for drainage losses) to potential transpiration and soil moisture deficit for each neutron access site for each of the periods is shown in Table 5.2.6. Losses from the individual sites vary significantly, more so than for the grass field (Table 5.1.2) suggesting that the grass cover may not have been completely uniform. Also shown in Table 5.2.6 are average values for each of the periods. Surprisingly, the ratios of actual/potential transpiration are remarkably consistent, considering that the soil moisture deficit varies between 9.6 mm and 61.6 mm. Certainly there is no sign of the ratio decreasing with increasing deficit as is the case of the grass field in 1990 (Fig. 5.1.1). Also, the mean values of the ratio of actual/potential transpiration do not approach unity, even at a deficit of 9.6 mm. It seems that some factor is restricting transpiration other than soil moisture.

In order to attempt to explain these values, Fig. 5.2.3 shows a plot of average actual/ potential transpiration ratios against soil moisture deficit for the temporary grass and the permanent grass for the periods shown in Table 5.2.6. Also shown is the regression obtained for the 1990 data over the soil moisture deficit range from the permanent grass field. This plot shows that, if the 1991 data for the two grass fields are taken together, there is a trend of a decrease in ETa/ETp with an increase in soil moisture deficit, admittedly with a great deal of scatter. More importantly perhaps, the data shown in Fig. 5.2.3 indicate that, with one exception, ETa/ETp values for 1991 are consistently lower for an equivalent soil moisture deficit, than for 1990. There are a number of possible reasons for this.

One obvious possibility was the occurrence of low temperatures during the periods selected for 1991, as was the case for 1990 (Section 5.1). Fig. 5.2.4 shows soil temperatures at 20 cm depth measured at 0900 GMT at the Field Centre at Slapton. Although the Field Centre is some 3 km away from the catchment, the soil temperatures shown were felt to be sufficiently representative to demonstrate the temperature differences between the two years. The horizontal dashed line is at 6°C, the soil temperature below which it is generally considered that growth is restricted. The vertical dashed lines for 1990/91 show approximately the limits of the period from which the data values shown in Fig. 5.2.3 were obtained. An inspection of the soil temperatures within these two vertical lines show that they were well above 6°C, this suggests that the temperatures experienced during these periods were not restricting growth to any appreciable extent.

Another possibility is antecedent conditions. Whereas soil temperatures in the winter 1989/90 rarely dropped below 6°C (top graph in Fig. 5.2.4), there were many instances of low temperatures in the winter 1990/91 (bottom graph in Fig. 5.2.4). In particular, there was a very cold spell in February 1991 with soil temperatures as low as 1°C. It is possible that such a cold spell may have had a 'knock-on' effect on growth in the spring. The pattern of soil moisture deficit also differed, for the grass field at least, for the two winters. Whilst field capacity extended from the beginning of November 1989 to the end of February 1990, there

was a lag of approximately one month in the following winter, with field capacity being attained from the beginning of December 1990 to the beginning of April 1991 (Fig. 5.1.2). Again, the delay of the onset of a deficit in the spring may have had some effect on crop growth.

*Table 5.2.6* *Ratio of actual/potential transpiration and soil moisture deficit for the established temporary grass sward*

| Period | | Tube 2 | Tube 3 | Tube 4 | Tube 5 | Tube 6 | Mean |
|---|---|---|---|---|---|---|---|
| 17.04-24.04.91 | ETa/ETp | 0.83 | | 0.92 | 0.59 | | 0.78 |
| | SMD | 17.3 | | 23.6 | 13.7 | | 18.2 |
| 01.05-08.05.91 | ETa/ETp | 0.69 | | | 0.68 | 0.79 | 0.72 |
| | SMD | 11.4 | | | 8.4 | 9.1 | 9.6 |
| 08.05-15.05.91 | ETa/ETp | 0.59 | | - | 0.57 | 0.95 | 0.70 |
| | SMD | 24.5 | | | 21.2 | 27.0 | 24.2 |
| 15.05-22.05.91 | ETa/ETp | 0.48 | | 0.75 | 0.74 | 0.93 | 0.73 |
| | SMD | 36.1 | | 53.1 | 35.6 | 47.5 | 43.1 |
| 22.05-29.05.91 | ETa/ETp | 0.47 | | 0.67 | 1.08 | 1.02 | 0.81 |
| | SMD | 47.5 | | 70.1 | 57.8 | 71.1 | 61.6 |
| 24.07-30.07.91 | ETa/ETp | 0.24 | | 0.69 | 0.69 | 0.48 | 0.53 |
| | SMD | 14.0 | | 14.5 | 14.5 | 10.8 | 11.3 |

Possibly a more realistic explanation of the differing transpiration rates during the two years, involves the effects of cutting the grass for silage. This practice has the result in severely reducing the leaf area index, and thus the transpiration rate, though, after a suitable lag, replacing mainly dying vegetation with young vigorous growth. Generally speaking, it can be assumed that transpiration will be restricted prior to and following cutting.

The permanent grass field was cut for silage on the 14th June 1990 and again between the 29th May and the 5th June 1991. The temporary grass field was cut between the 22nd and the 29th May 1991. For 1990, when obtaining the ETa/ETp against SMD relationship, data from only one period, 13th to the 19th June, would have been affected. For 1991, it is possible that a number of the periods shown in Table 5.2.6 and in Fig. 5.2.3 may have experienced reduced transpiration as a result of pre-harvesting senescence. This hypothesis is supported by overestimation of transpiration, manifest as overestimated soil moisture deficits for the permanent grass crop in late May and early June 1990 (Fig. 5.1.2).

Whatever the reason for the discrepancies shown in Fig. 5.2.3, it would seem that transpiration losses from this stage of the arable crop cycle are not controlled primarily by soil moisture deficit, and a mean value of ETa/ETp = 0.71 has been used, this given as the mean value for the six periods shown in Table 5.2.6.

In brief, the steps employed for calculating soil moisture losses for the established temporary grass sward stage were as follows:-

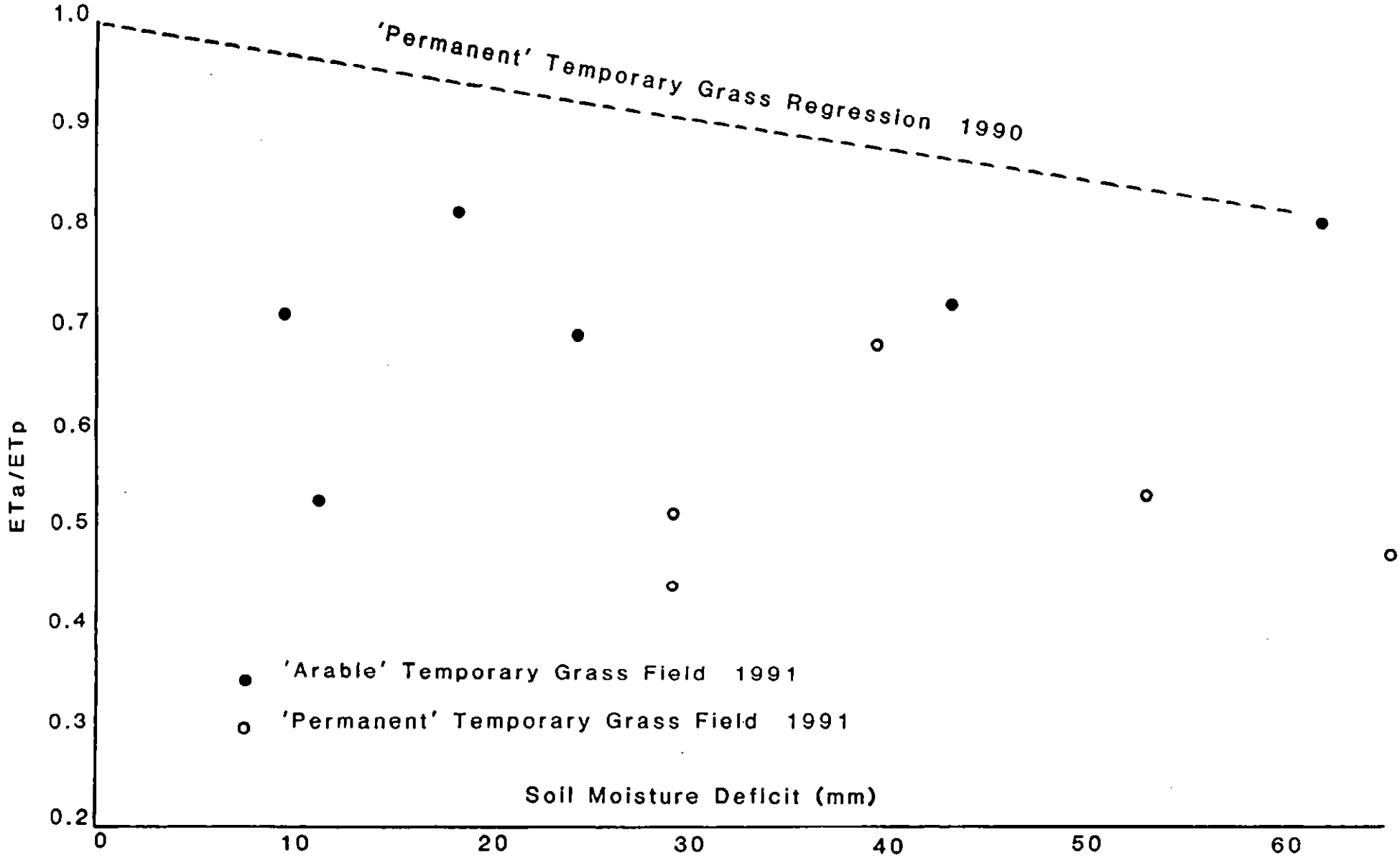


Fig. 5.2.3 Actual/Potential Transpiration against Soil Moisture Deficit for the 'arable' grass field and the 'permanent' grass field

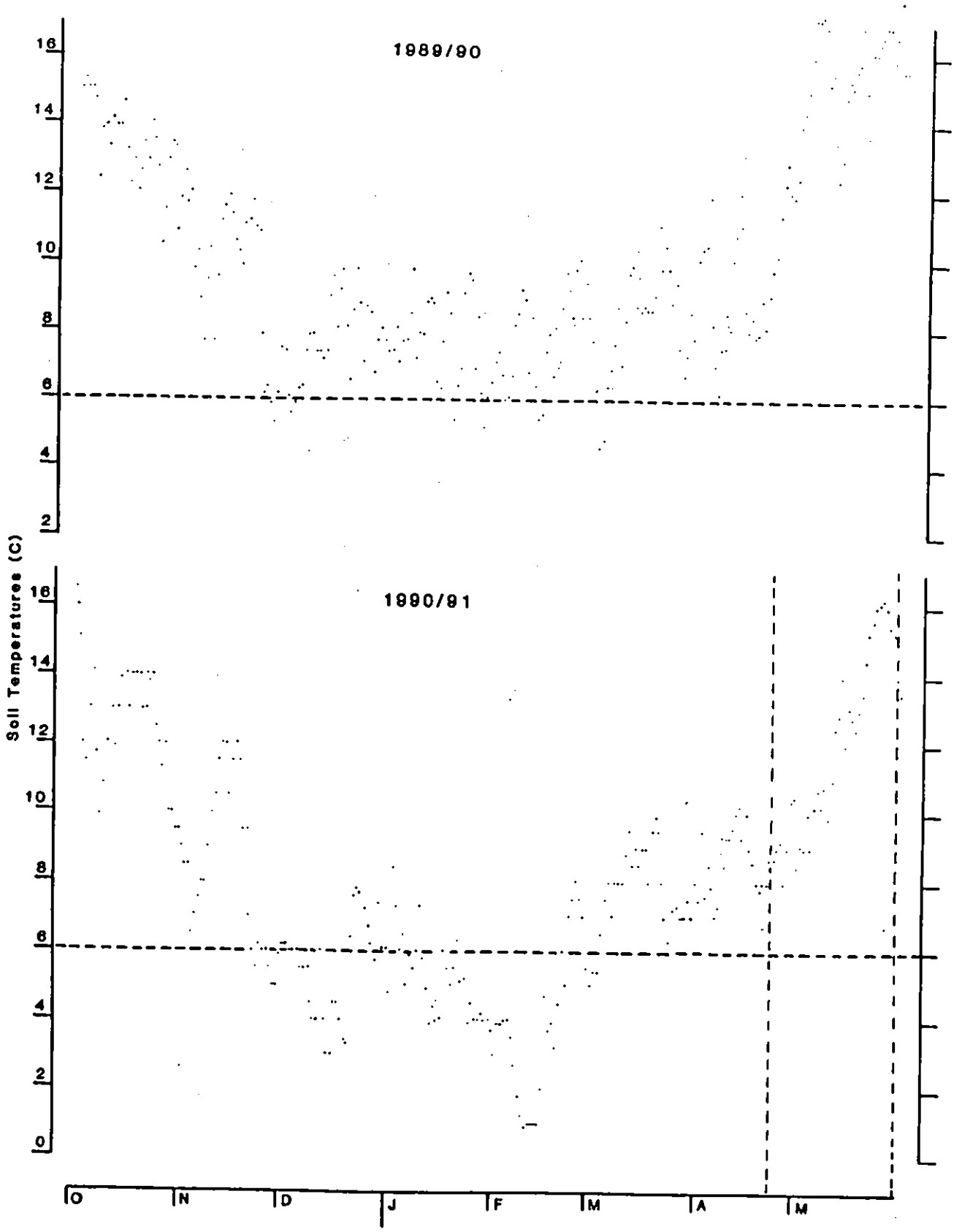


Fig. 5.2.4 Soil Temperatures at 20cm depth from the Field Centre at Slapton

(a) Calculate the drainage from the profile as:-

$$DRAINAGE = 0.05\ SMD + 1.015$$

(b) Calculate the actual transpiration as:-

$$ETa = 0.71\ ETp$$

(iii) Developing Temporary Grass Sward

Two stages (8 and 9) of the arable crop cycle are involved. Stage 8 covers the period between seedling emergence at the beginning of October to 10% crop cover at the end of February; whilst stage 9 is the next stage along and covers rapid growth to 70% crop cover during the month of May. Estimates of all significant processes have been made in the previous two sections; the difficulty in this part of the arable crop cycle is determining how much of the total evaporative loss is as a result of crop transpiration and how much is bare soil evaporation. This partitioning depends very much on the stage of growth of the grass for the periods considered.

In theory, this is given by the values quoted in Table 5.2.2 ie 0% crop cover at the beginning of October, 10% at the end of February, and 70% in the middle of May. However, when these percentages were applied, and estimated soil moisture deficits compared with those measured, it was found that evapotranspiration losses were significantly underestimated. The best fit was obtained by assuming that total evaporative losses could be partitioned into grass transpiration and bare soil evaporation as follows:-

| | | |
|---|---|---|
| Stage 8, germination → 10% crop cover:- | | 50% bare soil<br>50% grass |
| Stage 9, 10% → 70% crop cover:- | Bare soil | 50% → 0 |
| | Grass | 50% → 100% |

and these were the percentages adopted. Drainage and bare soil evaporation were as calculated for stages 1,6 and 7, grass transpiration was as calculated for stage 10, modified for low temperatures as indicated in Section 5.1.

(iv) The Winter Barley crop

Estimating actual evapotranspiration losses from the winter sown barley is difficult because of the other various processes that are likely to be occurring simultaneously. Because of this, the growth cycle has not been split into its various stages; instead assumptions have been made regarding these processes. The significance of these various processes - drainage, bare soil evaporation, crop transpiration, and interception by the crop, will vary according to the stage of the crop cycle. Drainage rates and bare soil evaporation have already been estimated; for the latter an estimate of percentage crop cover is required. Knowing all of these factors, it will then be possible to calculate crop transpiration losses and relate them to soil moisture deficit.

Percentage crop cover and rainfall interception losses by the crop canopy over the growth cycle of the winter barley are shown in Fig. 5.2.5. The former is as given in Table 5.2.2, based on local observations, whilst the latter is similar to the pattern used by Roberts and

Fig. 5.2.5 Percentage Crop Cover and Rainfall Interception for the Winter Barley Crop

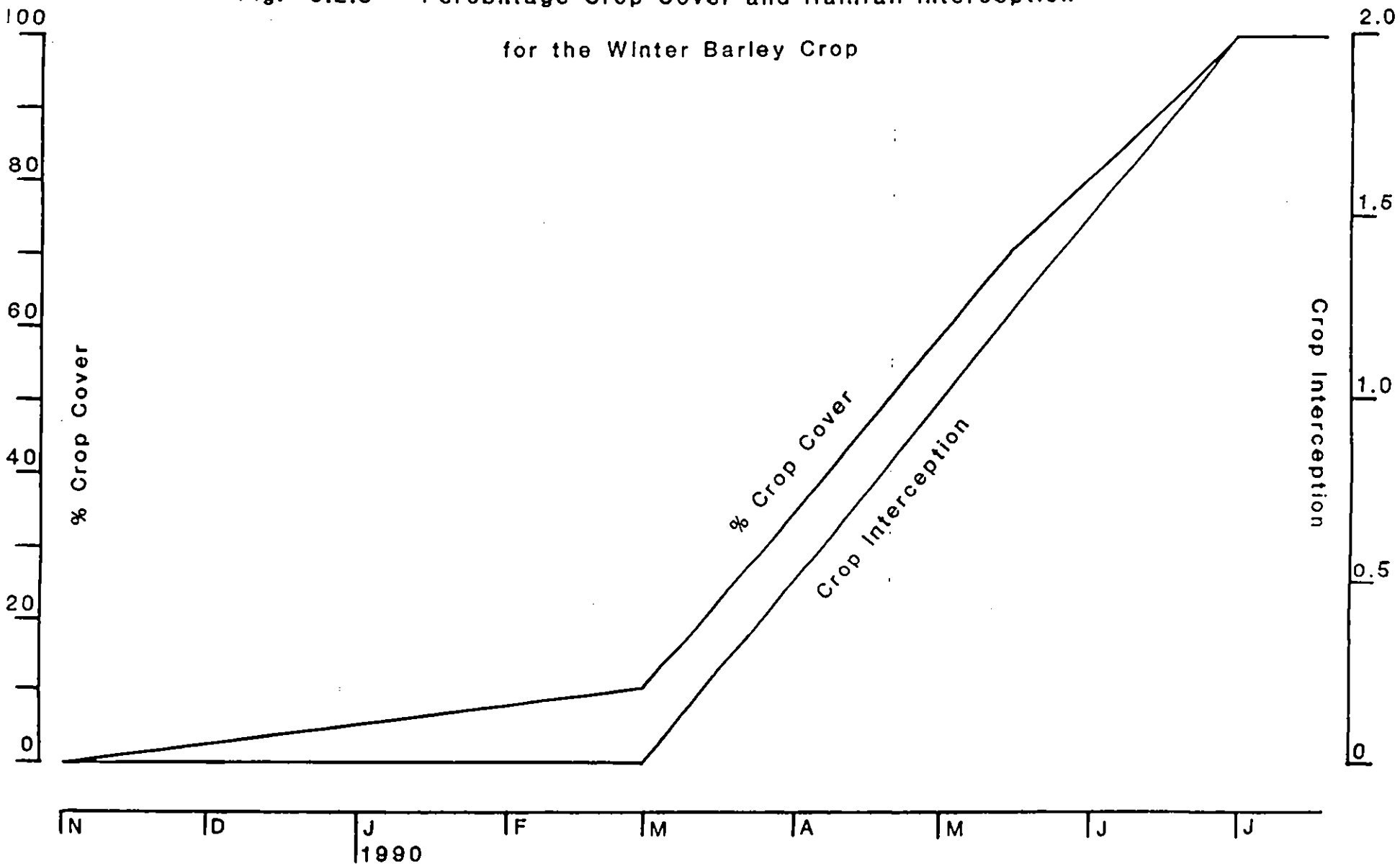

Roberts, 1992 based on observations made at Long Ashton Agricultural Research Center (LARC, 1982). Using these patterns, together with the previously estimated drainage and bare soil evaporation values, crop transpiration estimates have been made for seven low rainfall periods. These are shown in Table 5.2.7; also a plot of crop transpiration given as a fraction of the Penman potential evaporation against the average soil moisture deficit for each period is given in Fig. 5.2.6. The data show a great deal of scatter with, in particular high values of ETa/ETp during 25.4-28.4.90, and low values during 16.5-23.5.90. One possible reason for the latter is the emergence of the barley seed head, as unpublished previous work has suggested that, during this period, transpiration rates are low. This may have also contributed to the low values found for the permanent and temporary grain fields in May 1991. Unfortunately, insufficient data were available for this period to test this hypothesis further, and it was assumed that ETa/ETp for the barley crop declined linearly with SMD as shown in Fig. 5.2.6. A least squares regression of the points shown in Fig. 5.2.6 gave the following relationship:-

$$ETa/ETp = 1.10 - 0.0066\,SMD$$

and this is the relationship that has been used for calculating transpiration for the barley crop throughout the cycle.

This formulation and the others described previously was applied on a daily basis. The resulting soil moisture deficits were compared with measured values and, in general, the agreement was good, usually within $\pm 10$ mm.

Complete arable crop cycle

The formulations obtained for the various stages of the arable crop cycle were applied on a daily basis for the period 1.10.89 to 31.7.91. The initial soil moisture deficit at the beginning was set at 12.1 mm, as given by neutron probe measurements on 29.9.89. Also, it was found necessary to 'reset' the soil moisture deficit between two of the stages (7 and 8) shown in Fig. 5.2.1. This particular period coincided with the time that the field was ploughed, and it was found that, not surprisingly, the measured soil moisture deficit was much greater than that estimated. Apart from this, the estimated soil moisture deficit was passed over from one stage to the next. The resulting estimated daily soil moisture deficits, together with the less frequent values measured by neutron probe are shown in Fig. 5.2.7.

In general, the agreement between the measured and estimated soil moisture deficits is very good, normally within $\pm 10$ mm. The effect of 're-setting' the soil moisture deficit is seen as a discontinuity of approximately 11 mm in the middle of September. The reason for this is almost certainly as a result of enhanced bare soil evaporation following the burning of stubble and ploughing during the early part of September. This particular period was not used during the calibration.

Measured and estimated monthly totals of hydrological variables for the arable field are given in Table 5.2.8. For 1990, it was found that actual evaporation losses were 404.4 mm; comprised of 51.8 mm interception (12.8%), 155.2 mm bare soil evaporation (38.4%), and 197.9 mm crop transpiration (48.9%). These total losses were 61.4 mm less than those under grassland (Table 5.1.4). These reduced evaporation losses were compensated by increased drainage losses (116.4 mm) from the arable field and 51.1 mm from the grass field. Rapid flow losses were similar to those from the grass field.

*Table 5.2.7 Periods used for estimating transpiration losses from the winter barley at Slapton*

| Period | 23.3-28.3.90 | 4.4-11.4.90 | 25.4-28.4.90 | 28.4-2.5.90 | 10.5-16.5.90 | 16.5-23.5.90 | 13.6-19.6.90 |
|---|---|---|---|---|---|---|---|
| SOIL MOISTURE DEFICIT (mm) | 10.2 | 23.3 | 34.7 | 42.3 | 66.4 | 74.4 | 80.5 |
| RAINFALL (mm) | 0.5 | 0.5 | 0.5 | 0.0 | 2.0 | 2.0 | 7.0 |
| INTERCEPTION RATE (mm/day) | 0.4 | 0.7 | 0.9 | 1.0 | 1.2 | 1.3 | 1.7 |
| TOTAL INTERCEPTION (mm) | 0.4 | 0.5 | 0.5 | 0.0 | 1.2 | 1.8 | 1.7 |
| CHANGE IN SOIL MOISTURE (mm) | -7.3 | -9.3 | -6.0 | -9.2 | -7.6 | -8.4 | -5.5 |
| % CROP COVER | 31 | 41 | 55 | 57 | 69 | 73 | 91 |
| BARE EARTH EVAPORATION (mm) | 1.5 | 2.1 | 0.7 | 0.9 | 0.6 | 0.4 | 0.3 |
| DRAINAGE (mm) | 2.5 | - | - | - | - | - | - |
| CROP TRANSPIRATION (mm) | 10.6 | 17.5 | 9.8 | 14.7 | 11.3 | 11.2 | 11.6 |
| TRANSPIRATION/PENMAN POTENTIAL | 0.97 | 0.82 | 1.14 | 0.88 | 0.65 | 0.46 | 0.63 |

Fig. 5.2.6 Ratio of Crop Transpiration (ETa) to Penman Potential (ETp) against Soil Moisture Deficit for Winter Barley

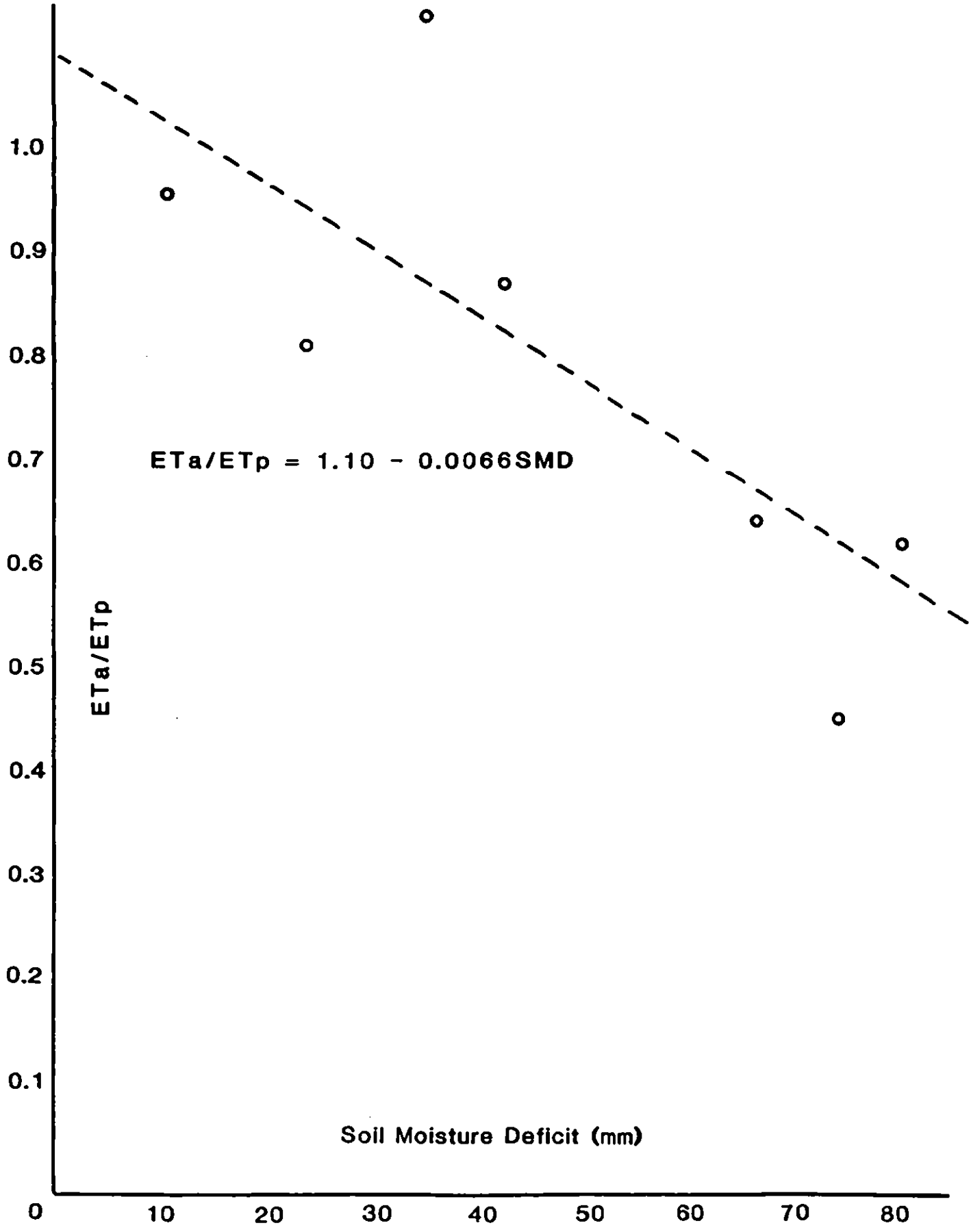

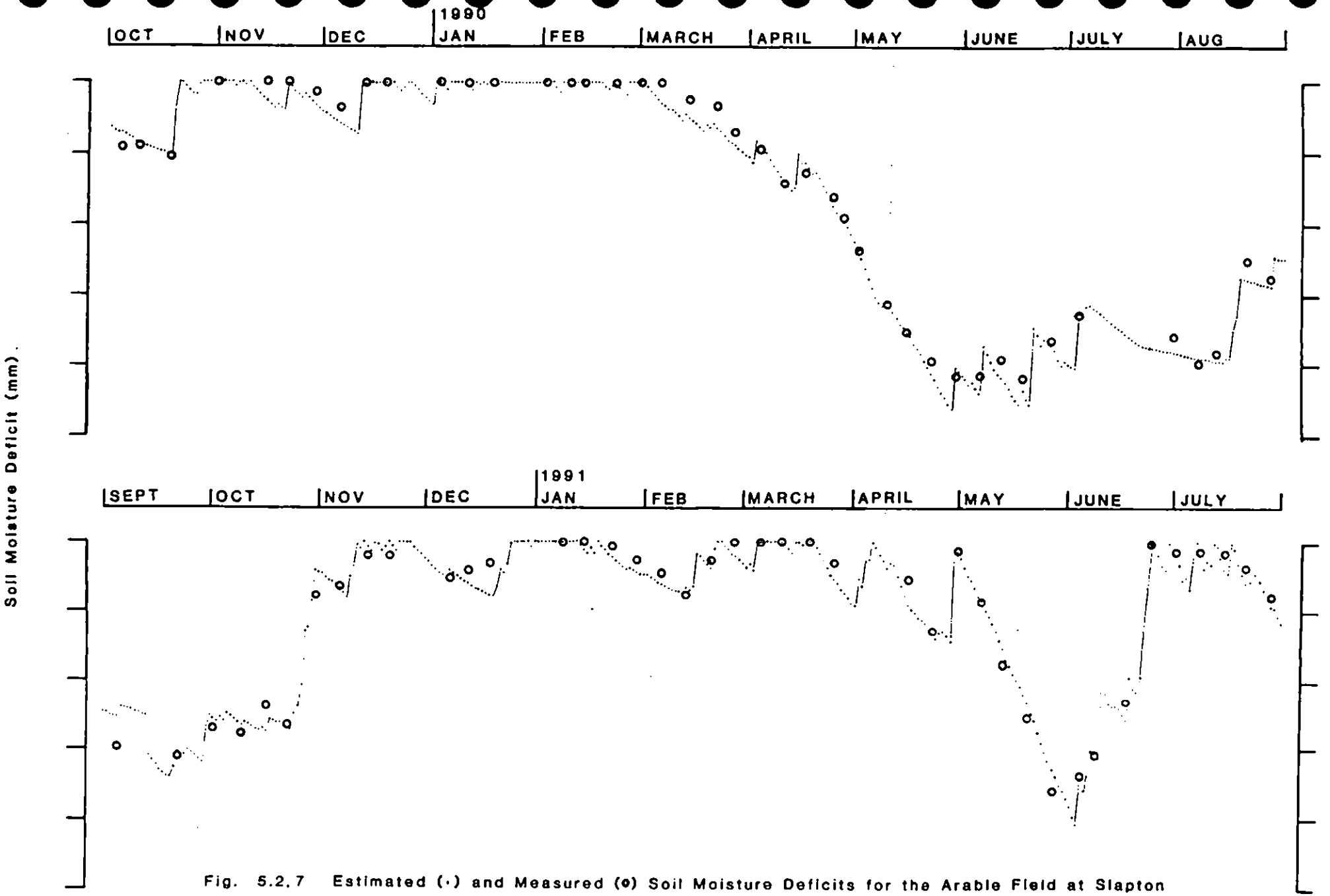


Fig. 5.2.7 Estimated (·) and Measured (o) Soil Moisture Deficits for the Arable Field at Slapton

The annual estimated actual evaporation losses from the arable field (404.4 mm) was 73 mm less than the water use of the whole catchment, given as the difference between the rainfall and runoff totals. However, allowance has to be made for the increased bare soil evaporation following stubble burning and ploughing, referred to earlier. The necessary correction, given by the difference between estimated and measured soil moisture was 10.3 mm; this must be added to the estimated evaporation, resulting in an annual total of 414.7 mm evaporative losses from the arable field.

This value is similar to transpiration losses from barley quoted in the literature. For example Kristensen (1974) estimated losses in the range 378 to 420 mm (average 395 mm), whilst McGowan and Williams (1980) quote estimates of 426 and 371 mm.

*Table 5.2.8* *Measured and estimated monthly totals (mm) of hydrological variables for the arable field at Slapton*

| Month | Measured | | | | Estimated | | |
|---|---|---|---|---|---|---|---|
| | Rainfall | Pot. Evap. | Flow | Act. Evap. | Drainage | Fast flow | Total flow |
| 1989 | | | | | | | |
| OCT | 105.5 | 44.3 | 15.0 | 25.8 | 14.6 | 54.0 | 68.7 |
| NOV | 70.9 | 26.4 | 50.8 | 15.5 | 25.6 | 36.8 | 62.3 |
| DEC | 191.5 | 25.6 | 155.9 | 18.5 | 24.0 | 147.1 | 171.1 |
| 1990 | | | | | | | |
| JAN | 191.0 | 5.6 | 107.3 | 4.3 | 30.5 | 149.7 | 180.4 |
| FEB | 287.5 | 18.9 | 274.5 | 17.4 | 27.3 | 242.3 | 269.6 |
| MARCH | 15.5 | 37.6 | 57.8 | 20.9 | 15.3 | 0.1 | 15.4 |
| APRIL | 36.0 | 87.0 | 21.2 | 59.5 | 0.4 | - | 0.4 |
| MAY | 23.5 | 110.1 | 14.1 | 61.8 | - | - | - |
| JUNE | 78.5 | 85.8 | 11.5 | 74.6 | - | - | - |
| JULY | 38.0 | 133.6 | 10.0 | 35.2 | - | - | - |
| AUG | 53.0 | 109.5 | 8.0 | 26.5 | - | - | - |
| SEPT | 43.5 | 83.5 | 6.7 | 34.3 | - | - | - |
| OCT | 76.5 | 48.3 | 8.9 | 33.6 | 0.8 | - | 0.8 |
| NOV | 87.0 | 30.7 | 9.5 | 19.7 | 23.2 | 40.4 | 63.6 |
| DEC | 89.5 | 27.8 | 12.9 | 16.6 | 18.9 | 49.0 | 67.9 |
| ANNUALS TOTALS | 1019.5 | 778.4 | 542.4 | 404.4 | 116.4 | 481.5 | 597.9 |
| 1991 | | | | | | | |
| JAN | 136.5 | 27.4 | 90.1 | 18.9 | 27.1 | 99.9 | 127.1 |
| FEB | 69.5 | 24.0 | 41.1 | 10.7 | 16.7 | 38.8 | 55.5 |
| MARCH | 136.0 | 45.4 | 129.8 | 26.5 | 24.5 | 95.5 | 120.3 |
| APRIL | 67.0 | 68.4 | 38.6 | 40.1 | 10.1 | 1.9 | 12.0 |
| MAY | 3.5 | 96.8 | 19.8 | 65.6 | 4.2 | - | 4.2 |
| JUNE | 150.0 | 82.8 | 17.1 | 58.3 | 4.7 | 14.8 | 19.5 |
| JULY | 88.0 | 94.4 | 24.6 | 67.1 | 19.2 | 25.6 | 44.8 |

## 5.3 FORESTRY SITE

Six neutron access tubes were installed in the forested area during September 1989. The depth of installation varied between 74 and 170 cm below ground level.

In contrast to the grassland and arable sites, it was found that significant changes in soil moisture occurred throughout the soil profile and it was not realistic to adopt a common depth for computing transpiration losses for the six sites. Field capacity values, given as the total profile water contents on the 7th March 1990, and the depths of installation for the six forestry neutron access tubes are given in Table 5.3.1.

*Table 5.3.1 Field capacity values (mm) and depth of installation (cm) for the forestry site*

| Tube | 1 | 2 | 3 | 4 | 5 | 6 |
|---|---|---|---|---|---|---|
| F.C. | 131.5 | 271.9 | 347.9 | 193.5 | 176.4 | 287.6 |
| Depth | 74 | 120 | 170 | 94 | 100 | 100 |

Three processes need to be considered for the forested area. These are forest transpiration, canopy interception, and drainage. The techniques employed are similar to those described for the arable site.

Table 5.3.2 shows the zero or low rainfall periods used to calculate forest transpiration and drainage for the six neutron access tubes. When calculating transpiration and drainage rates for non-zero rainfall periods, a maximum daily rainfall interception of 0.5 mm has been assumed. Although this introduces some degree of uncertainty into the calculations, any error resulting is likely to be small as the changes in soil moisture are much greater than the rainfall input. In any case, as will be seen later, a canopy interception value of 0.5 mm/day is appropriate for most of the periods considered.

An initial analysis of the data in Table 5.3.2 showed that the ratio of actual to potential transpiration was negatively correlated with both potential evapotranspiration and specific humidity deficit. In the event, it was decided to use a regression based on potential evapotranspiration, as suggested for beech and ash plantations in southern England by Harding *et al.*, (in press).

It was also found that the set of six access tubes could be separated into two groups according to the soil moisture deficits generated in the summer months. This was as a result of difficulties in installing the access tubes due to the presence of rocks, whilst it is likely that the roots of trees would be able to abstract water from deeper down the profile. In general, the shallower tubes (1, 4, and 5) had lower transpiration rates, and hence lower deficits, than the deeper tubes (2, 3, and 6). The difference was so pronounced that the analysis had to be conducted separately on the two sets of tubes. It is likely that both sets of tubes underestimate transpiration by the trees but, in the absence of changes in soil moisture at greater depth, some estimate has to be made using the available data.

For those periods where the ratio of actual to potential transpiration was greater than unity, it has been assumed that transpiration is at potential, and the difference is equal to drainage from the soil profile. Interception by the forest canopy was estimated by carrying out a water balance for all the soil moisture periods and minimizing the differences between the observed and predicted soil moisture totals. An analysis of the rainfall totals in the four period gauges within the catchment (Fig. 2.1) suggested that the rainfall totals in the valley bottom were significantly smaller than those in the interfluve areas. Therefore, the daily rainfall totals from the automatic weather station were reduced (by 13%) to compensate for this whilst computing these interception losses.

***Table 5.3.2*** *Periods used for estimating actual transpiration from the forested area showing precipitation (P), actual/potential daily transpiration (ETa/ETp) and average soil moisture deficit (SMD)*

| Period | P | Tube | 1 | 2 | 3 | 4 | 5 | 6 |
|---|---|---|---|---|---|---|---|---|
| 10.10-18.10.89 | 0.0 | ETa/ETp | | 0.73 | | | 0.61 | |
| | | SMD | | 56.8 | | | 34.2 | |
| 30.11-6.12.89 | 0.0 | ETa/ETp | | | 1.84 | | 0.74 | |
| | | SMD | | | 12.1 | | 10.0 | |
| 1.8-8.8.90 | 0.0 | ETa/ETp | 0.17 | 0.30 | 0.45 | 0.38 | 0.18 | 0.65 |
| | | SMD | 57.5 | 118.3 | 125.0 | 45.2 | 53.7 | 119.0 |
| 8.8-13.8.90 | 0.0 | ETa/ETp | 0.07 | 0.06 | 0.25 | | 0.05 | 0.32 |
| | | SMD | 61.1 | 124.0 | 135.0 | | 57.2 | 133.0 |
| 22.8-29.8.90 | 0.0 | ETa/ETp | 0.12 | 0.48 | 0.37 | 0.13 | 0.27 | 0.14 |
| | | SMD | 59.6 | 120.4 | 126.4 | 43.0 | 52.5 | 131.8 |
| 12.9-17.9.90 | 0.0 | ETa/ETp | | 0.20 | 0.18 | | 0.23 | 0.22 |
| | | SMD | | 122.4 | 146.7 | | 57.6 | 137.1 |
| 17.10-23.10.90 | 0.0 | ETa/ETp | | | | 0.45 | 0.35 | |
| | | SMD | | | | 49.5 | 63.0 | |
| 8.5-15.5.91 | 0.0 | ETa/ETp | 0.33 | 0.37 | 0.83 | 0.35 | 0.40 | 0.33 |
| | | SMD | 4.7 | 26.9 | 25.1 | 10.7 | 16.5 | 23.4 |
| 15.5-22.5.91 | 0.0 | ETa/ETp | 0.24 | 0.45 | 0.27 | 0.27 | 0.63 | 0.29 |
| | | SMD | 11.4 | 38.0 | 37.0 | 17.4 | 25.8 | 29.7 |
| 22.5-29.5.91 | 0.0 | ETa/ETp | 0.27 | 0.42 | 0.48 | 0.30 | 0.28 | 0.40 |
| | | SMD | 18.1 | 50.6 | 46.3 | 24.3 | 34.5 | 37.6 |
| 23.3-28.3.90 | 0.5 | ETa/ETp | 0.25 | 0.47 | 0.97 | 0.23 | 0.44 | 0.37 |
| | | SMD | 6.2 | 16.1 | 9.3 | 4.8 | 12.9 | 14.5 |
| 4.4-11.4.90 | 0.5 | ETa/ETp | 0.26 | 0.15 | 0.17 | 0.07 | 0.30 | 0.25 |
| | | SMD | 9.2 | 23.3 | 21.6 | 8.0 | 19.3 | 24.5 |
| 25.4-2.5.90 | 0.5 | ETa/ETp | 0.33 | 0.43 | 0.31 | 0.31 | 0.21 | 0.14 |
| | | SMD | 17.0 | 38.2 | 33.4 | 12.1 | 26.7 | 30.6 |
| 17.4-24.4.91 | 0.5 | ETa/ETp | | 0.47 | 0.42 | 0.37 | 0.42 | 0.35 |
| | | SMD | | 19.6 | 16.9 | 9.6 | 15.0 | 24.1 |
| 1.3-7.3.90 | 2.0 | ETa/ETp | | 2.90 | 6.92 | 1.21 | 1.88 | 5.06 |
| | | SMD | | -7.0 | -16.6 | -2.9 | -4.5 | -12.2 |
| 16.5-23.5.90 | 2.0 | ETa/ETp | 0.19 | 0.31 | 0.55 | 0.25 | 0.11 | 0.24 |
| | | SMD | 32.0 | 67.5 | 61.3 | 33.3 | 41.6 | 49.5 |
| 31.10-7.11.90 | 3.0 | ETa/ETp | | 1.29 | 1.19 | 0.88 | | |
| | | SMD | | 106.4 | 109.8 | 8.2 | | |
| 23.1-30.1.91 | 2.0 | ETa/ETp | 1.22 | | 3.51 | | 2.04 | 2.55 |
| | | SMD | 0.4 | | 5.3 | | 7.9 | 15.1 |
| 1.5-8.5.91 | 3.0 | ETa/ETp | 0.41 | 0.33 | 0.26 | 0.37 | 0.38 | 0.31 |
| | | SMD | -2.7 | 19.9 | 13.9 | 3.6 | 8.6 | 17.0 |
| 4.9-11.9.91 | 0.5 | ETa/ETp | 0.24 | 0.23 | 0.22 | 0.31 | 0.28 | 0.23 |
| | | SMD | 37.6 | 67.1 | 50.8 | 13.5 | 41.0 | 72.6 |

(i) **Shallow tubes (1, 4, and 5)**

Figure 5.3.1 shows plots of the ratio of actual to potential transpiration against potential, and of drainage against soil moisture deficit. For the former, it was found that the ratio of actual to potential transpiration initially fell sharply against potential before levelling out at higher potentials. Two straight line regressions, crossing at a potential transpiration value of 2.2 mm/day, were used to describe this relationship. The regression coefficients obtained by least squares were:-

$$ETa/ETp = 1.08 - 0.34\ ETp \qquad ETp \leq 2.2 \text{ mm/day}$$

$$ETa/ETp = 0.46 - 0.058\ ETp \qquad ETp > 2.2 \text{ mm/day}$$

There is no real pattern in the plot of drainage against soil moisture deficit though, at positive deficits, the drainage rates were either zero or so low that they could be ignored.

Applying the above transpiration regressions with zero drainage rates to the whole soil moisture data set produced the following daily equivalent canopy capacities (mm) for each month;

| J | F | M | A | M | J | J | A | S | O | N | D |
|---|---|---|---|---|---|---|---|---|---|---|---|
| 0.5 | 0.5 | 0.5 | 2.0 | 2.0 | 3.5 | 3.5 | 3.5 | 2.0 | 1.0 | 0.5 | 0.5 |

A time series plot of measured and daily estimated soil moisture deficit is given in Figure 5.3.2. In general, the agreement is good, normally within 10 mm. The only significant differences occur during November and December 1990. Here, estimated soil moisture deficits are much lower than measured ie. the model predicts that the profile reaches field capacity quicker than it actually does. Most of these differences are due to one particular period, 23.10 → 31.10.90. During this period, 57.3 mm of rainfall was recorded at the met. site, and it is quite possible that much of this may have actually been lost as surface runoff without contributing to the profile soil water.

(ii) **Deep tubes (2, 3, and 6)**

Figure 5.3.3 shows plots of the ratio of actual to potential transpiration against potential for the three deep tubes in the forested area. The pattern is similar to that shown for the shallow tubes. Again, two straight line regressions were derived, in this case crossing at a potential transpiration of about 2.7 mm/day. Above this value, the ratio of actual to potential transpiration seemed to increase, unlike the situation for the shallow tubes. The regression coefficients obtained by least squares were:-

$$ETa/ETp = 1.24 - 0.34\ ETp \qquad ETp \leq 2.7 \text{ mm/day}$$

$$ETa/ETp = 0.18 + 0.044\ ETp \qquad ETp > 2.7 \text{ mm/day}$$

A plot of drainage rate (mm/day) against soil moisture deficit (mm) for positive and one slightly negative deficit is given in Fig. 5.3.4. It was found that drainage was linearly inversely proportional to deficit, and the following straight line regression was obtained by

Fig. 5.3.1 Actual/Potential Transpiration against Potential and Drainage against Soil Moisture Deficit for the Shallow Forest Tubes (1,4, and 5)

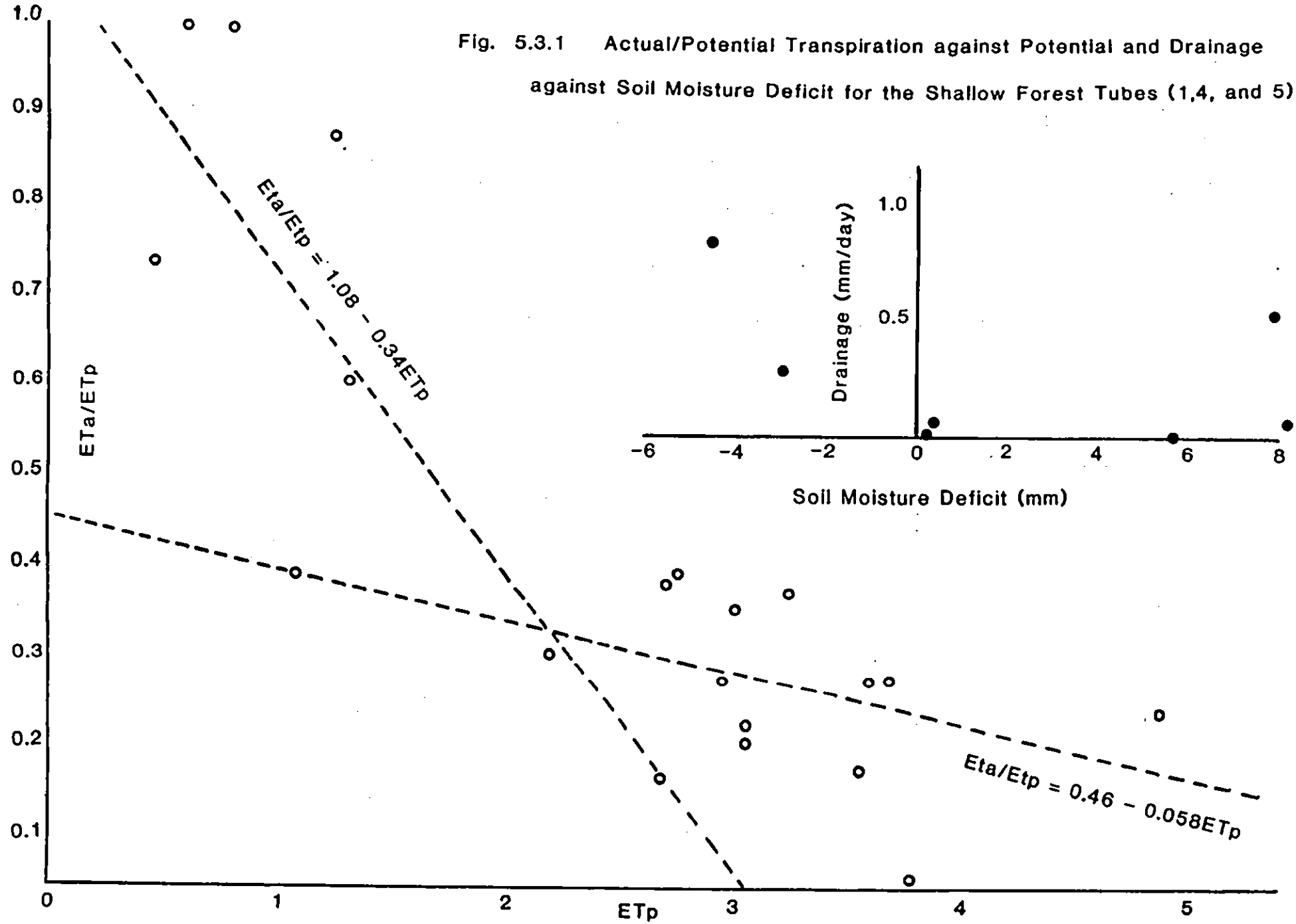

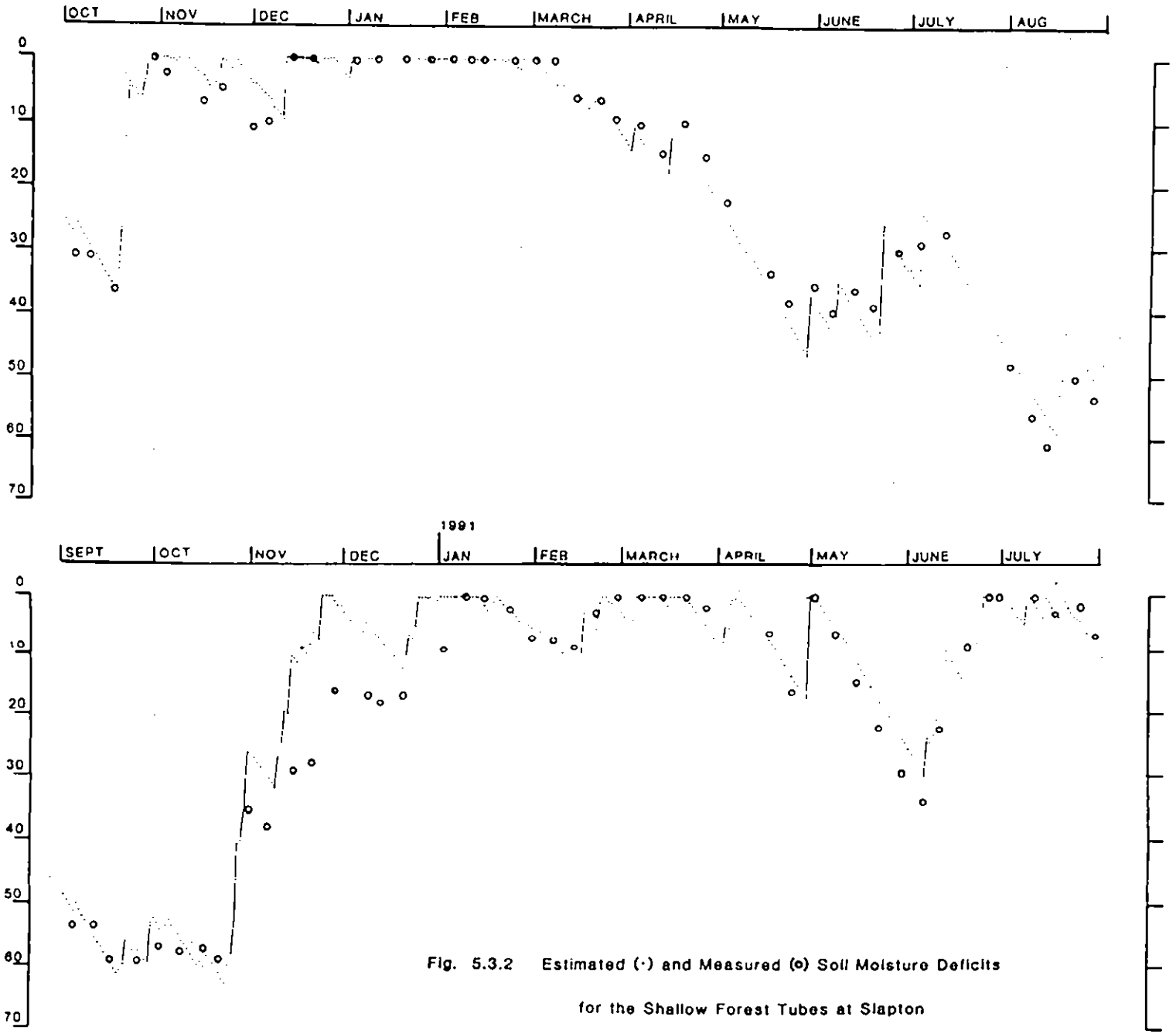


Fig. 5.3.2 Estimated (·) and Measured (o) Soil Moisture Deficits for the Shallow Forest Tubes at Slapton

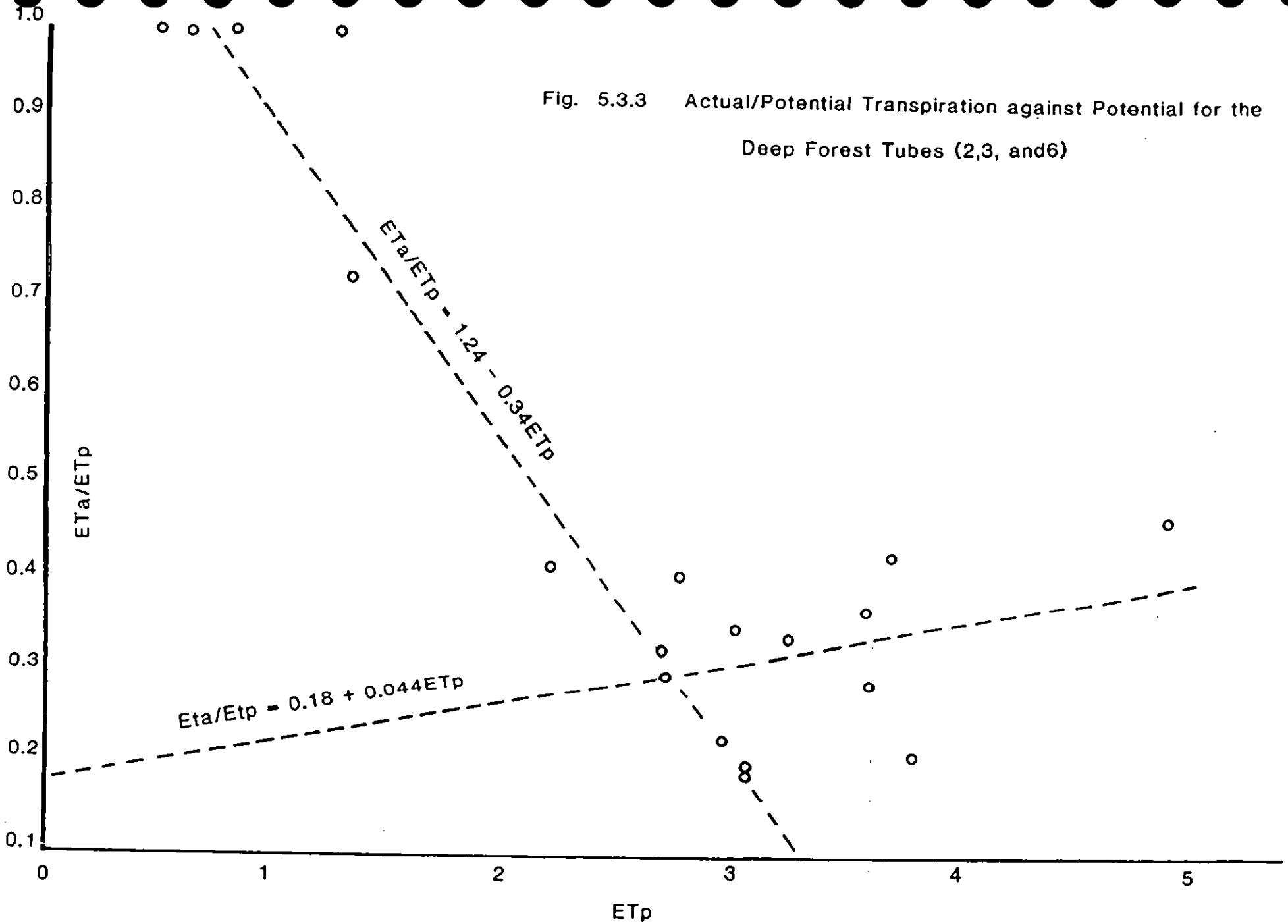


Fig. 5.3.3 Actual/Potential Transpiration against Potential for the Deep Forest Tubes (2,3, and6)

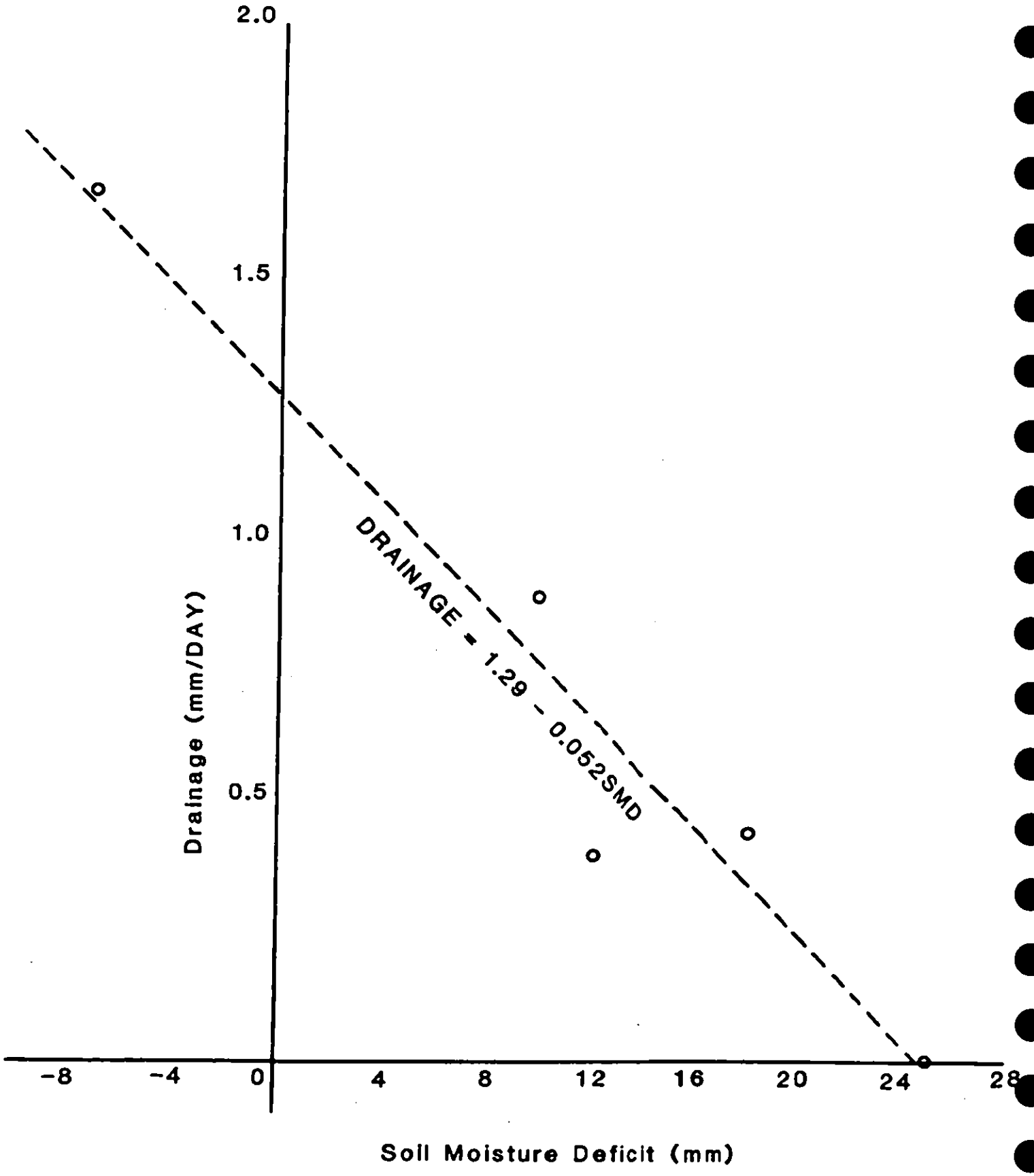


Fig. 5.3.4 Drainage Rate (mm/DAY) against Soil Moisture Deficit (mm) for the Deep Forest Tubes

least squares:-

DRAINAGE = 1.29 - 0.052 SMD

Applying the above transpiration and drainage regressions to the whole soil moisture data set produced the following daily equivalent canopy capacities (mm) for each month;

| J | F | M | A | M | J | J | A | S | O | N | D |
|---|---|---|---|---|---|---|---|---|---|---|---|
| 0.5 | 0.5 | 0.5 | 1.0 | 2.0 | 2.5 | 3.0 | 3.0 | 2.0 | 1.0 | 0.5 | 0.5 |

these are similar to, but slightly smaller, than those for the shallow tubes.

A time series plot of measured and daily estimated soil moisture deficit is given in Figure 5.3.5. The agreement between observed and estimated is again very good apart from two periods. The first is during the spring 1990 when the estimated soil moisture deficit is consistently greater than observed by about 10 mm. This is solely due to differences during one period, the 1st to the 7th March. During this period, 2 mm of rain fell, and the model predicted that the deficit would increase from 0.6 mm to 10.7 mm, most of which was as a result of drainage from the soil profile. When the measured soil moisture changes were averaged, no change in deficit was suggested, though there was a great deal of variation between the three sites.

The second period was at the end of 1990 when, as was the case of the shallow tubes, the estimated soil moisture deficits suggest that the profile reached field capacity sooner than observed. In the case of the deeper tubes, this was due to changes during one period only, 20.12.90 - 1.1.91. For this, the model predicted a fall in deficit of 76.6 mm whilst the observed values gave a fall of 5.2 mm. This was a particularly wet period when 73.8 mm of rainfall occurred. It is quite possible that most of this may have been lost as surface runoff without contributing to the soil moisture store.

The soil moisture deficits generated at the deep forest sites (Fig. 5.3.5) in the summer months are approximately twice those at the shallow sites (Fig. 5.3.2). This is as a result of higher evaporation losses (120 mm over the 22 months period) from the deeper sites compared to the shallow sites (Table 5.3.3). These greater evaporation losses are balanced by higher flows from the shallower sites.

Average values from the shallow and deep soil moisture sites have been used in Table 5.3.4, where measured and estimated monthly totals of hydrological variables for the forested area are tabulated. The rainfall totals shown as those recorded by the automatic weather station (Fig. 2.1) reduced by 13% to compensate for lower rainfall rates in the valley bottom.

For 1990, it was found that actual evaporation losses were 486.6 mm, of which 310.9 mm (64%) was transpiration, and 175.3 mm (36%) was evaporation from the forest canopy. The latter shows that approximately 20% of the incoming rainfall was intercepted by the forest canopy. These values agree well with others quoted in the literature eg. Roberts (1983), in his review of a number of forests in the UK and western Europe, quoted an annual transpiration loss of 320-344 mm, whilst Hall and Roberts, 1990 showed that between 10 and 36% of incoming rainfall was intercepted by broadleaved woodland. These losses were greater than those found for the grass and the arable field. Estimated total flow for 1990 was

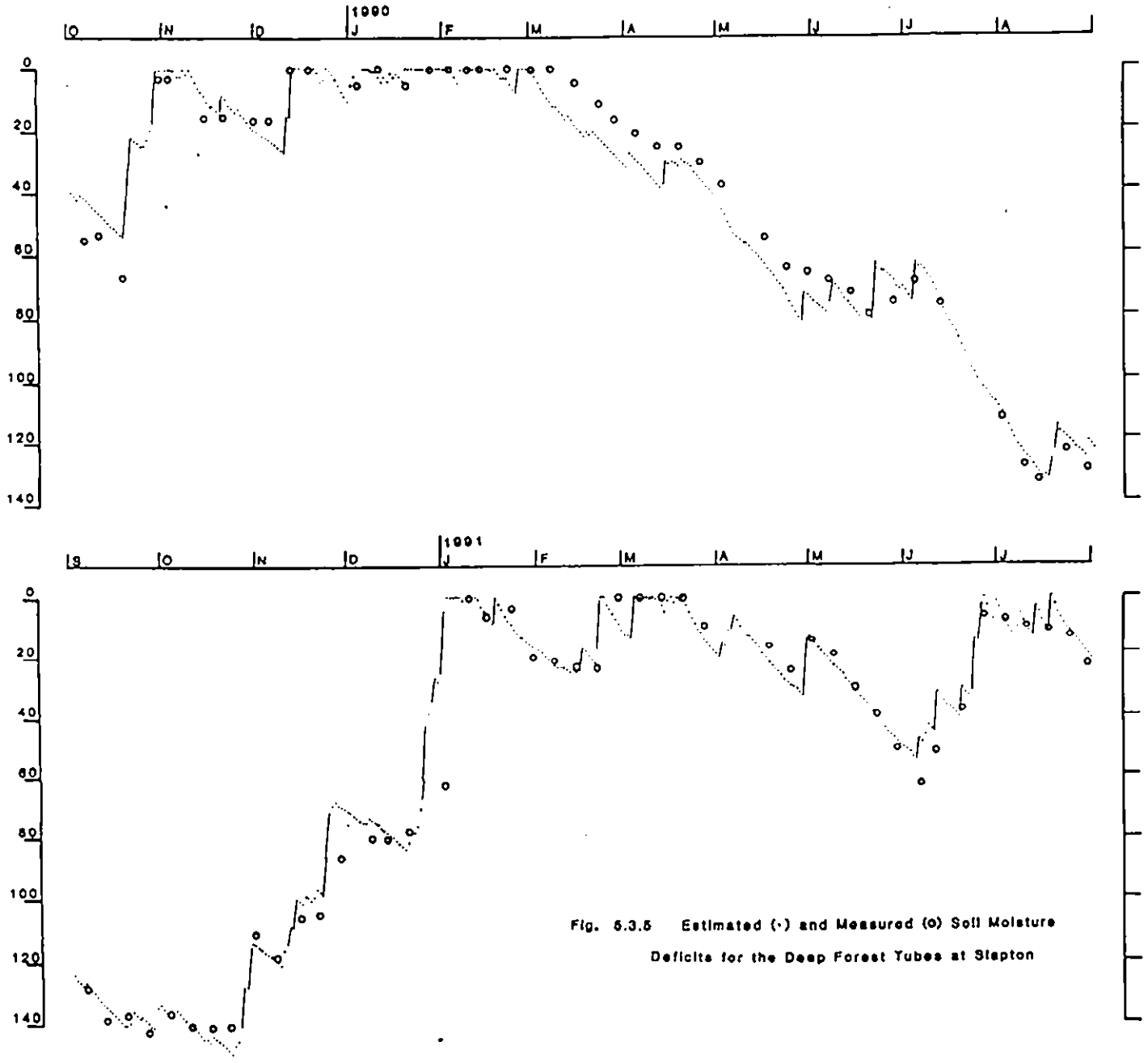


Fig. 5.3.5 Estimated (·) and Measured (o) Soil Moisture Deficits for the Deep Forest Tubes at Slapton

*Table 5.3.3 Monthly evaporation and runoff losses (mm) from the shallow and deep forest sites*

| Month | Shallow tubes | | | | Deep tubes | | | |
|---|---|---|---|---|---|---|---|---|
| | Transpiration | Interception | Drainage | Surface Runoff | Transpiration | Interception | Drainage | Surface Runoff |
| 1989 | | | | | | | | |
| OCT | 23.8 | 12.1 | 0.0 | 31.9 | 29.4 | 12.1 | 3.8 | 10.6 |
| NOV | 18.8 | 6.0 | 0.0 | 39.9 | 22.4 | 6.0 | 26.6 | 23.7 |
| DEC | 18.4 | 7.3 | 0.0 | 140.1 | 22.0 | 7.3 | 23.4 | 105.1 |
| 1990 | | | | | | | | |
| JAN | 5.3 | 13.2 | 0.0 | 144.6 | 5.7 | 13.2 | 37.1 | 99.6 |
| FEB | 13.6 | 11.5 | 0.0 | 225.0 | 16.1 | 11.5 | 34.1 | 188.4 |
| MARCH | 21.3 | 4.7 | 0.0 | 0.7 | 26.1 | 4.7 | 13.8 | 0.0 |
| APRIL | 25.3 | 15.9 | 0.0 | 0.0 | 33.4 | 9.6 | 0.0 | 0.0 |
| MAY | 26.7 | 9.4 | 0.0 | 0.0 | 42.2 | 9.4 | 0.0 | 0.0 |
| JUNE | 25.2 | 37.1 | 0.0 | 0.0 | 34.3 | 30.6 | 0.0 | 0.0 |
| JULY | 25.9 | 20.0 | 0.0 | 0.0 | 52.8 | 19.0 | 0.0 | 0.0 |
| AUG | 26.3 | 21.8 | 0.0 | 0.0 | 40.8 | 18.8 | 0.0 | 0.0 |
| SEPT | 25.0 | 17.4 | 0.0 | 0.0 | 31.5 | 17.4 | 0.0 | 0.0 |
| OCT | 24.4 | 16.5 | 0.0 | 0.0 | 30.9 | 16.5 | 0.0 | 0.0 |
| NOV | 19.6 | 8.7 | 0.0 | 23.4 | 23.5 | 8.7 | 0.0 | 0.0 |
| DEC | 20.9 | 7.5 | 0.0 | 46.9 | 25.0 | 7.5 | 0.0 | 0.0 |
| TOTAL | 259.5 | 183.7 | 0.0 | 440.6 | 362.3 | 166.9 | 85.0 | 288.0 |
| 1991 | | | | | | | | |
| JAN | 19.6 | 9.5 | 0.0 | 95.4 | 23.2 | 9.5 | 30.5 | 46.8 |
| FEB | 17.2 | 5.7 | 0.0 | 35.2 | 20.6 | 5.7 | 11.1 | 16.4 |
| MARCH | 21.2 | 8.9 | 0.0 | 93.7 | 26.2 | 8.9 | 31.2 | 61.2 |
| APRIL | 24.0 | 19.5 | 0.0 | 5.9 | 30.5 | 11.2 | 10.0 | 0.0 |
| MAY | 26.3 | 3.0 | 0.0 | 0.0 | 34.7 | 3.0 | 3.0 | 0.0 |
| JUNE | 24.7 | 51.4 | 0.0 | 28.2 | 32.4 | 40.4 | 6.5 | 2.0 |
| JULY | 26.4 | 36.0 | 0.0 | 24.8 | 36.1 | 32.5 | 24.3 | 4.5 |
| GRAND TOTAL | 479.9 | 343.1 | 0.0 | 935.7 | 639.8 | 303.5 | 255.4 | 558.3 |
| | 823.0 | | | 935.7 | 943.3 | | | 813.7 |

395.0 mm composed of 30.6 mm of drainage from the soil profile and 364.4 mm (92%) surface runoff.

*Table 5.3.4* *Measured and estimated monthly totals (mm) of hydrological variables for the forested areas at Slapton*

| Month | Measured | | | | Estimated | | |
|---|---|---|---|---|---|---|---|
| | Rainfall | Pot. Evap | Flow | Act. Evap | Drainage | Fast flow | Total flow |
| 1989 | | | | | | | |
| OCT | 91.8 | 44.3 | 15.0 | 38.7 | 1.9 | 21.3 | 23.2 |
| NOV | 61.7 | 26.4 | 50.8 | 26.6 | 13.3 | 31.8 | 45.1 |
| DEC | 166.6 | 25.6 | 155.9 | 27.5 | 11.7 | 122.6 | 134.3 |
| 1990 | | | | | | | |
| JAN | 166.2 | 5.6 | 107.3 | 18.7 | 6.6 | 122.1 | 128.7 |
| FEB | 250.1 | 18.9 | 274.5 | 26.4 | 17.1 | 206.7 | 223.8 |
| MARCH | 13.5 | 37.6 | 57.8 | 28.4 | 6.9 | 0.4 | 7.3 |
| APRIL | 31.3 | 87.0 | 21.2 | 42.1 | 0.0 | 0.0 | 0.0 |
| MAY | 20.4 | 110.1 | 14.1 | 43.9 | 0.0 | 0.0 | 0.0 |
| JUNE | 68.3 | 85.8 | 11.5 | 63.6 | 0.0 | 0.0 | 0.0 |
| JULY | 33.1 | 133.6 | 10.0 | 58.9 | 0.0 | 0.0 | 0.0 |
| AUG | 46.1 | 109.5 | 8.0 | 53.9 | 0.0 | 0.0 | 0.0 |
| SEPT | 37.8 | 83.5 | 6.7 | 45.7 | 0.0 | 0.0 | 0.0 |
| OCT | 66.6 | 48.3 | 8.9 | 44.2 | 0.0 | 0.0 | 0.0 |
| NOV | 75.7 | 30.7 | 9.5 | 30.3 | 0.0 | 11.7 | 11.7 |
| DEC | 77.9 | 27.8 | 12.9 | 30.5 | 0.0 | 23.5 | 23.5 |
| ANNUAL TOTALS | 887.1 | 778.4 | 542.4 | 486.6 | 30.6 | 364.4 | 395.0 |
| 1991 | | | | | | | |
| JAN | 118.8 | 27.4 | 90.1 | 30.9 | 15.3 | 71.1 | 86.4 |
| FEB | 60.5 | 24.0 | 41.1 | 24.6 | 5.6 | 25.8 | 31.4 |
| MARCH | 118.3 | 45.4 | 129.8 | 32.6 | 15.6 | 77.5 | 93.1 |
| APRIL | 58.3 | 68.4 | 38.6 | 42.6 | 5.0 | 3.0 | 8.0 |
| MAY | 3.0 | 96.8 | 19.8 | 33.5 | 1.5 | 0.0 | 1.5 |
| JUNE | 130.5 | 82.8 | 17.1 | 74.5 | 3.3 | 15.1 | 18.4 |
| JULY | 76.6 | 94.4 | 24.6 | 65.5 | 12.1 | 14.7 | 26.8 |

# 6. Water balance Calculations

Having estimated evapotranspiration losses from the three vegetation types and knowing their areal extent, it is now possible to calculate the actual evapotranspiration losses from the Slapton wood catchment, and to insert this into a water balance. For a given period, rainfall to the catchment should be balanced by streamflow plus evapotranspiration losses, assuming no change in the unsaturated zone soil moisture, and no deep percolation to groundwater. In order to ensure that the first assumption is valid, the start and finish of the accounting period are normally chosen so that there is no soil moisture deficit at either time. In this case, the start and end of 1990 can be conveniently used. Also, for the Slapton wood catchment, it can be reasonably assumed that deep percolation to groundwater is minimal through the Dartmouth slates underlying the catchment.

Table 6.1 gives measured and estimated monthly totals of hydrological variables for the Slapton wood catchment. The estimated actual evapotranspiration losses (ETa) are based on the Landsat classification. Also shown are annual totals (January to January) for 1990. For the latter, the difference between measured rainfall and flow gives an annual 'water use' of 477.1 mm; this is in excellent agreement with the estimate of actual evapotranspiration of 456.9 mm. It would seem, therefore, on an annual basis at least, that the methods used to estimate actual evapotranspiration are sensible.

On a shorter time scale, the situation is not so clear. Fig. 6.1 shows daily rainfall and measured and estimated total flow for the period 10th December 1989 to the 4th January 1990. During this period, 205 mm of rainfall occurred. Of this, 178.9 mm (87%) was estimated to be net rainfall ie. gross rainfall-actual evapotranspiration , whilst 155.6 mm (76% of gross rainfall) was lost as actual runoff. This suggests that, even for a small 'flashy' catchment such as Slapton wood, some additional store is present to modulate the rainfall. This is confirmed in Fig. 6.1 by the difference between the net rainfall and actual streamflow hydrographs. Also, the fact that the stream never dried out during the 22 months of study points to the presence of an additional soil moisture store. Obviously, some means of routing the net rainfall is required before the stream hydrograph can be modelled.

The model used in this report has not really addressed the problem of apportioning 'excess' water. It has been assumed that surface or 'quick' runoff occurs when the soil is above field capacity, and drainage reduces exponentially with soil moisture deficit. In reality, rapid runoff can occur either when the surface layer has reached saturation, not the same as field capacity, or when the rainfall intensity exceeds the infiltration rate. Both processes can occur long before the entire profile has reach field capacity. On the other hand, drainage will also occur, at a higher rate, up to soil saturation and beyond, and it is incorrect to assign all rainfall to rapid runoff when the soil is at field capacity.

All of these considerations must be taken into account when routing net rainfall though, provided that soil moisture and groundwater stores are similar at the beginning and end of the accounting period, then long term inputs and outputs should balance, as demonstrated above.

*Table 6.1* *Measured and estimated monthly totals (mm) of Hydrological variables for the Slapton wood catchment*

| Month | Measured | | | Estimated | | | |
|---|---|---|---|---|---|---|---|
| | Rain | ETp | Flow | ETa | Drainage | Surface Runoff | Total flow |
| 1989 | | | | | | | |
| OCT | 105.5 | 44.3 | 15.0 | 37.2 | 5.3 | 37.3 | 42.6 |
| NOV | 70.9 | 26.4 | 50.8 | 22.4 | 14.2 | 40.0 | 54.3 |
| DEC | 191.5 | 25.6 | 155.9 | 22.3 | 13.7 | 150.9 | 164.7 |
| 1990 | | | | | | | |
| JAN | 191.0 | 5.6 | 107.3 | 6.6 | 16.7 | 157.9 | 174.7 |
| FEB | 287.5 | 18.9 | 274.5 | 18.2 | 16.3 | 249.1 | 265.4 |
| MARCH | 15.5 | 37.6 | 57.8 | 29.4 | 9.0 | 1.0 | 10.0 |
| APRIL | 36.0 | 87.0 | 21.2 | 62.3 | 0.9 | 0.0 | 0.9 |
| MAY | 23.5 | 110.1 | 14.1 | 65.2 | 0.0 | 0.0 | 0.0 |
| JUNE | 78.5 | 85.8 | 11.5 | 59.6 | 0.0 | 0.0 | 0.0 |
| JULY | 38.0 | 133.6 | 10.0 | 62.6 | 0.0 | 0.0 | 0.0 |
| AUG | 53.0 | 109.5 | 8.0 | 37.4 | 0.0 | 0.0 | 0.0 |
| SEPT | 43.5 | 83.5 | 6.7 | 37.0 | 0.0 | 0.0 | 0.0 |
| OCT | 76.5 | 48.3 | 8.9 | 35.3 | 0.1 | 0.0 | 0.1 |
| NOV | 87.0 | 30.7 | 9.5 | 23.1 | 6.9 | 21.0 | 27.9 |
| DEC | 89.5 | 27.8 | 12.9 | 20.2 | 10.3 | 52.4 | 62.8 |
| ANNUAL TOTALS | 1019.5 | 778.4 | 542.4 | 456.9 | 60.2 | 481.4 | 541.8 |
| 1991 | | | | | | | |
| JAN | 136.5 | 27.4 | 90.1 | 19.4 | 16.0 | 104.1 | 120.2 |
| FEB | 69.5 | 24.0 | 41.1 | 12.1 | 10.8 | 44.4 | 55.2 |
| MARCH | 136.0 | 45.4 | 129.8 | 35.2 | 14.4 | 99.6 | 114.1 |
| APRIL | 67.0 | 68.4 | 38.6 | 49.8 | 5.2 | 0.7 | 5.8 |
| MAY | 3.5 | 96.8 | 19.8 | 71.8 | 1.6 | 0.0 | 1.6 |
| JUNE | 150.0 | 82.8 | 17.1 | 64.8 | 1.9 | 4.2 | 6.1 |
| JULY | 88.0 | 94.4 | 24.6 | 82.3 | 9.8 | 18.0 | 27.8 |

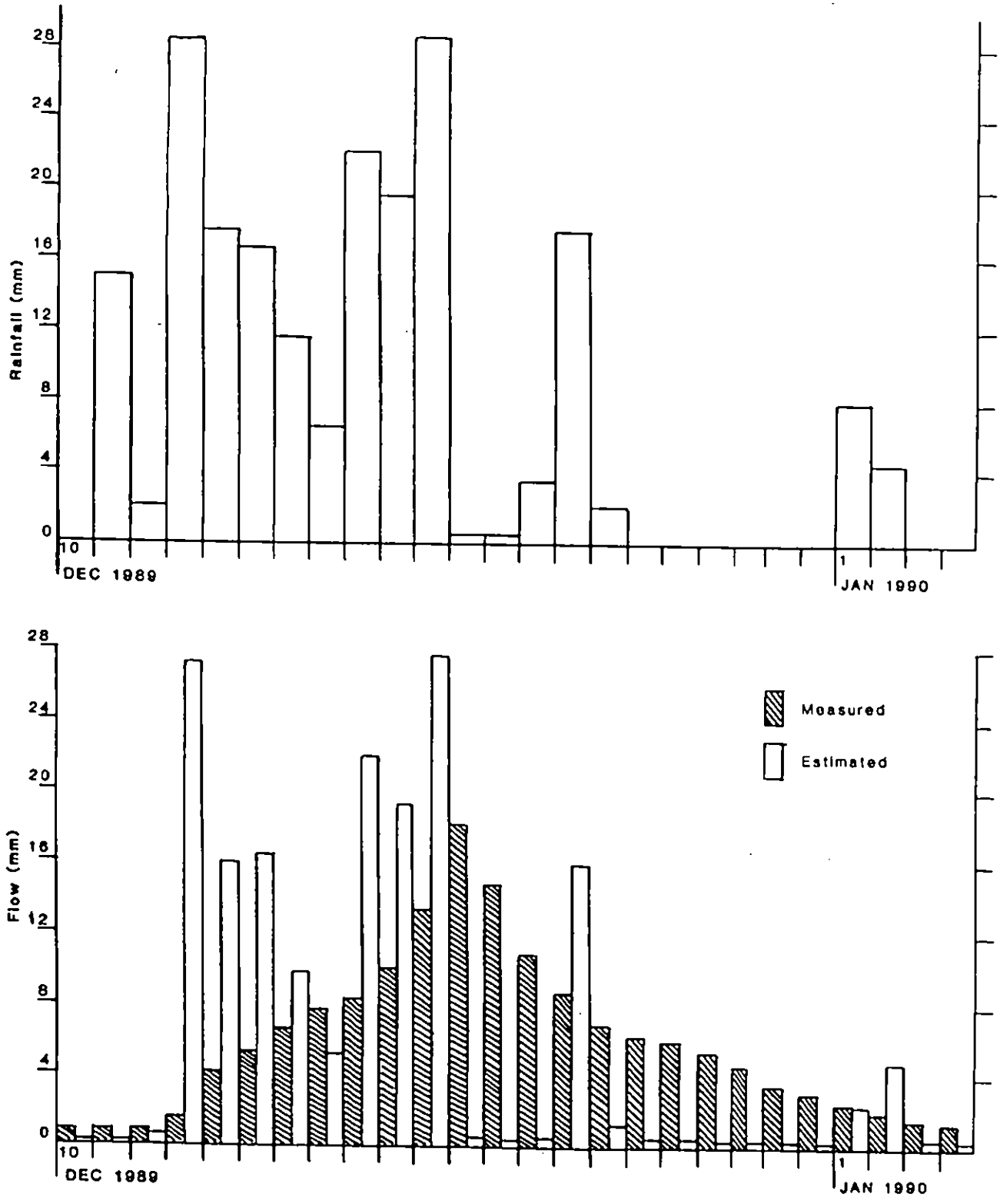


Fig. 6.1 Time series graph of Daily Rainfall and Measured and Estimated Flow

for the period 10th December 1989 to the 4th January 1990

# 7. Discussion

This report describes the techniques involved in analysing remotely sensed imagery and the usefulness of the resulting data, when combined with data from conventional field experiments, in solving hydrological problems. In this particular case, the images were acquired from a low flying aircraft, as it was felt that these high resolution images were required to adequately describe the heterogeneous nature of the small area under consideration. However, similar techniques could be applied to satellite images of larger, more homogeneous, areas.

Aerial photographs have been used extensively in the past for many hydrological applications. This was also true for Slapton, where the black and white photographs taken with the Wild RC8 camera were analysed under a stereo viewer to pinpoint the position of the flow gauging station at the outfall of the catchment (difficult on the ground because of the trees), and also to help delineate the catchment boundary. Some of the interfluve areas were so flat that the boundary could only be identified by ground survey. The use of a digital stereo plotter may have reduced the amount of field work required.

The images from the Daedalus scanner were analysed to provide a land use classification and the distribution of near surface soil moisture in the grassland areas of the catchment. The latter was disappointing, the resulting classification being more of a distinction between the temporary and permanent grassland areas, than the distribution of soil moisture. One of the reasons for this was the very dry conditions and lack of spatial variability in soil moisture experienced during the overflights. Hopefully, more positive results will be obtained during the 1994 airborne campaign over the Wye catchment at Plynlimon.

Problems were also encountered with the land classifications, these being mainly due to large variations in spectral response from the areas of forest affected by windthrow. Satisfactory classifications were eventually obtained, particularly for the April ATM image, though the effort involved was much greater than would normally have been expected. In this particular case, such a detailed classification as given by the aircraft imagery was not required, and the Landsat classification used. The reason for this was the lack of soil moisture data from under the different agricultural crops. As a result, it had to be assumed that changes in soil moisture observed under winter barley and temporary grass were applicable to all of the arable areas. This assumption is clearly not valid as there will be differences in the cropping cycles, rooting depths and transpiration demands of different agricultural crops. The same is true for the grassland areas, where it has been assumed that soil moisture conditions under one flat, temporary grass field could be applied to all of the grassland areas of the catchment, including the steep valley sides, covered by permanent grassland. The soil moisture distribution in the forested sites were seen to vary a great deal, though an attempt was made to minimize this by considering 'shallow' and 'deep' soil moisture profiles. Windthrow areas within the forest will also be problematic. In the Landsat classification, these have mostly been classed as grassland. In terms of the soil moisture distribution, this is probably more realistic than regarding them as forestry, as there will be no canopy interception to reduce rainfall inputs to these areas.

This attempt to estimate areal evapotranspiration is a simple example of how formulations obtained at single points can be extrapolated to larger areas using a spatial data set, in this case a land classification. For such a small, accessible area, a more accurate classification (with reservations about the forested area) could, and has been, obtained more cheaply by a

ground survey. However, comparisons between the land classifications from the remotely sensed images and the field surveys shows that the analysis of these images can produce classifications with an acceptable degree of accuracy which may be useful for larger, remote areas where maps are not available and ground surveys difficult.

The same applies to the formulations applied. Provided that the required process studies have been done, estimates of a number of hydrologically relevant parameters, such as evaporation, chemical and sediment losses, can be made over large areas. Also such as an approach need not be limited to one particular spatial data set or need be confined to bulked areas. Advances in the manipulating of spatial data sets, such as land cover, soil type, and topography, using Geographic Information Systems, will provide a number of discrete conditions within the areas of interest, and enable a fully distributed approach to be adopted to hydrological modelling.

# Acknowledgements

Some of the hydrological data used in this paper were collected during a study funded by UK NIREX. The work of staff who helped with data collection and processing at Slapton and Wallingford is greatly acknowledged. The aircraft images were acquired during a Natural Environment Research Council airborne campaign.

# References


Andersson, L. & Harding, R.J. 1991. Soil-moisture deficit simulations with models of varying complexity for Forest and Grassland sites in Sweden and the UK. Water Resources Management 5: 25-46.

Atkinson, P., Cushnie, J.L., Townshend, J.R.G. & Wilson, A. 1985. Improving Thematic Mapper land cover classification using filtered data. Int. J. Remote Sensing, 6: 955-963.

Bathurst, J.C. 1986. Physically-based distributed modelling of an upland catchment using the Systems Hydrologique European. J. Hydrol., 87, 79-102.

Bell, J.P, 1976. Neutron Probe Practice. Institute of Hydrology report no. 19.

Blakeman, R.H. 1990. The identification of crop disease by aerial photography. In: Clark, J.A. and Steven, M.D. (eds), Applications of Remote Sensing in Agriculture, Butterworths, 229-254.

Boyle, S.A. 1991. Institute of Hydrology Instrumentation of the Slapton wood catchment. Report to UK Nirex Ltd under contract number UX/96/242.

BSI, 1981. British Standard Institution. Methods of measurement of liquid flow in open channels. Part 4A. Thin plate weirs. BS 3680.

Burt, T.P., Butcher, D.P., Coles, N. & Thomas, A.D. 1983. The natural history of the Slapton Ley nature reserve. XV. Hydrological processes in the Slapton wood catchment. Field Studies, 5, 731-752.

Burt, T.P., Arkell, B.P., Trudgill, S.T. & Walling, D.E. 1988. Stream nitrate levels in a small catchment in south west England over a period of 15 years (1970-1985). Hydrological Processes 2, 267-284.

Calder, I.R., Harding, R.J. & Rosier, P.T.W. 1983. An objective assessment of soil-moisture deficit models. J. Hydrol., 60, 329-355.

Curran, P.J. 1985. Principles of remote sensing. John Wiley and sons, Inc., New York.

Dean, T.J., Bell, J.P. & Baty, A.J.B. 1987. Soil moisture measurement by an improved capacitance technique, Part I. Sensor design and performance. J. Hydrol., 93, 67-78.

Devereaux, B.J., Fuller, R.M., Carter, L. & Parsell, R.J. 1990. Geometric correction of airborne scanner imagery by matching Delauney triangles. Int. J. Remote Sensing, Vol. II, no.12, 2237-2251.

Doorenbos, J & Pruitt, W.O. 1984. Guidelines for prediction of crop water requirements. FAO irrigation and drainage paper 24. Food and agriculture organisation of the United Nations, Rome, pp. 144.

Fuller, R.M., Parsell, R.J., Oliver, M. & Wyatt, G. 1989. Visual and computer classifications of remotely-sensed images: a case study of grasslands in Cambridgeshire. Int. J. Remote Sensing, 10: 193-211.

Gurnell, A.M., Gregory, K.J., Hollis, S. & Hill, C.T. 1985. Detrended correspondence analysis of heathland vegetation; the identification of runoff contributing areas. Earth Surface Processes and Landforms, Vol.10, 343-351.

Hall, R.L. & Roberts, J.M. 1990. Hydrological aspects of new broadleaf plantations. SEESOIL, 6: 2-38.

Harding, R.J., Hall, R.L. & Rosier, P.T.W. (in press) Measurement and modelling of the water use of beech and ash plantations in southern Britain.

Idso, S.B., Jackson, R.D. & Reginato, R.J. 1975. Detection of soil moisture by remote surveillance. American Scientist, 63, 549-557.

Iqbal, Muhammad. 1983. An introduction to Solar Radiation. Academic Press, Canada.

Kristensen, K.J. 1974. Actual evapotranspiration in relation to leaf area. Nordic Hydrology 5, 173-182.

LARC, 1982. Long Ashton Research Center Annual Report, 137-139.

McGowan, M. & Williams, J.B. 1980. The water balance of an agricultural catchment. II Crop evaporation: Seasonal and soil factors. J. Soil Science, 31, 231-244.

Musick, H. Brad & Pelletier, R.E. 1986. Response of some Thematic Mapper Band Ratios to Variation in Soil Water Content. Photogrammetric Engineering and Remote Sensing, Vol. 52, No.10, pp. 1661-1668.

Olesen, J.E. 1992. MVTOOL version 1.00. A tool for developing MARKVAND. Research Note No.30, Research Centre Foulum, Denmark.

Penman, H.L. 1948. Natural evaporation from open water, bare soil and grass. Proc. R. Soc. London, Ser. A, 193, 120-146.

Richardson, A.J. & Everitt, J.H. 1987. Monitoring water stress in buffelgrass using hand-held radiometers. Int. J. Remote Sensing, 8, 1797-1806.

Ripple, W.J. 1986. Spectral reflectance relationships to leaf water stress. Photogrammetric Engineering and Remote Sensing, 52, 1669-1675.

Roberts, G. & Roberts, A.M. 1992. Computing the water balance of a small agricultural catchment in southern England by consideration of different land-use type. II. Evaporative losses from different vegetation types. Agricultural Water Management, 21, 155-166.

Roberts, J.M. 1983. Forest transpiration: a conservative hydrological process? J. Hydrol., 66, 131-141.

Roberts G. 1972. The processing of soil moisture data. Institute of Hydrology Report no.18.

Roberts, G. 1981. The processing of hydrological data. Institute of Hydrology Report no.70.

Rollin, E.M. & Milton, E.J. 1988. The role of field spectroscopy in NERC airborne scanner campaigns. Proceedings of the Natural Environment Research Council 1987 Airborne Campaign Workshop, 15th December 1988, University of Southampton, pp. 1-19.

Singh, S.M. 1988. Atmosphere correction algorithm for ATM data. Proceedings of the NERC 1987 Airborne Campaign Workshop, University of Southampton, 15th December 1988, pp. 19-29.

Strangeways, I.C. 1972. Automatic weather stations for network operation. Weather 27: 403-408.

Strangeways, I.C. & Templeman, R.F. 1974. Logging river level on magnetic tape. Water Services 178(936), 57-60.

Thiessen, A.H. 1911. Precipitation averages for large areas. Monthly Weather Review 39, 1082-4.

Trudgill, S.T. 1983. The natural history of the Slapton Ley nature reserve. XVI. The soils of Slapton wood. Field Studies, 5, 833-840.

Tucker, C.J., Holden, B.N., Elgin, Jr. J.E. & McMurtney III, J.E. 1980. The relationship of spectral data to grain yield variations, Photogrammetric Engr. and Remote Sensing , 46(5), 657-666.

Wellings, S.R., Bell, J.P. & Raynor, R.J. 1985. The use of gypsum blocks for measuring soil water potential in the field. Institute of Hydrology Report no.92.

Wilson, A.K. 1986. Calibration of ATM data. Proceedings of the NERC 1985 Airborne Campaign Workshop, Natural Environment Research Council, Swindon, pages E.25-E.40.

Wilson, A.K. 1990. Retrieval of atmospheric parameters and validation of correction algorithms for remote sensing. Proceedings of the NERC symposium on airborne remote sensing 1990. British Geological Survey, Keyworth. December 1990, pp. 325-337.

Wilson, A.K. 1988. The critical dependence of remote sensing on sensor calibration and atmospheric transparency. Proceedings of the NERC 1987 Airborne Campaign Workshop, 15 Sept. 1988, University of Southampton, p. 29-58.

# Appendix I Reflectance spectra measured over various land covers in the range 350 to 2500 nanometer using the IRIS spectroradiometer. July 11th 1990.

Fig. 1 Temporary Grass

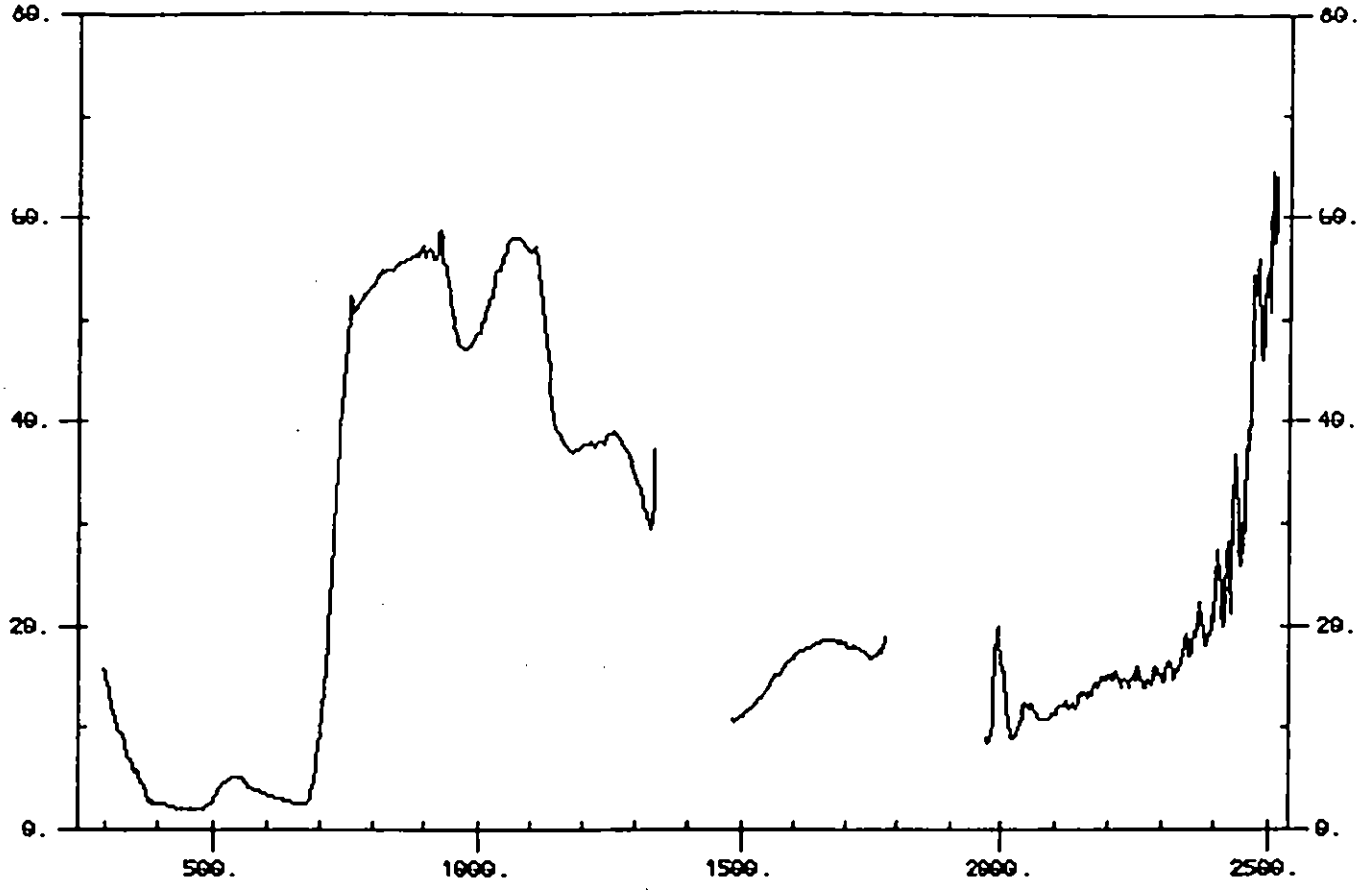


Fig. 2 Temporary Grass

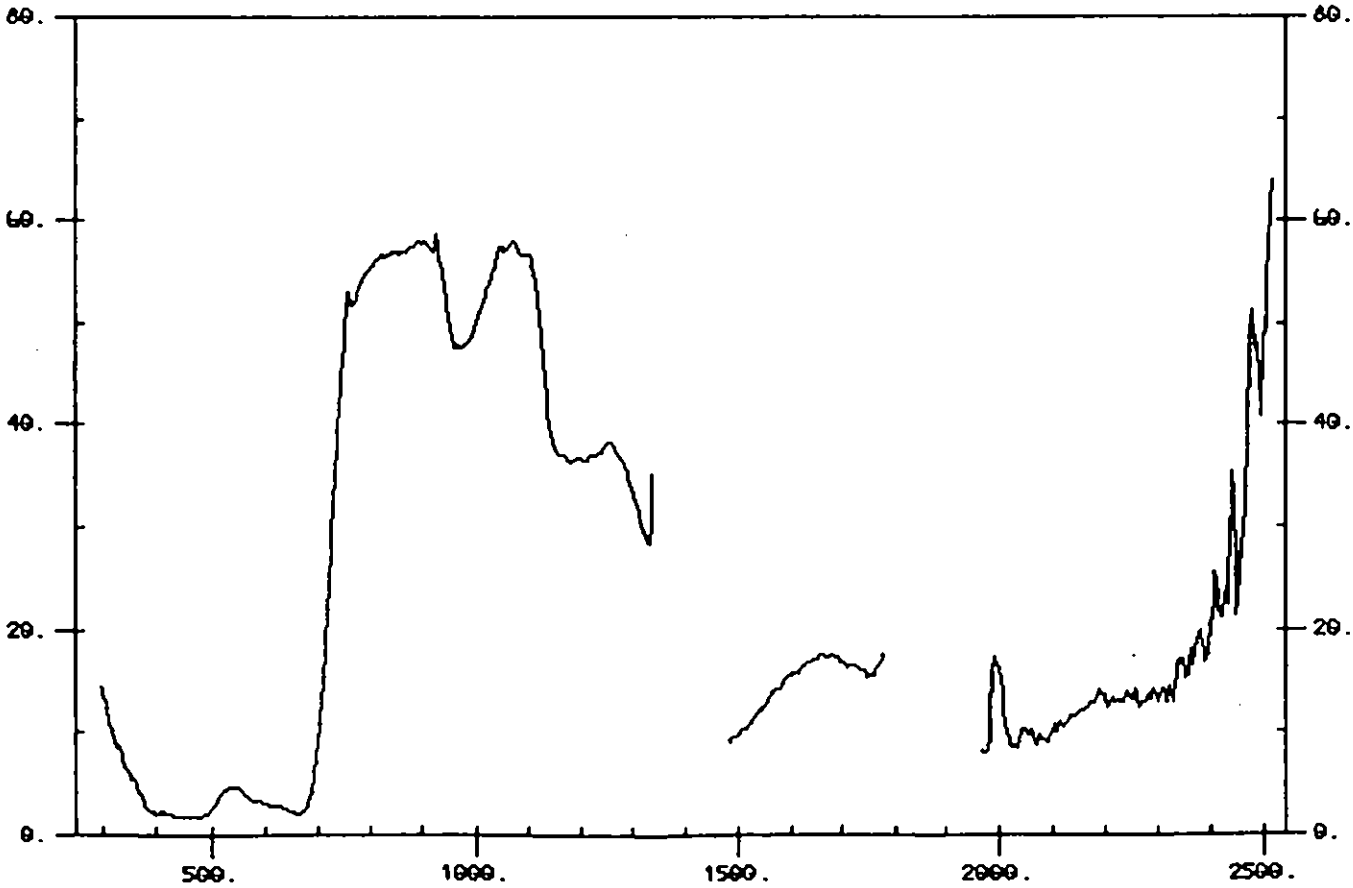

Fig. 3 Winter Barley

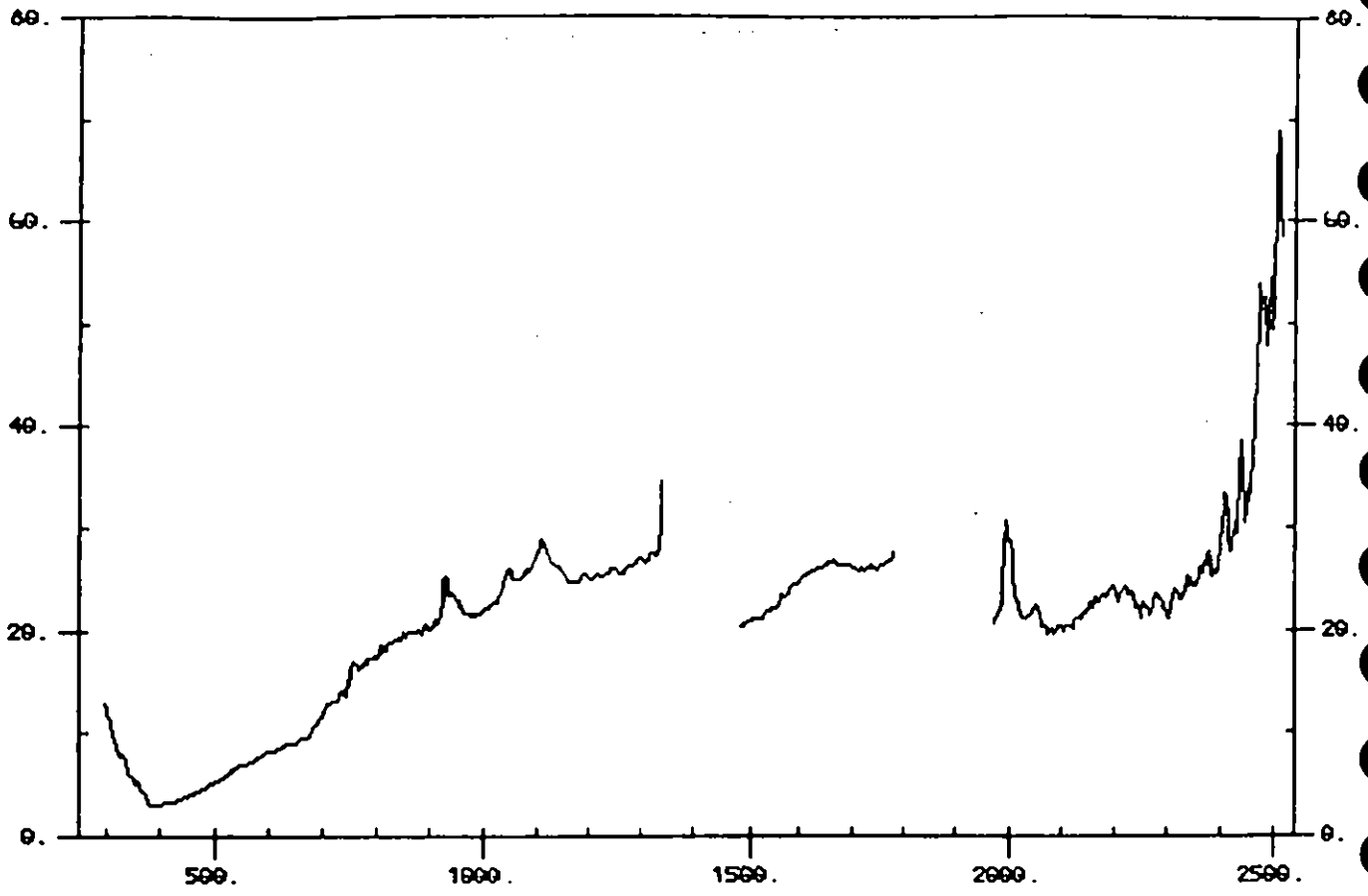


Fig. 4 Winter Barley

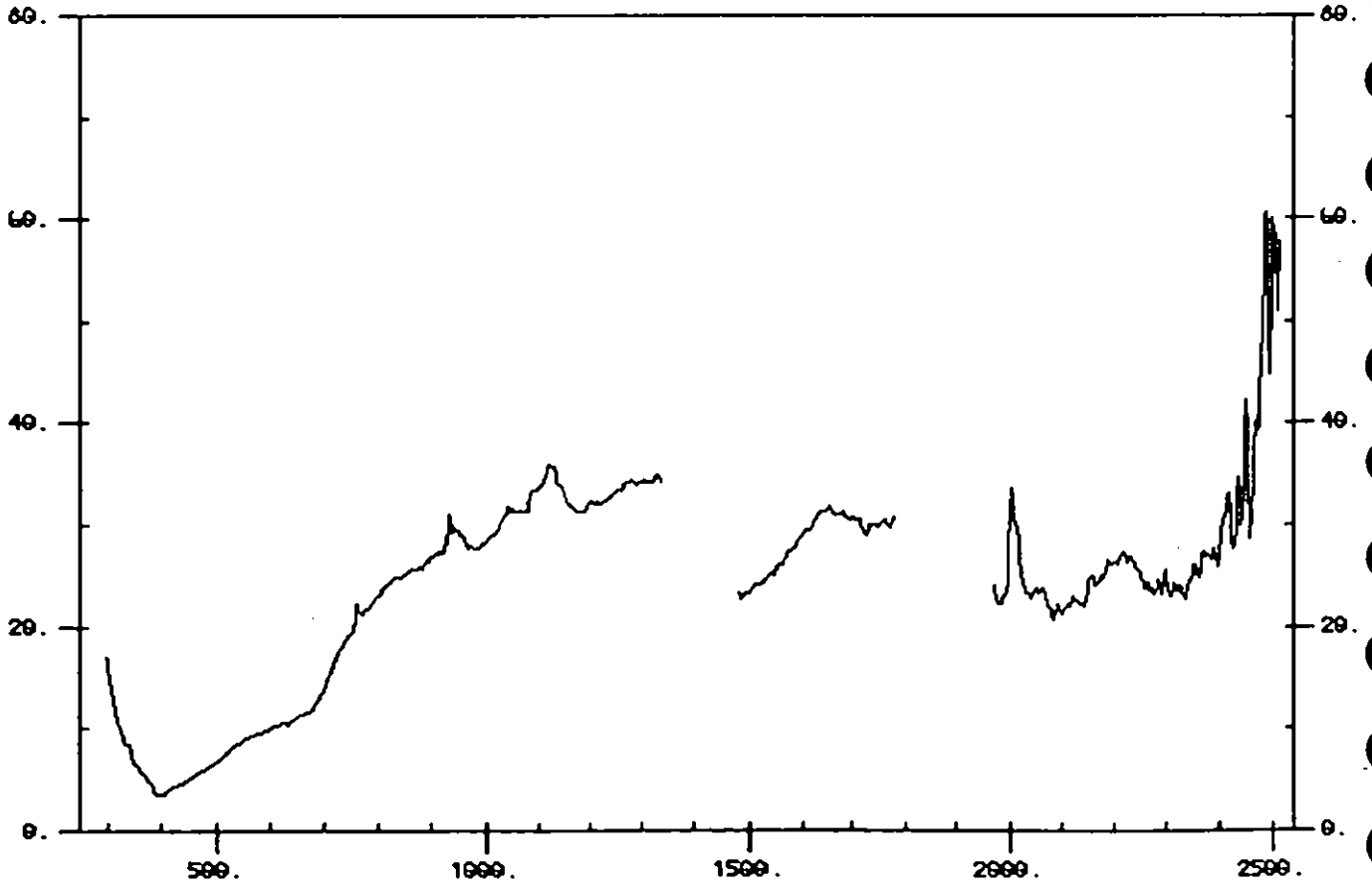

Fig. 5 Spring Barley

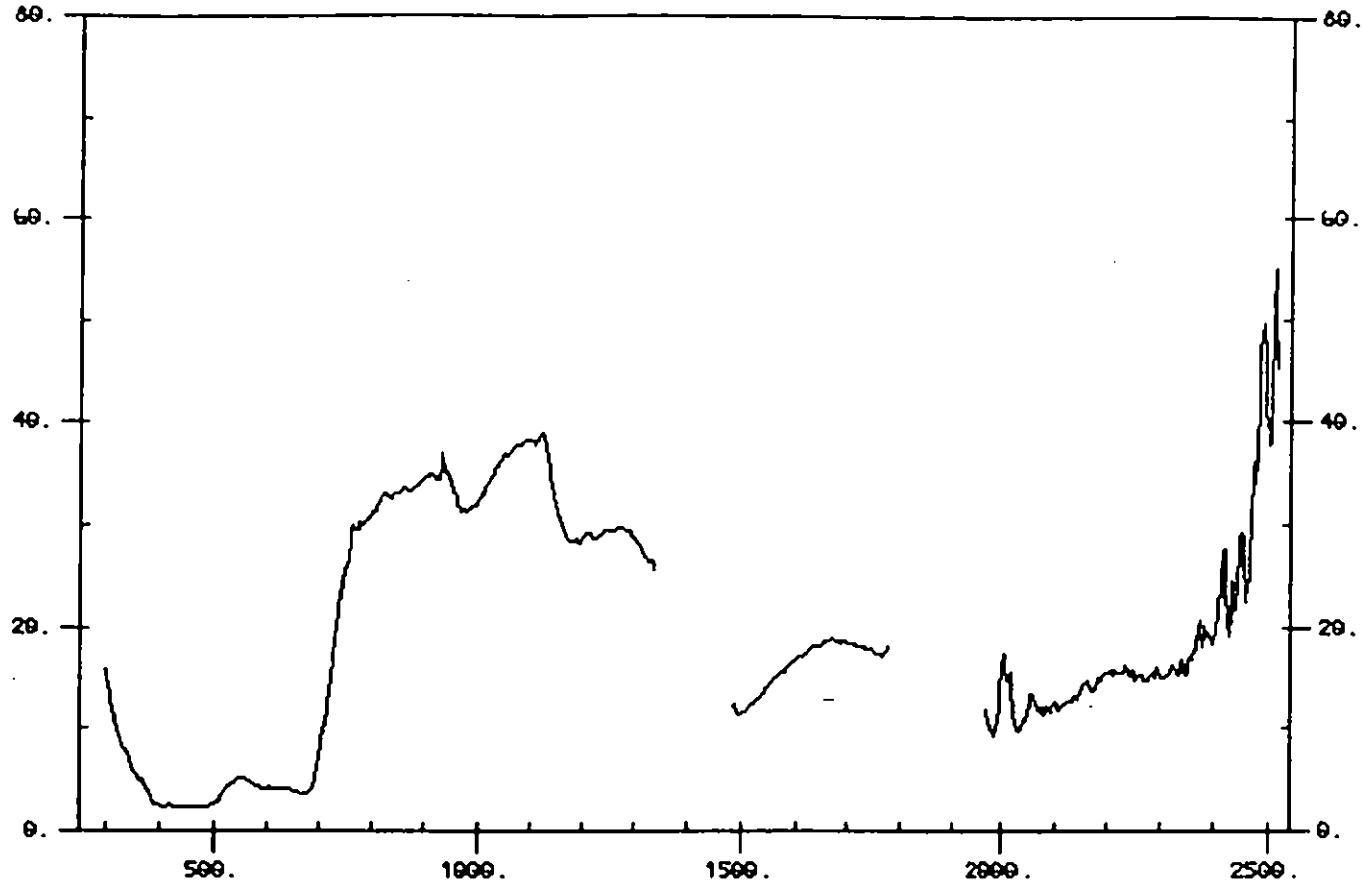


Fig. 6 Spring Barley

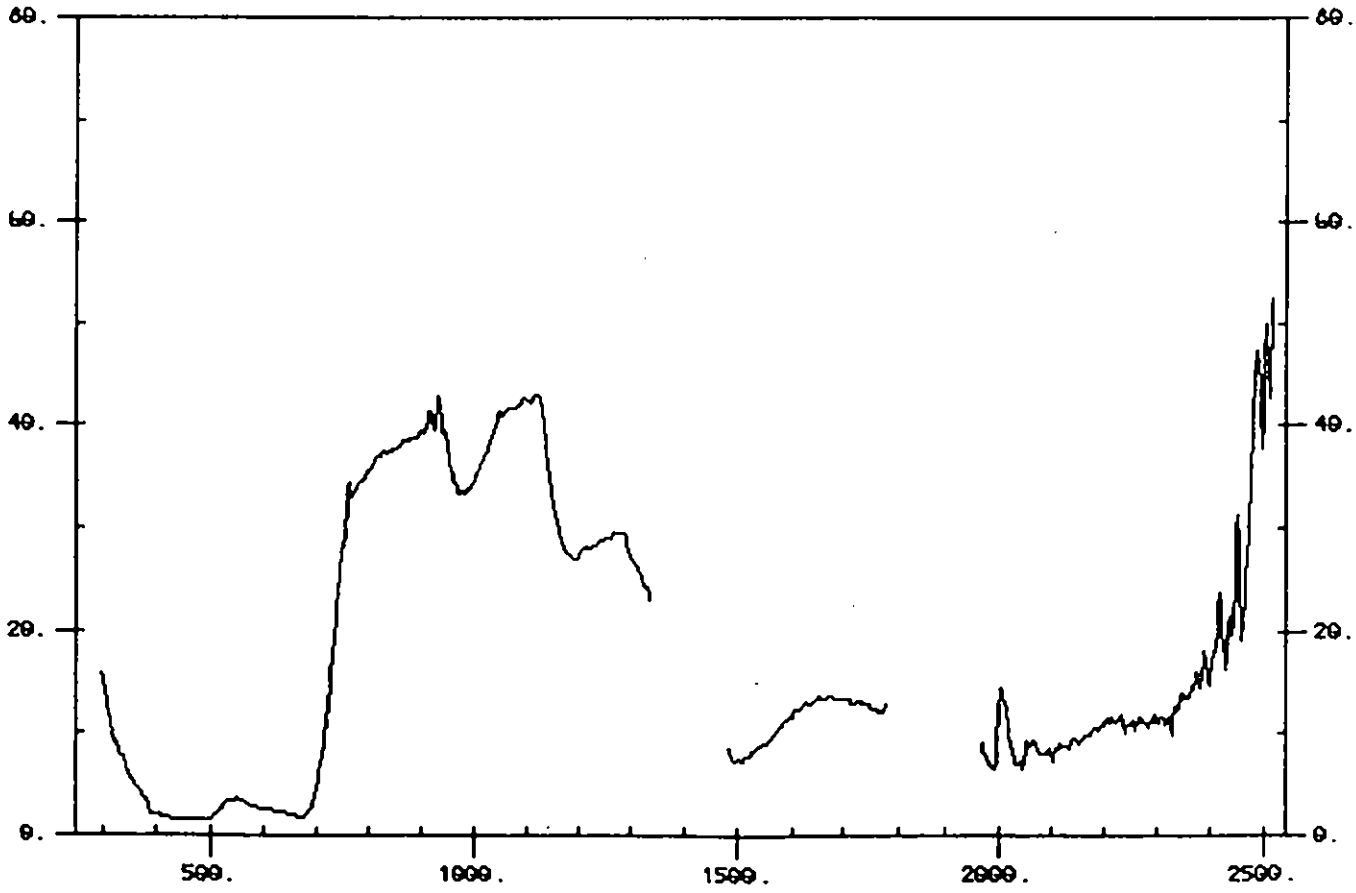

Fig. 7 Bare Earth

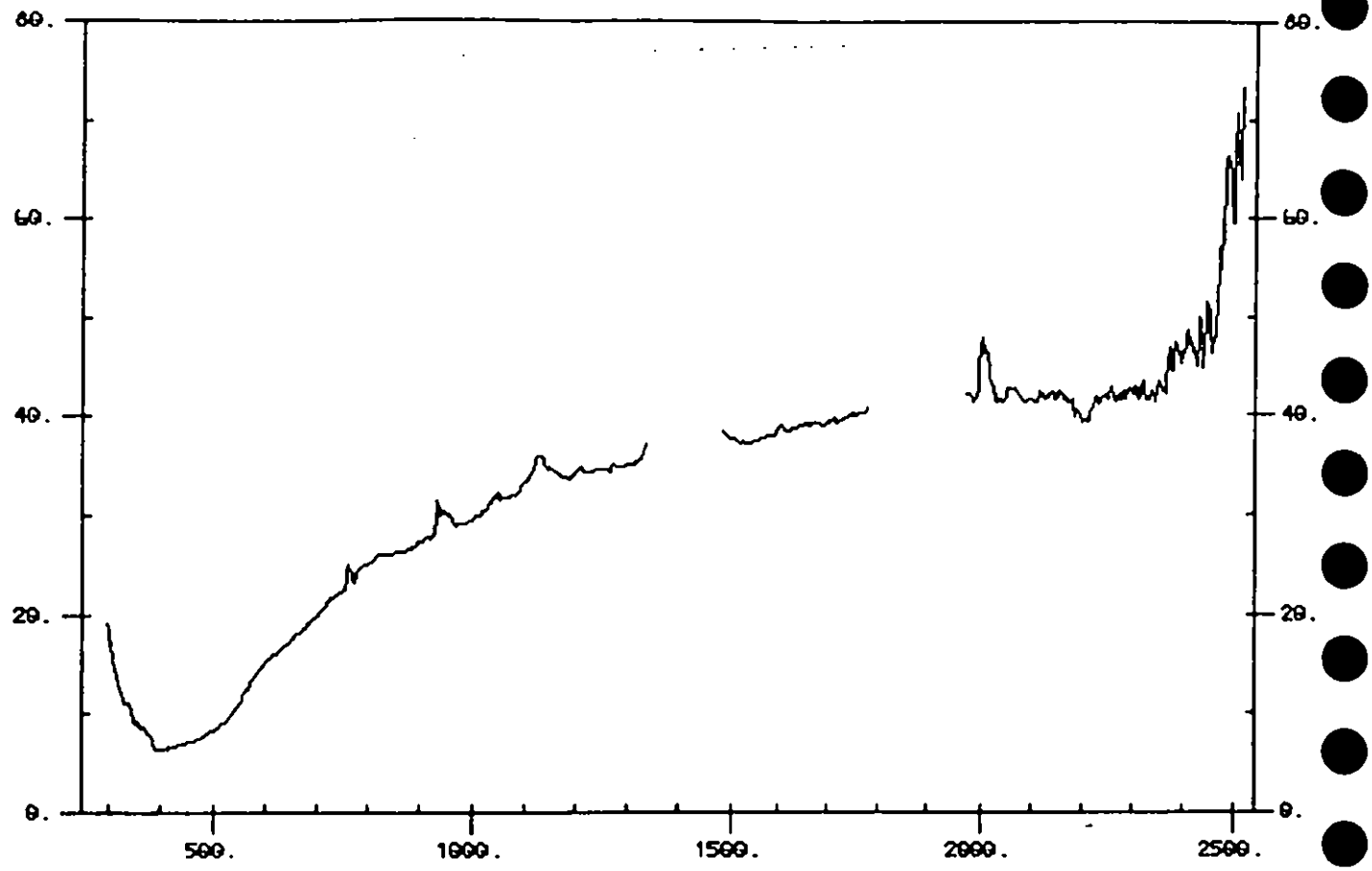


Fig. 8 Bare Earth

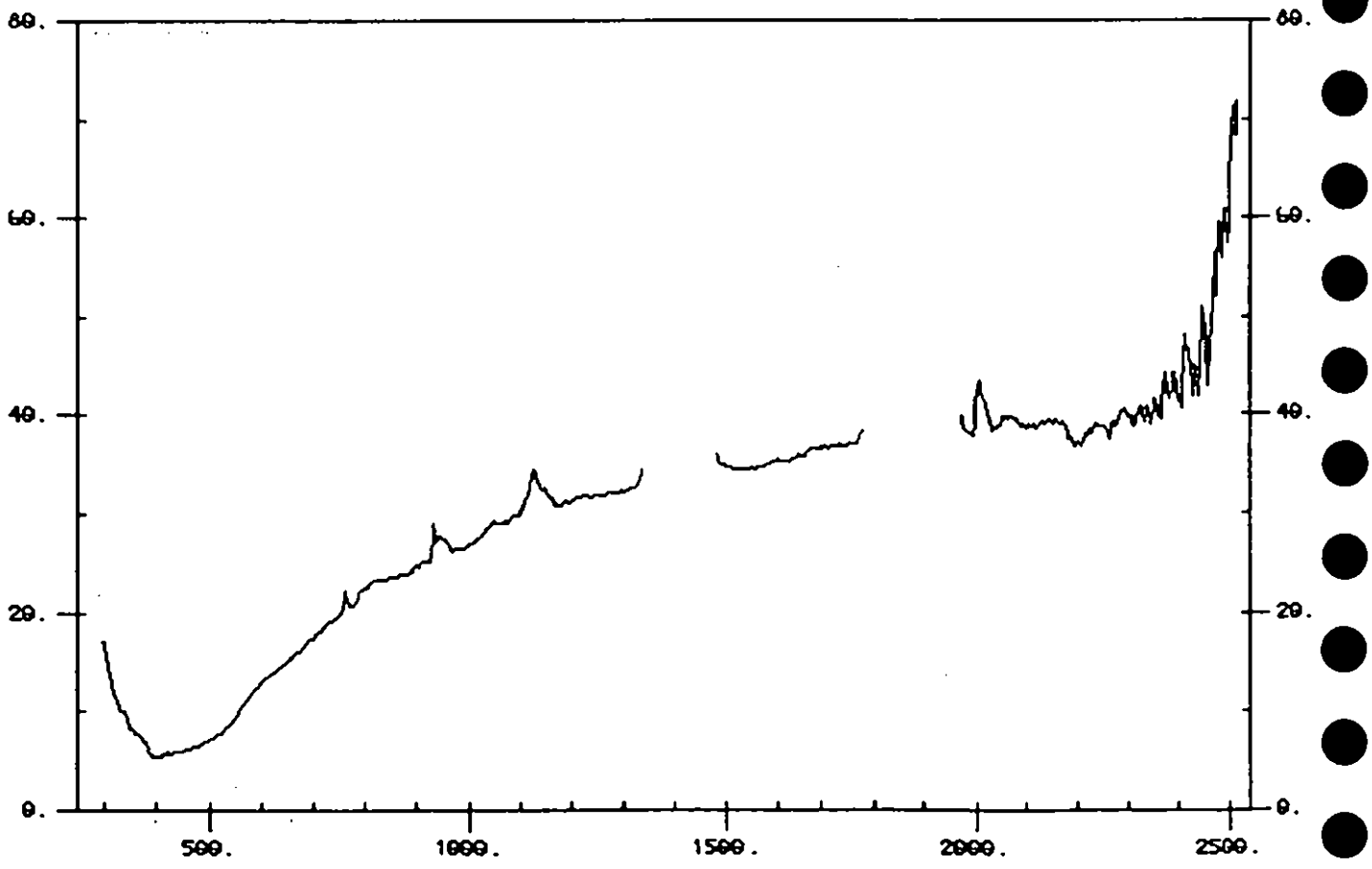

Fig. 9 Permanent Grass

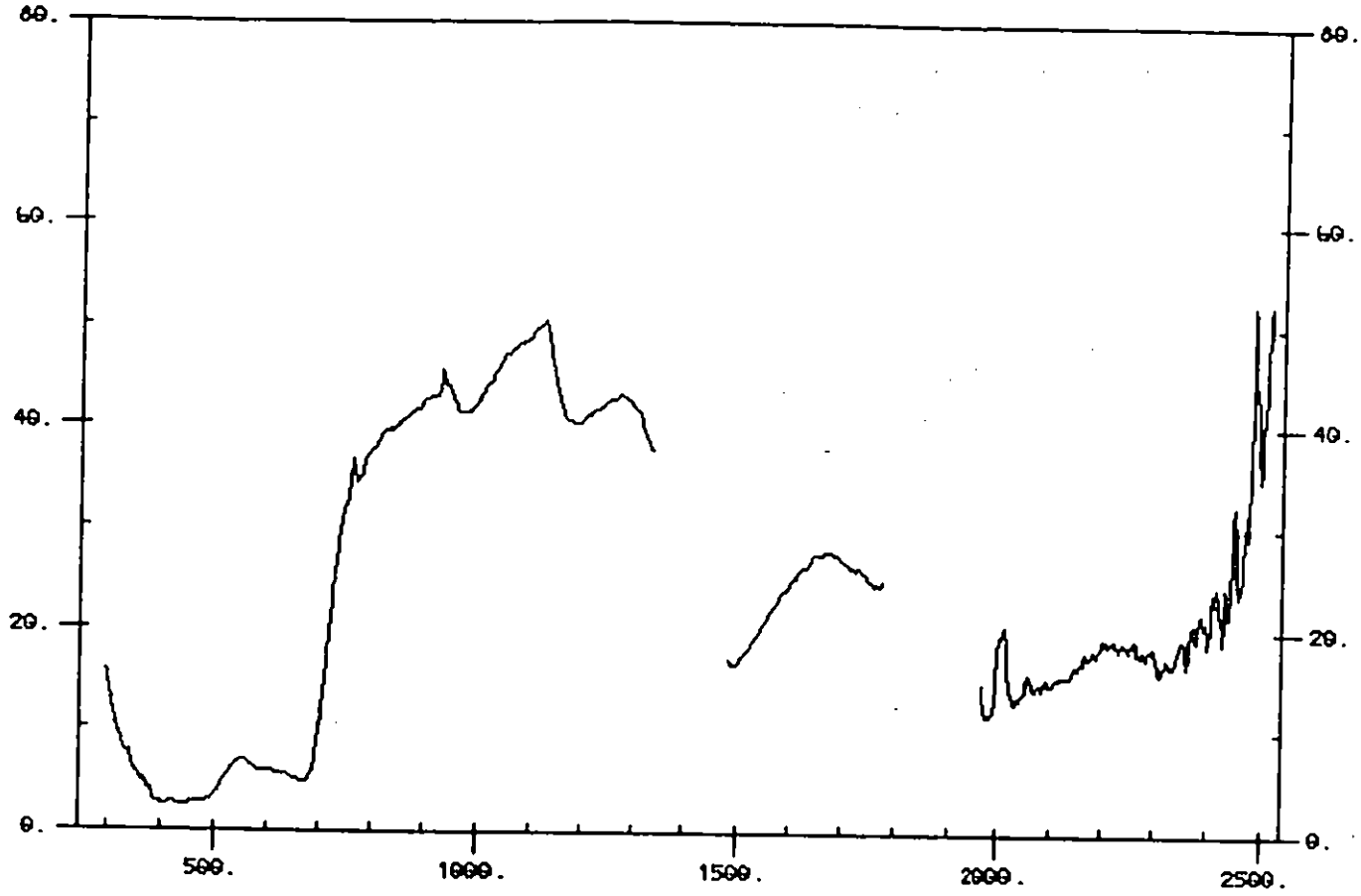


Fig. 10 Permanent Grass

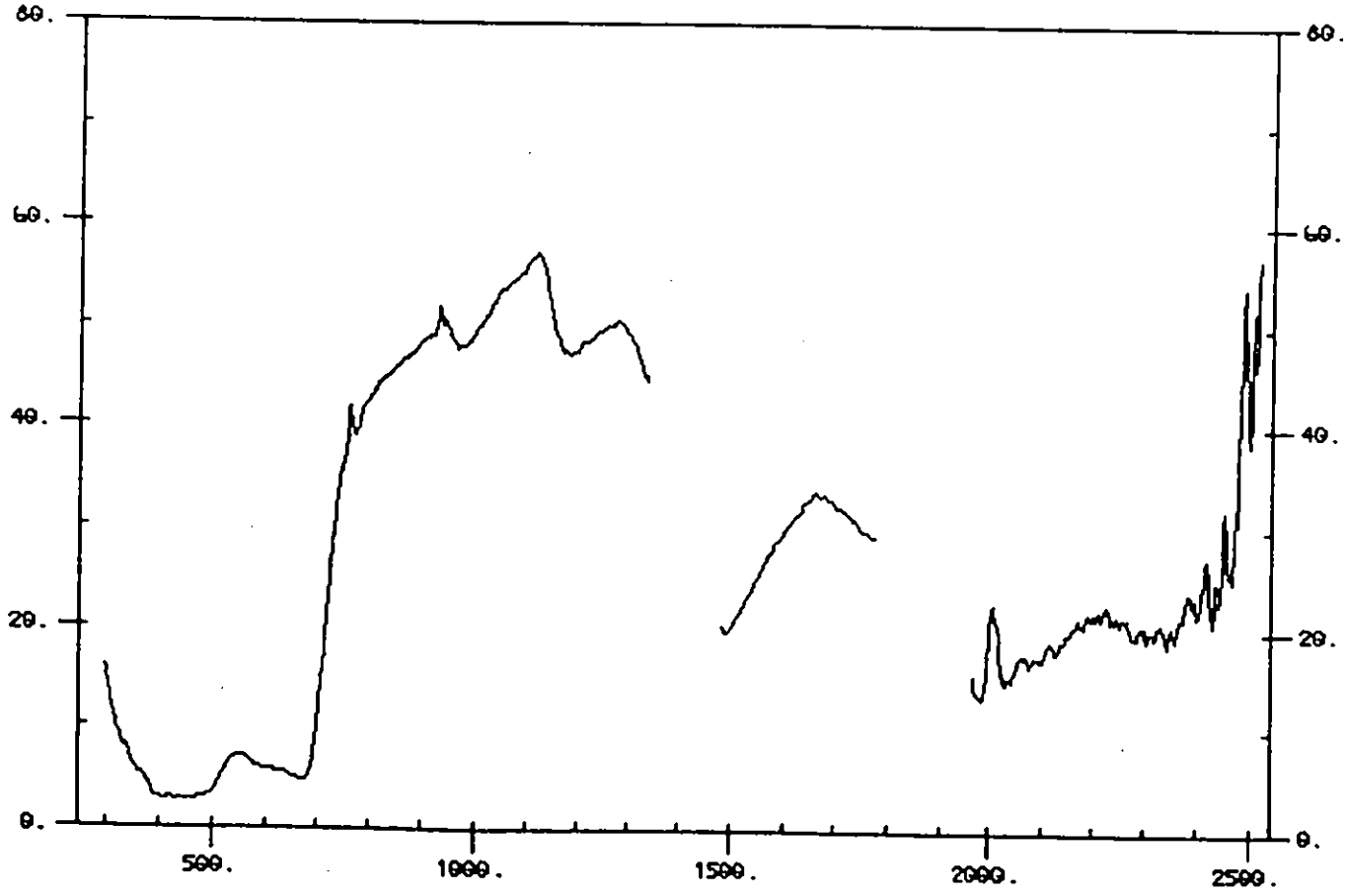

Fig.11 Bare Earth

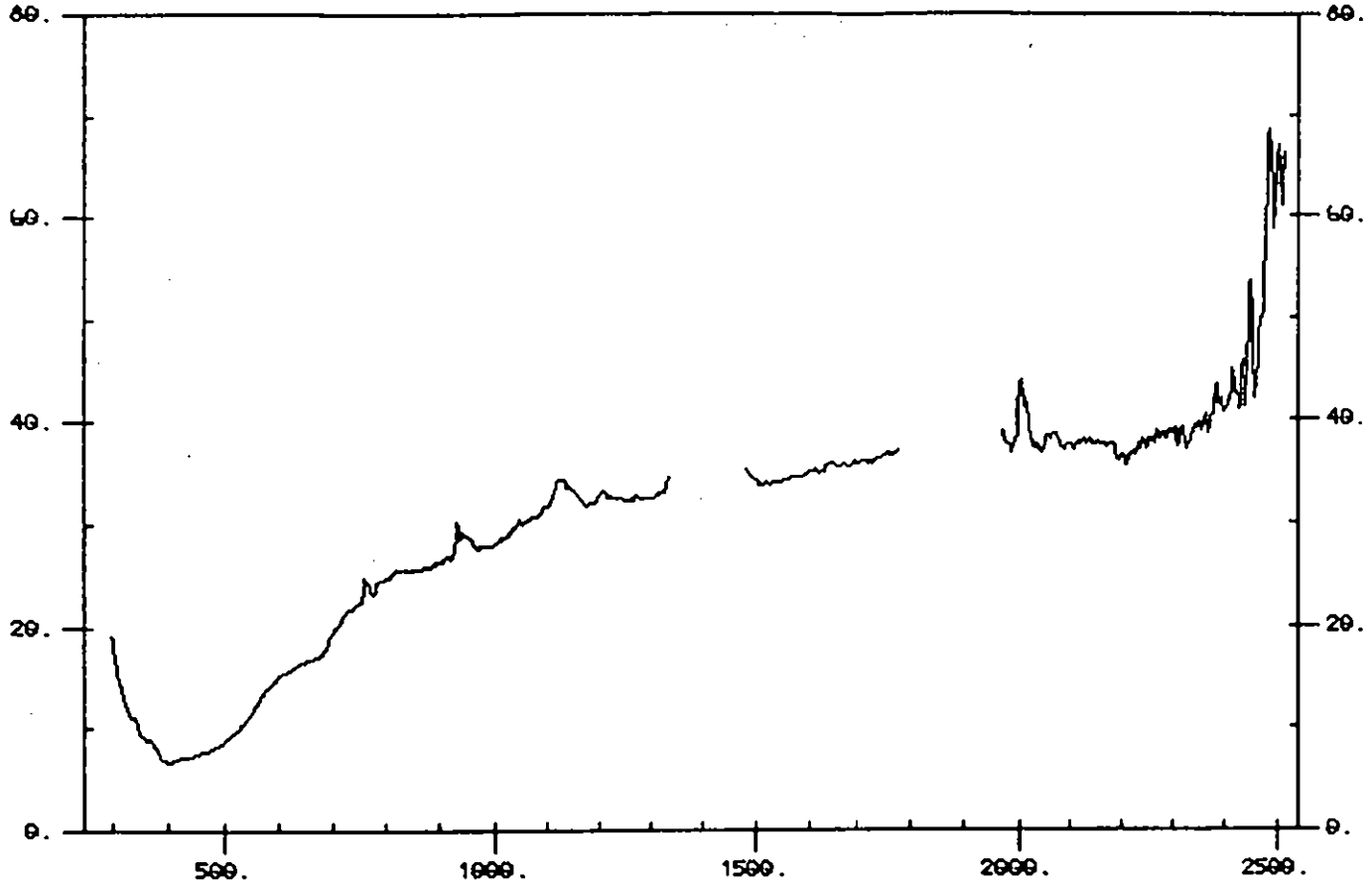


Fig. 12 Bare Earth

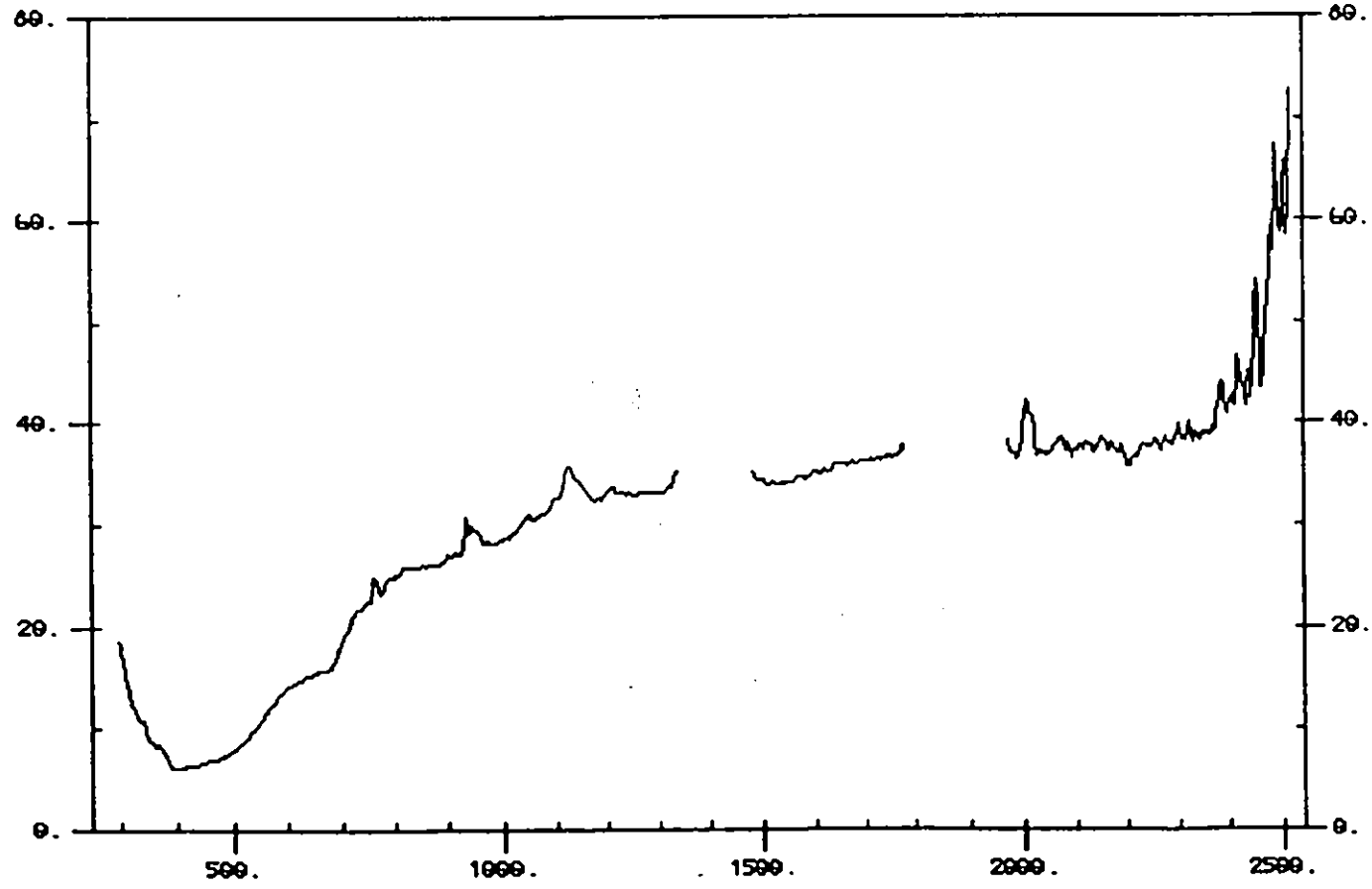

Fig. 13 Cauliflowers

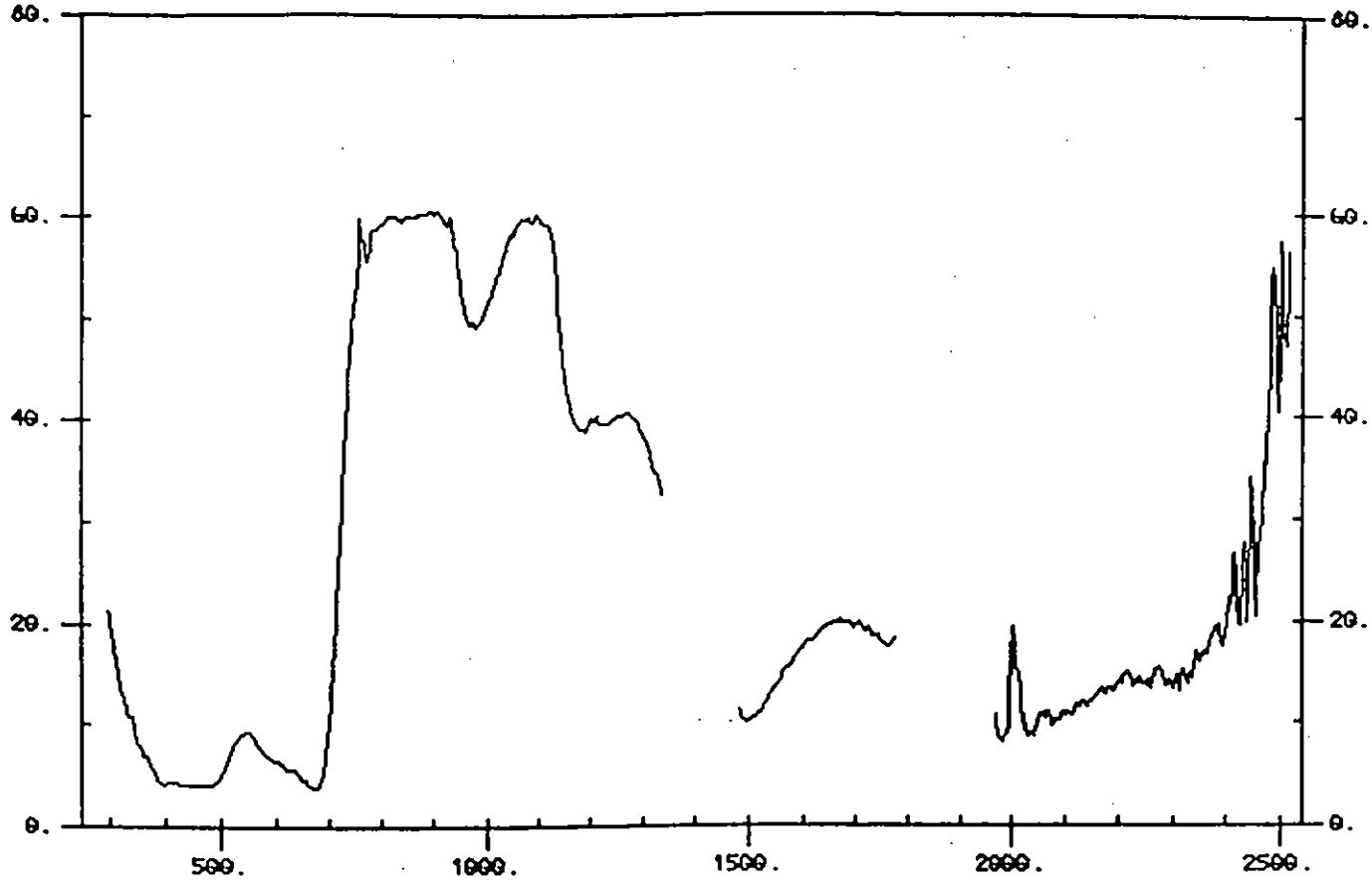


Fig. 14 Nettles

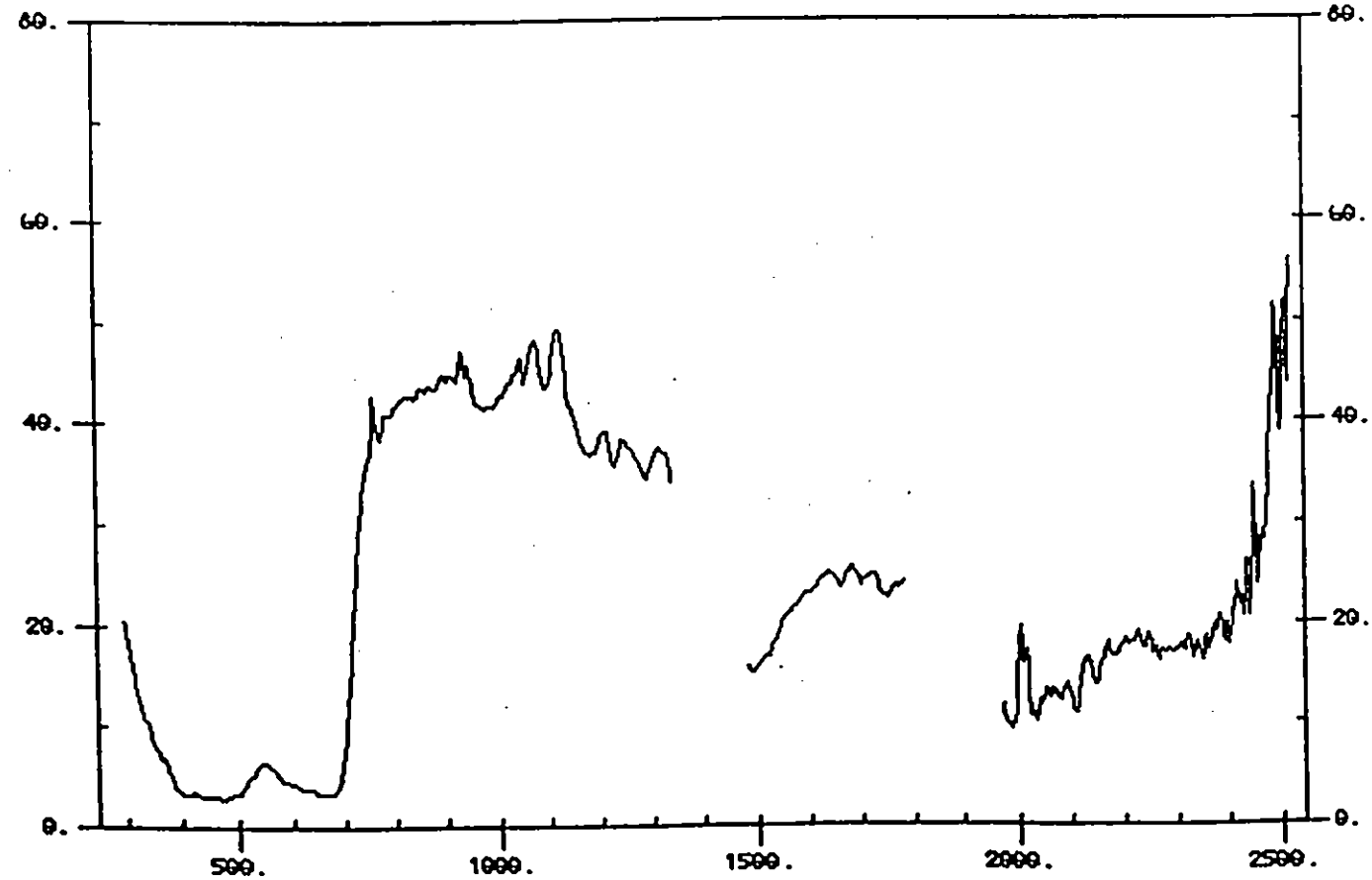

Fig. 15 Swedes

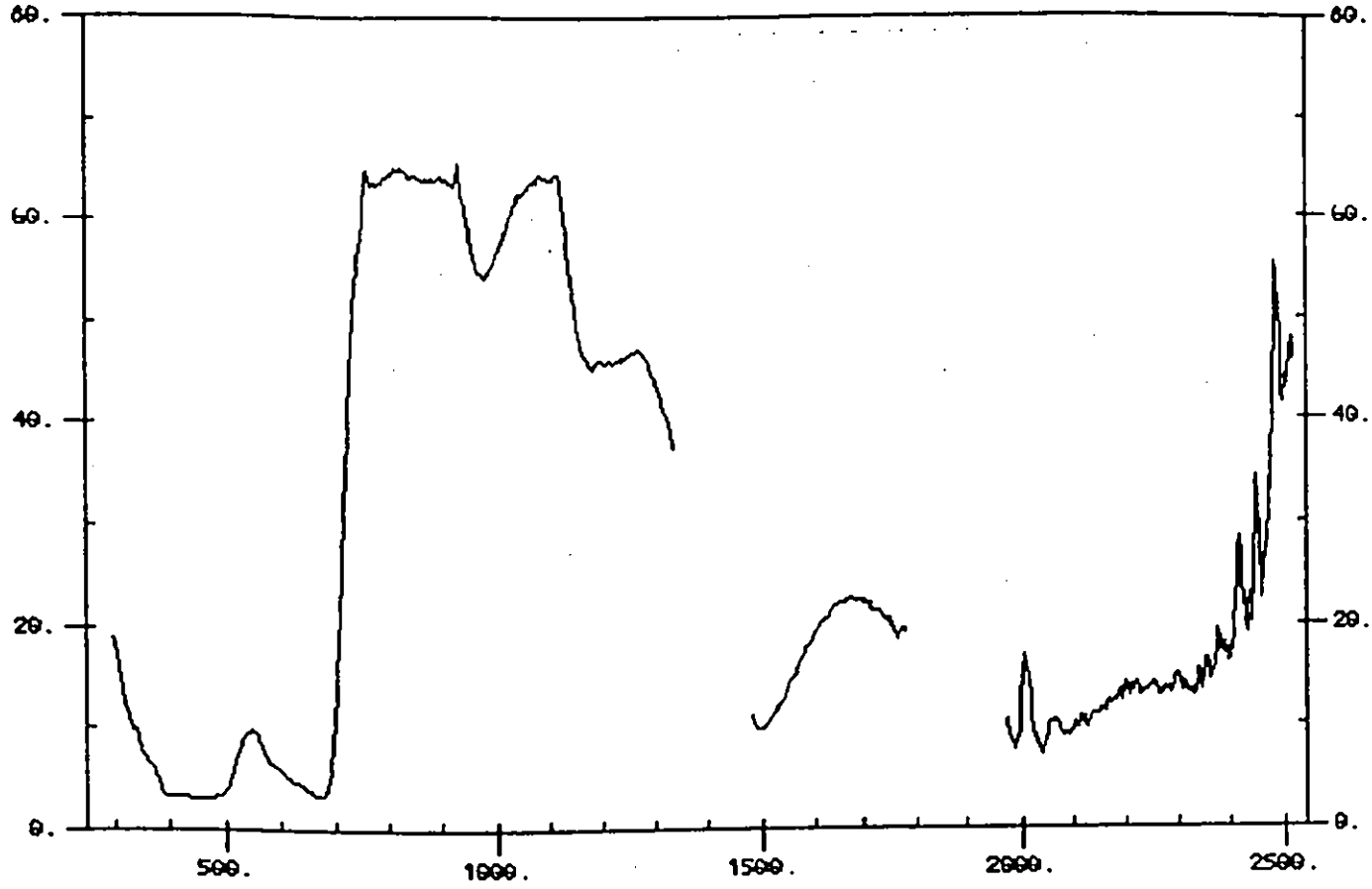


Fig. 16 Cut Grass

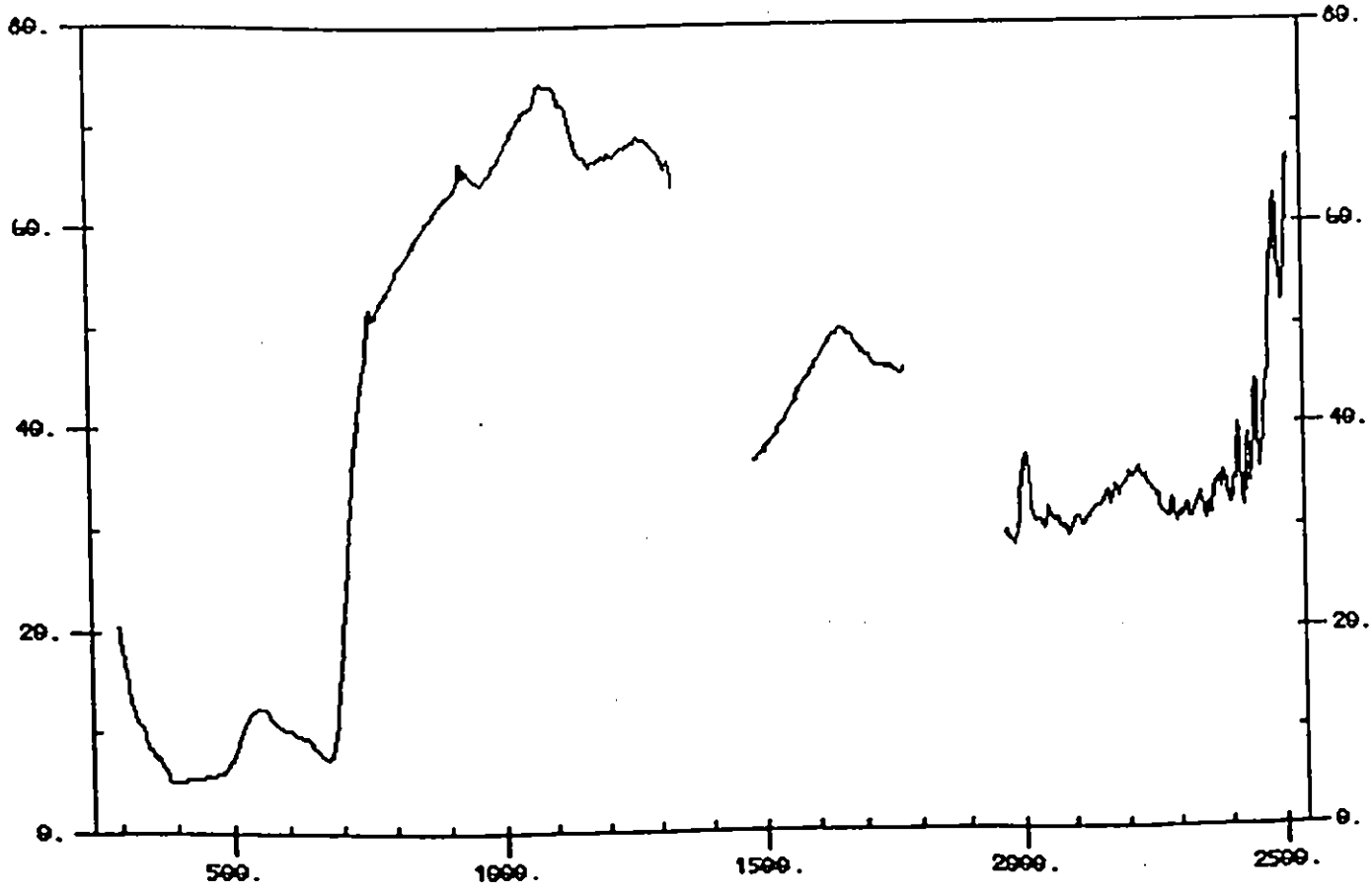

# Appendix II Comparison of reflectance spectra obtained using the IRIS spectroradiometer for fields under identical vegetation types.

Fig. 1 Temporary Grass

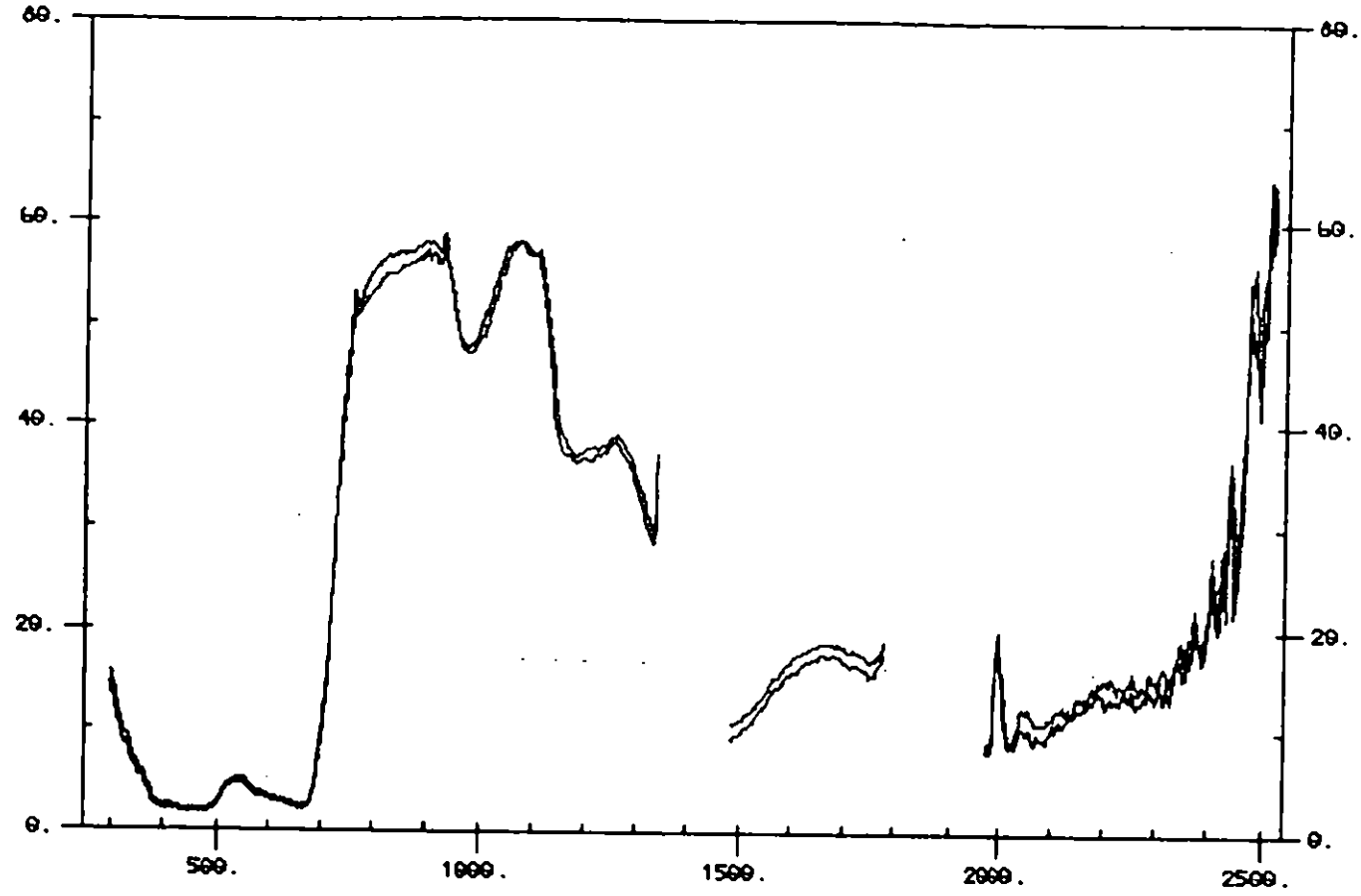


Fig. 2 Winter Barley

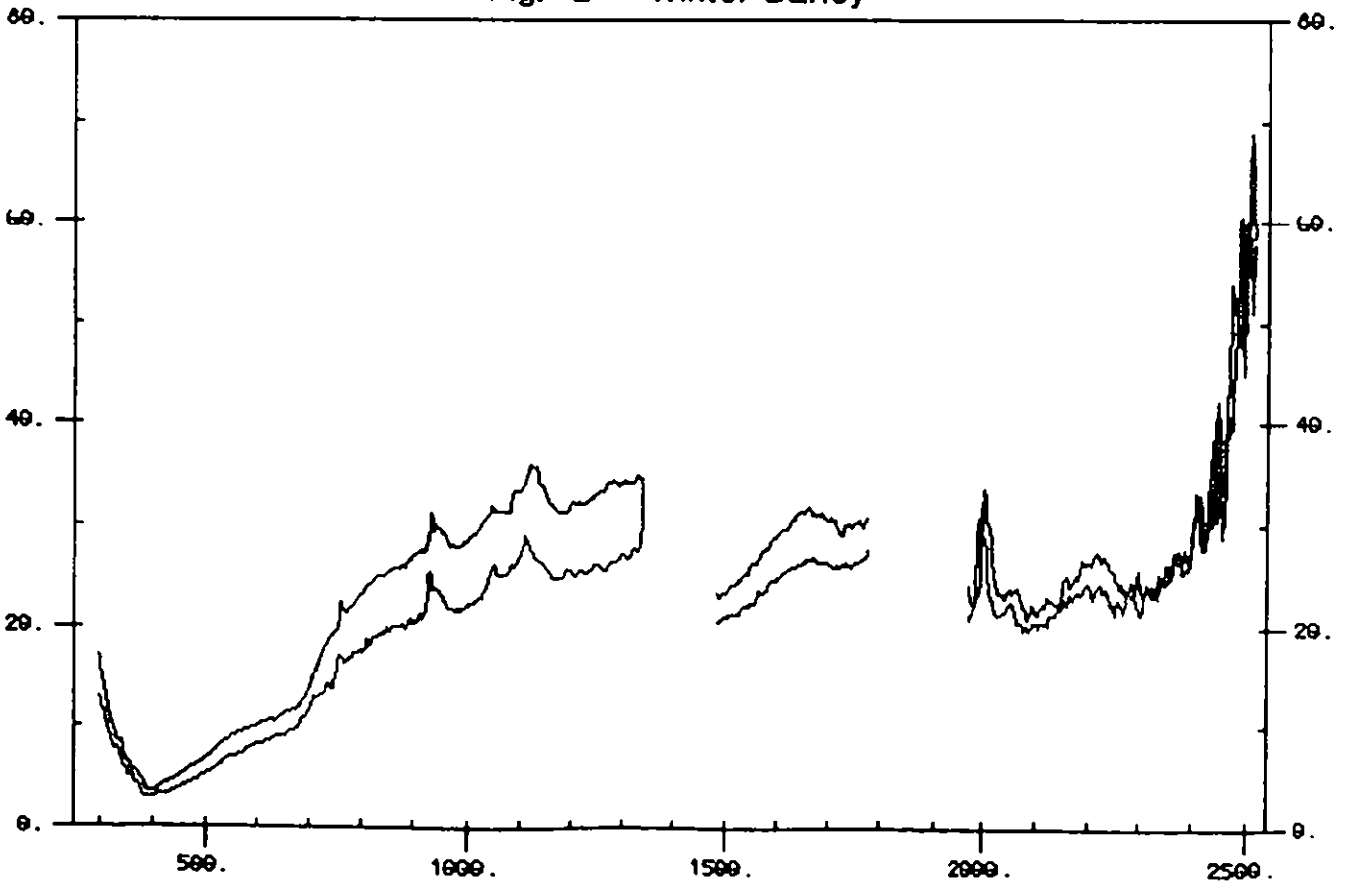

Fig. 3 Spring Barley

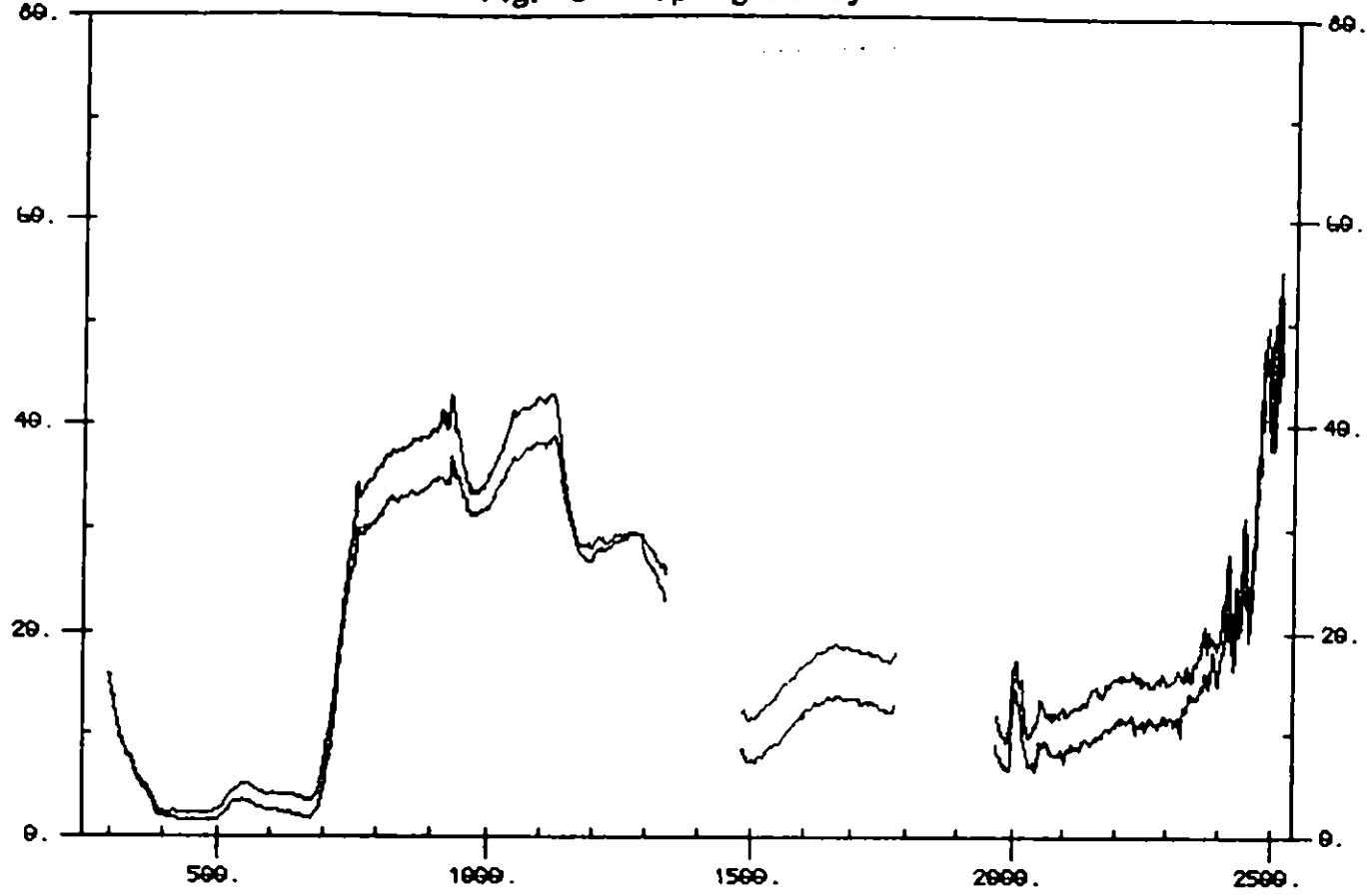


Fig. 4 Bare Earth

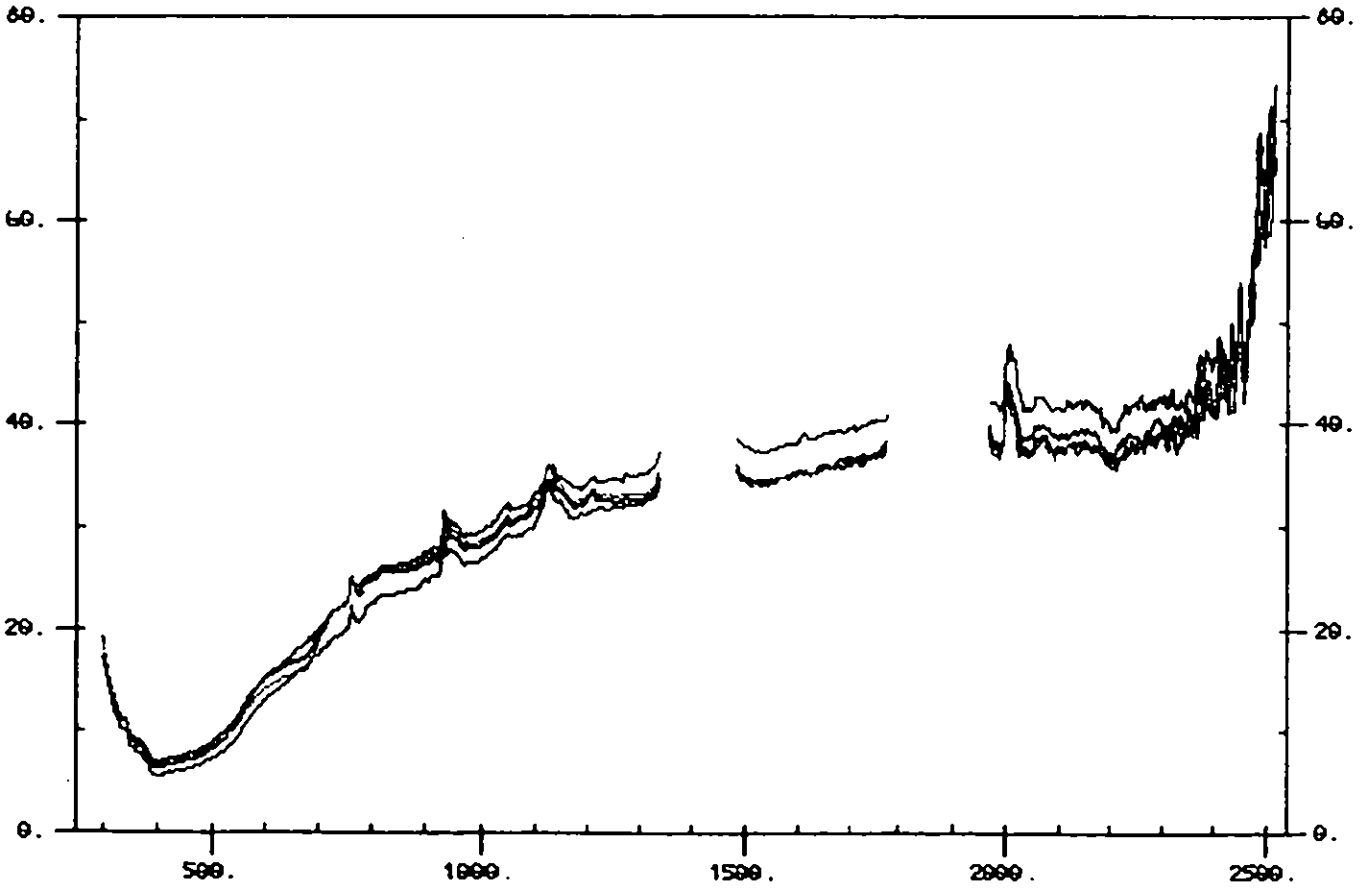

Fig. 5 Permanent Grass

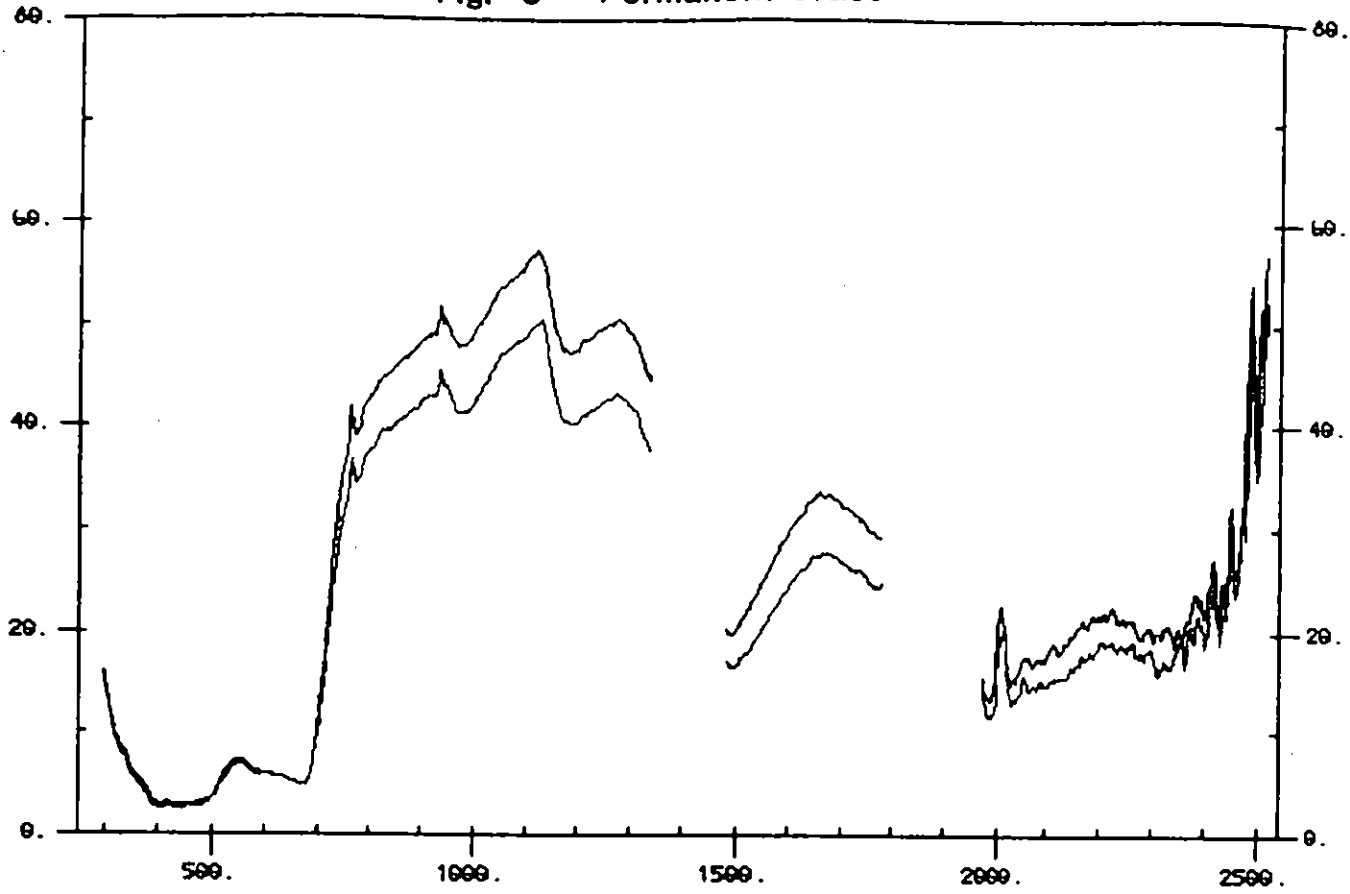

# Appendix III Regression of ATM vs IRIS radiances (w x $10^{-7}$ $cm^{-2}$ $sr^{-1}$ $nm^{-1}$) for the ATM band widths

ATM Band 1

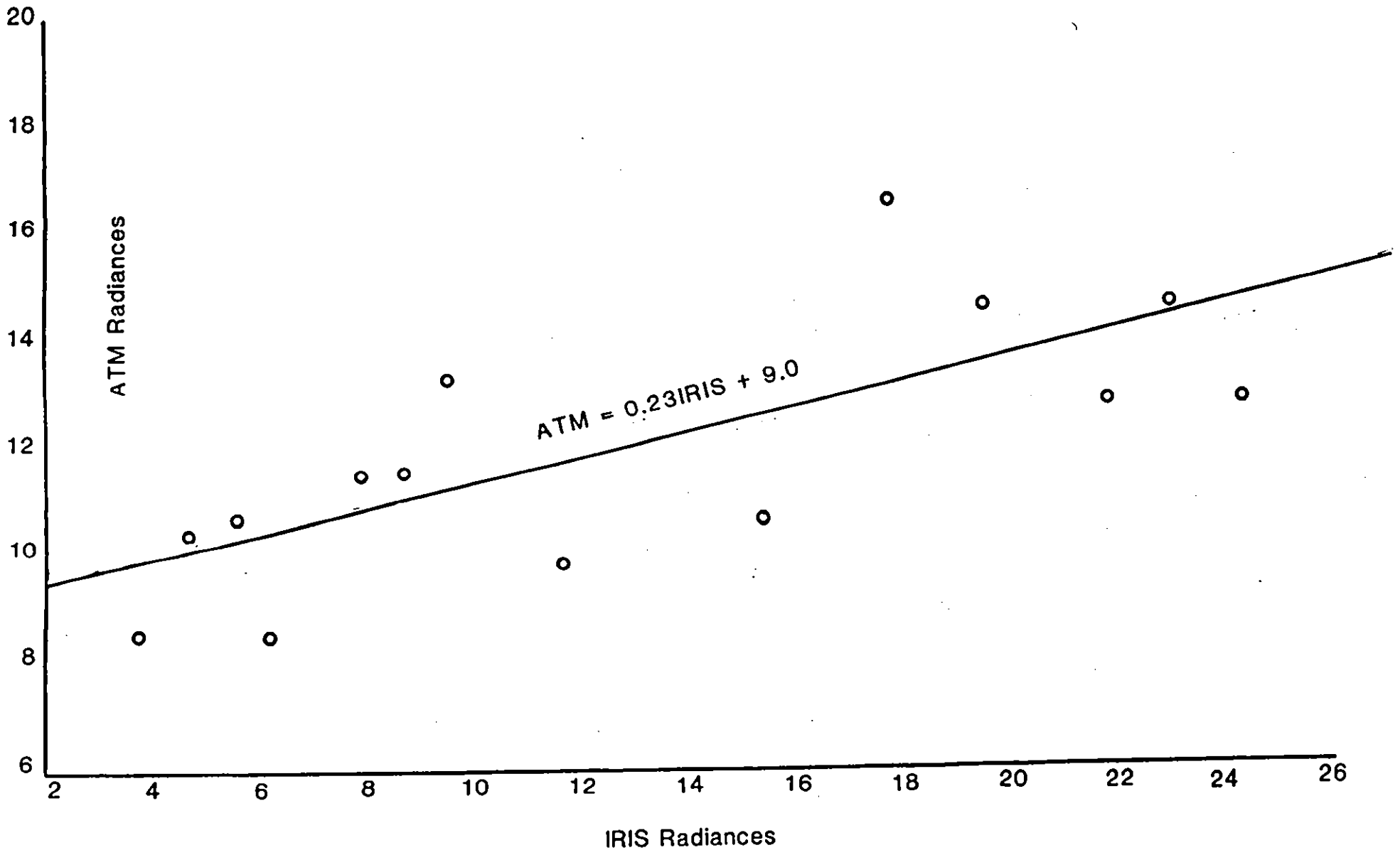
20
18
16
14
12
10
8
6
ATM Radiances
ATM = 0.23IRIS + 9.0
2
4
6
8
10
12
14
16
18
20
22
24
26
IRIS Radiances

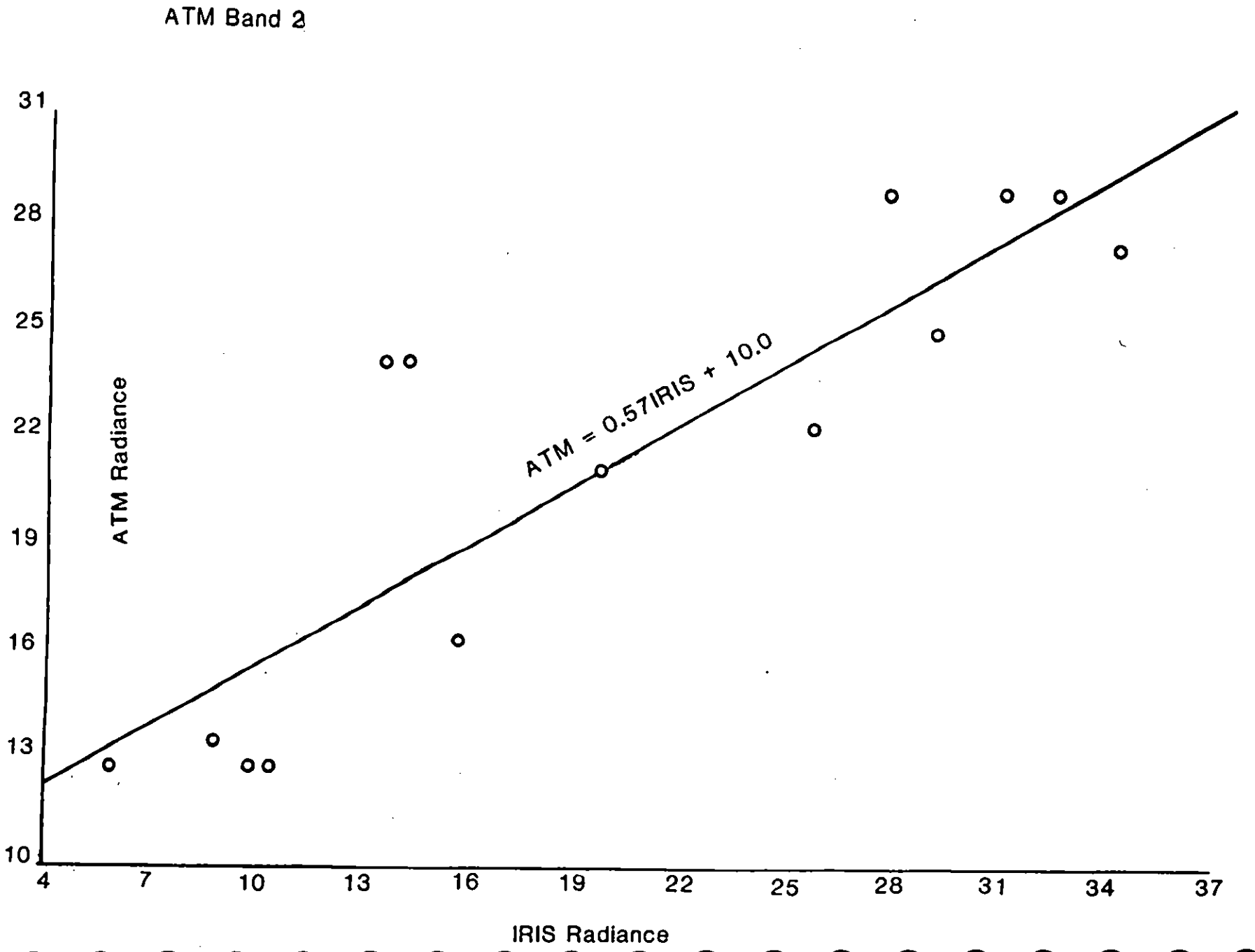
ATM Band 2
31
28
25
22
19
16
13
10
ATM Radiance
ATM = 0.571IRIS + 10.0
4
7
10
13
16
19
22
25
28
31
34
37
IRIS Radiance

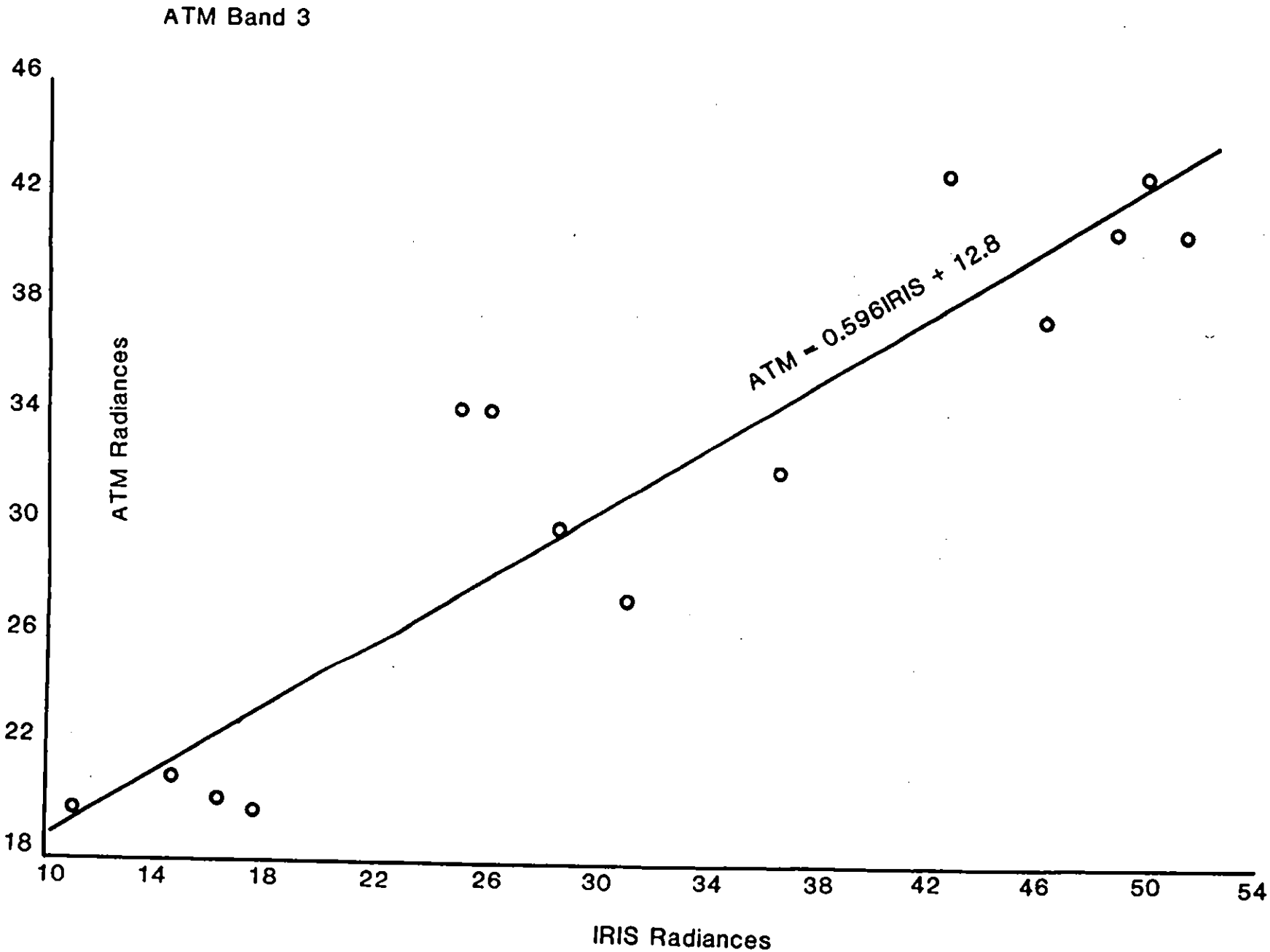
ATM Band 3
ATM Radiances
IRIS Radiances
ATM = 0.596IRIS + 12.8
46
42
38
34
30
26
22
18
10
14
18
22
26
30
34
38
42
46
50
54

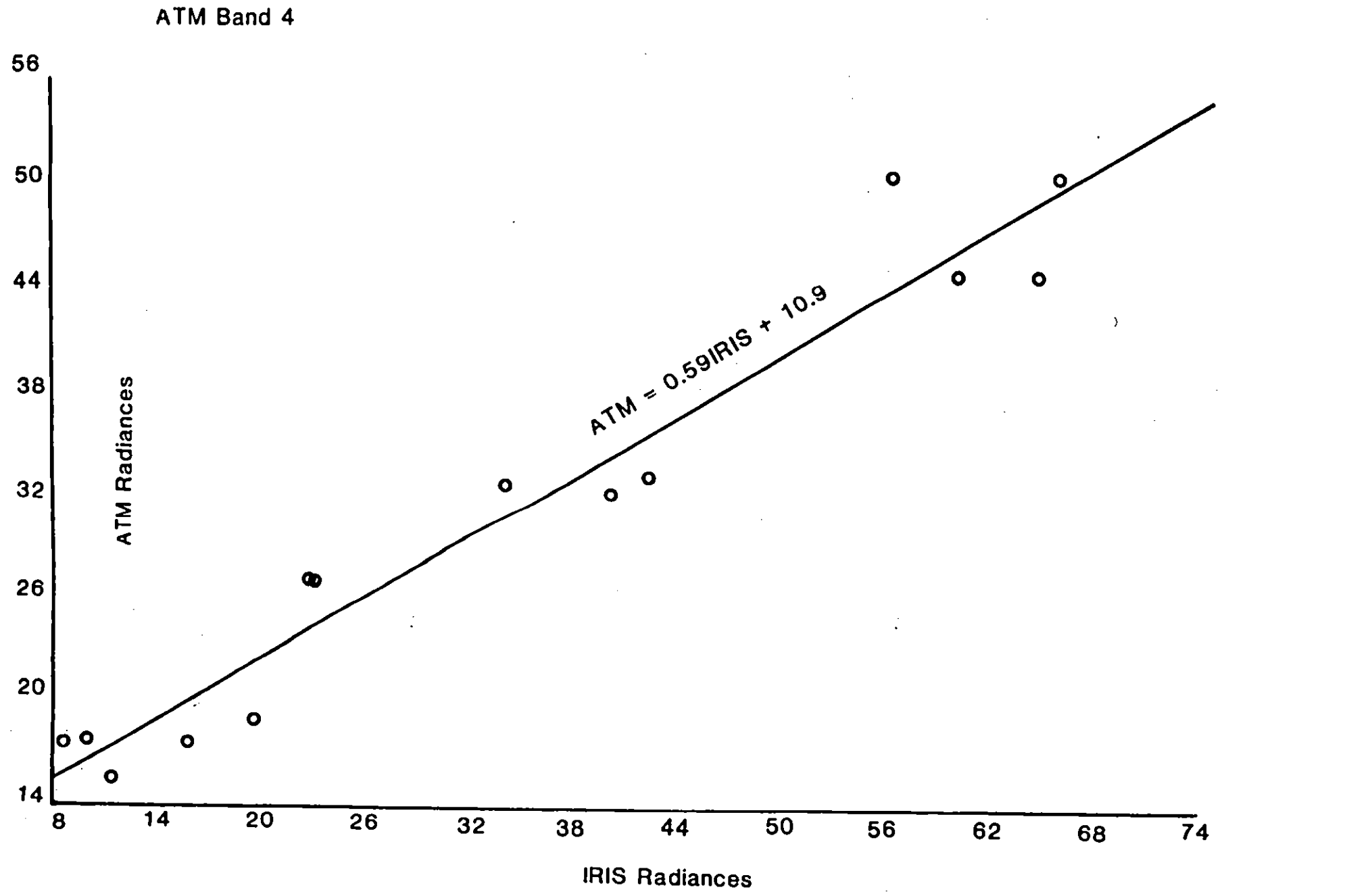
ATM Band 4
56
50
44
38
32
26
20
14
ATM Radiances
ATM = 0.59IRIS + 10.9
8
14
20
26
32
38
44
50
56
62
68
74
IRIS Radiances

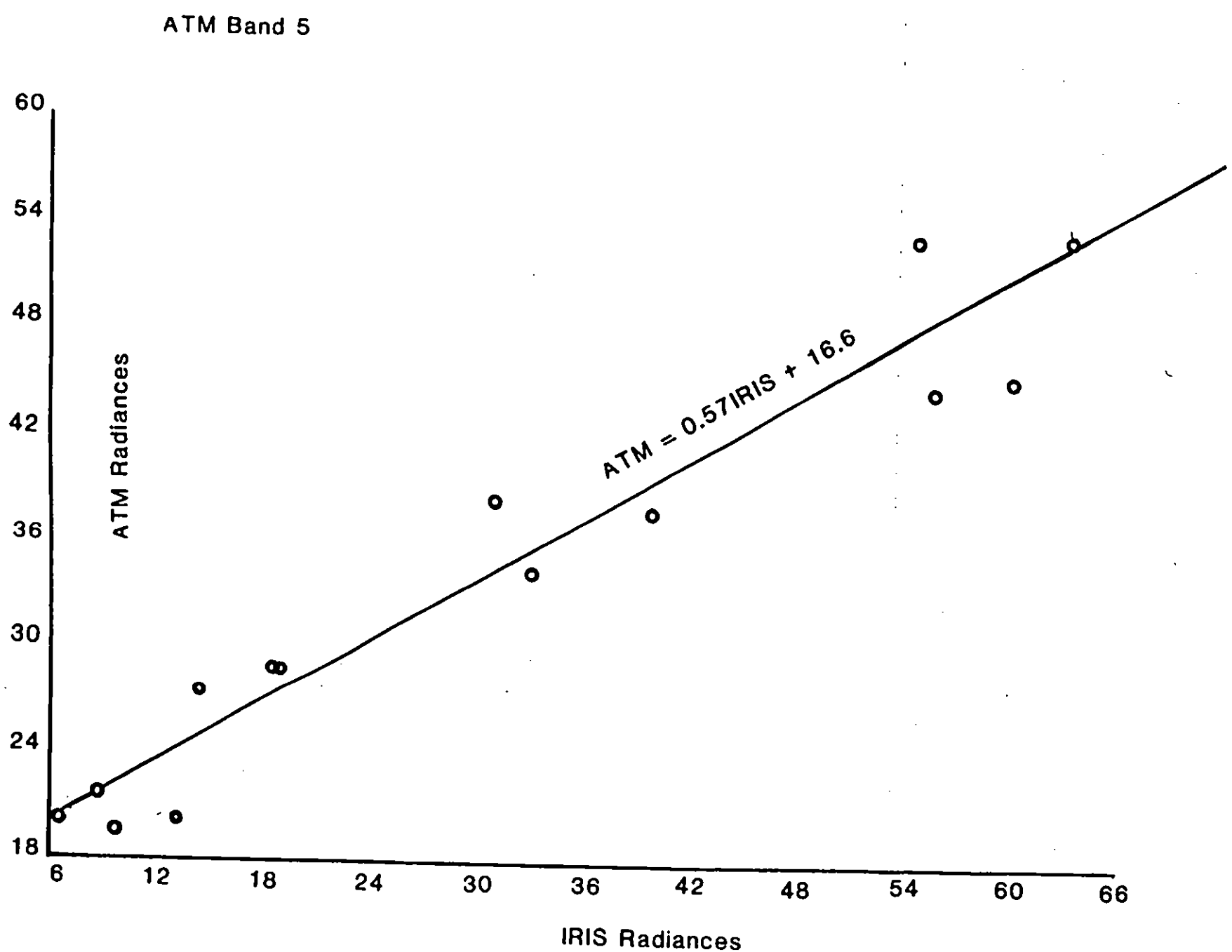
ATM Band 5
ATM Radiances
IRIS Radiances
ATM = 0.57IRIS + 16.6
60
54
48
42
36
30
24
18
6
12
18
24
30
36
42
48
54
60
66

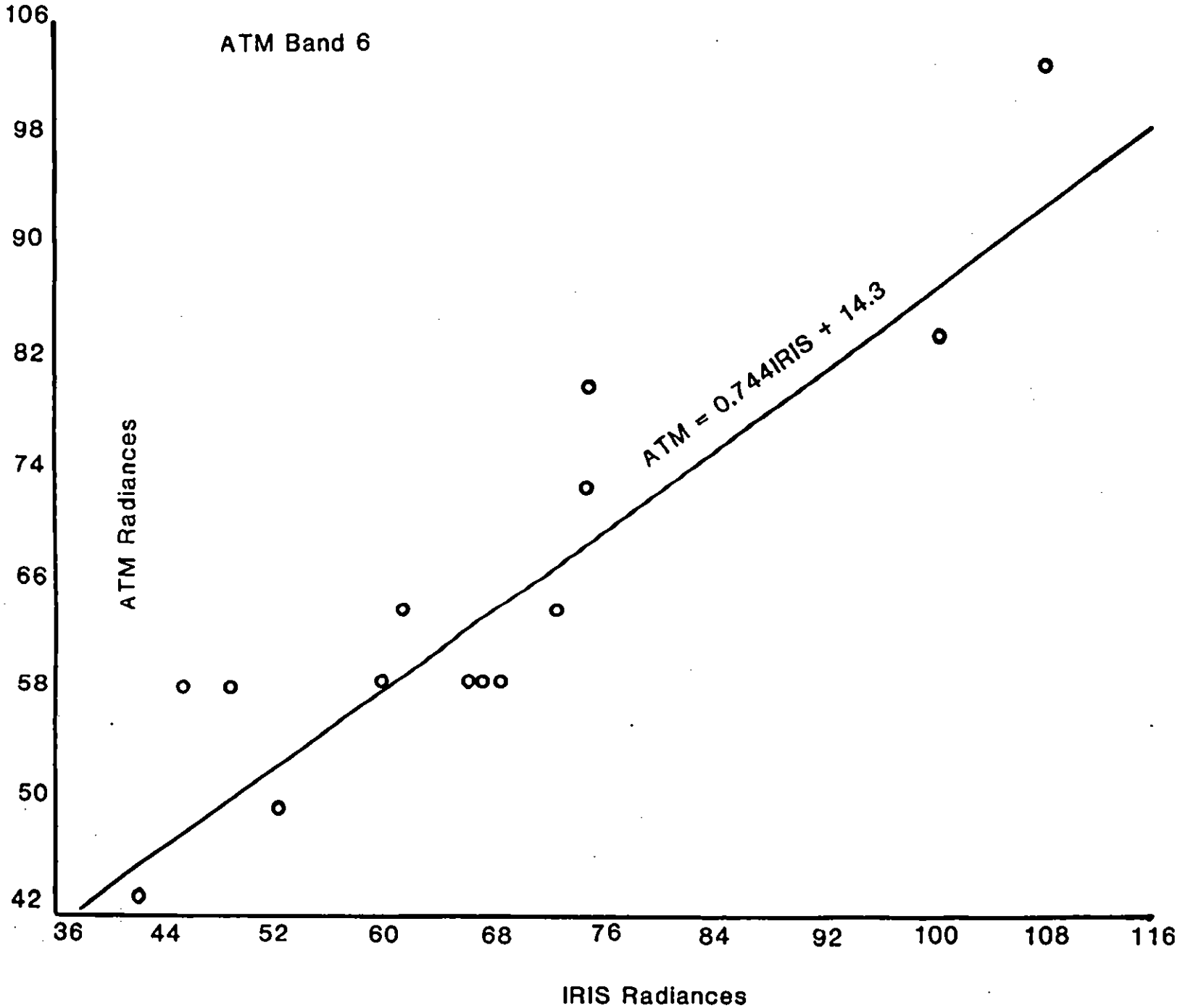
ATM Band 6
ATM = 0.744IRIS + 14.3
ATM Radiances
IRIS Radiances
106
98
90
82
74
66
58
50
42
36
44
52
60
68
76
84
92
100
108
116

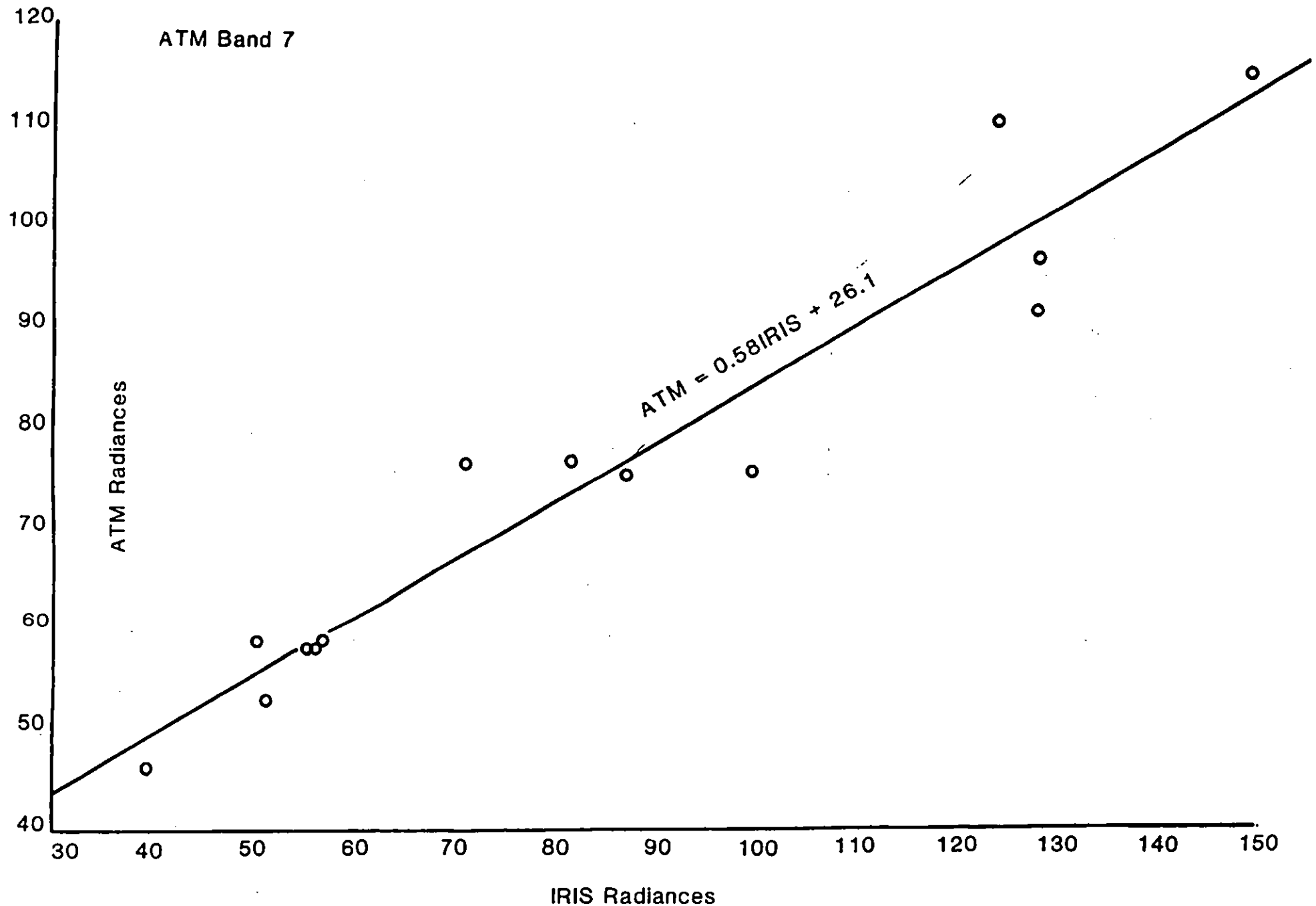
ATM Band 7
ATM = 0.58IRIS + 26.1
ATM Radiances
IRIS Radiances
120
110
100
90
80
70
60
50
40
30
40
50
60
70
80
90
100
110
120
130
140
150

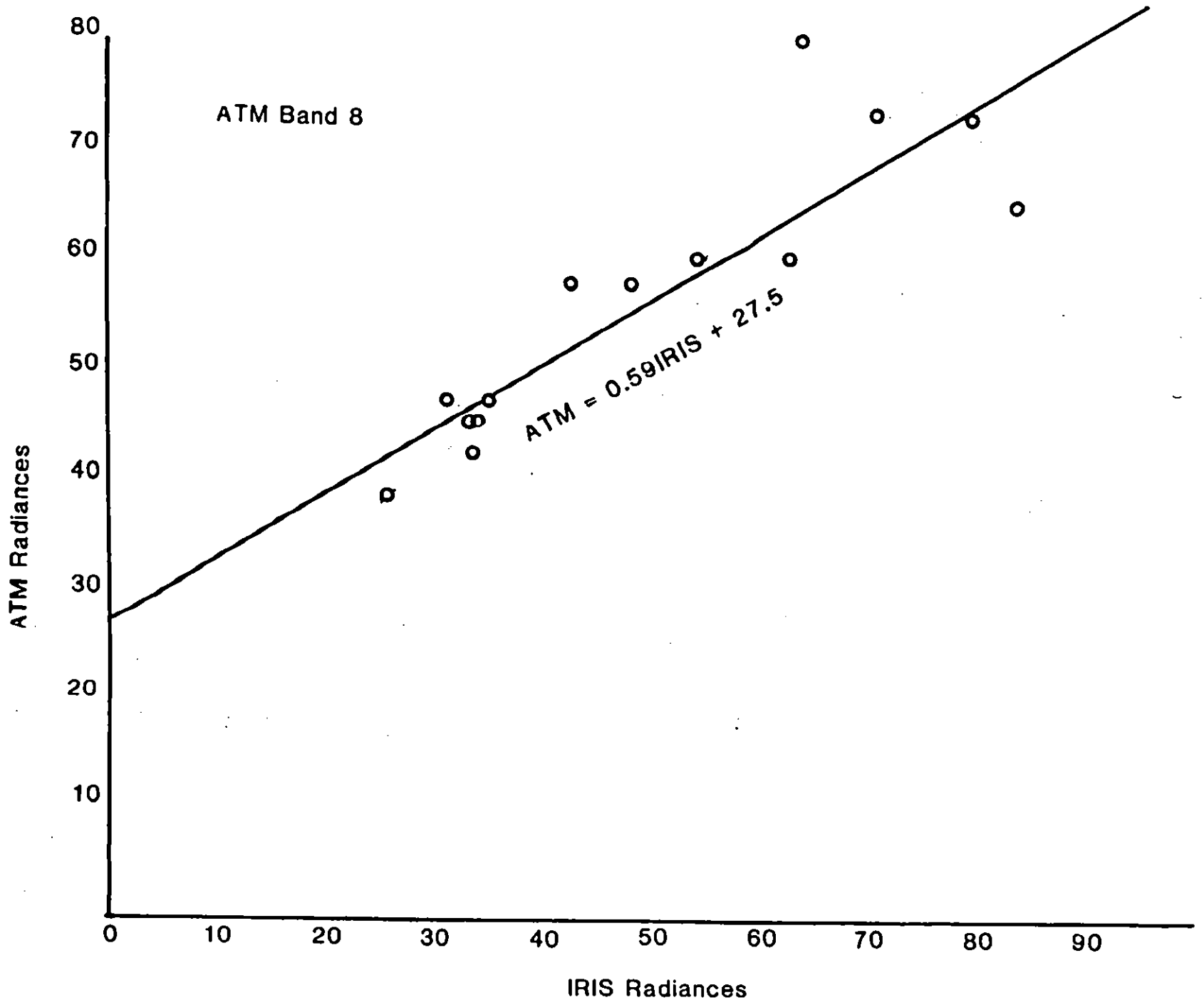
ATM Band 8
ATM = 0.59IRIS + 27.5
ATM Radiances
IRIS Radiances
80
70
60
50
40
30
20
10
0
10
20
30
40
50
60
70
80
90

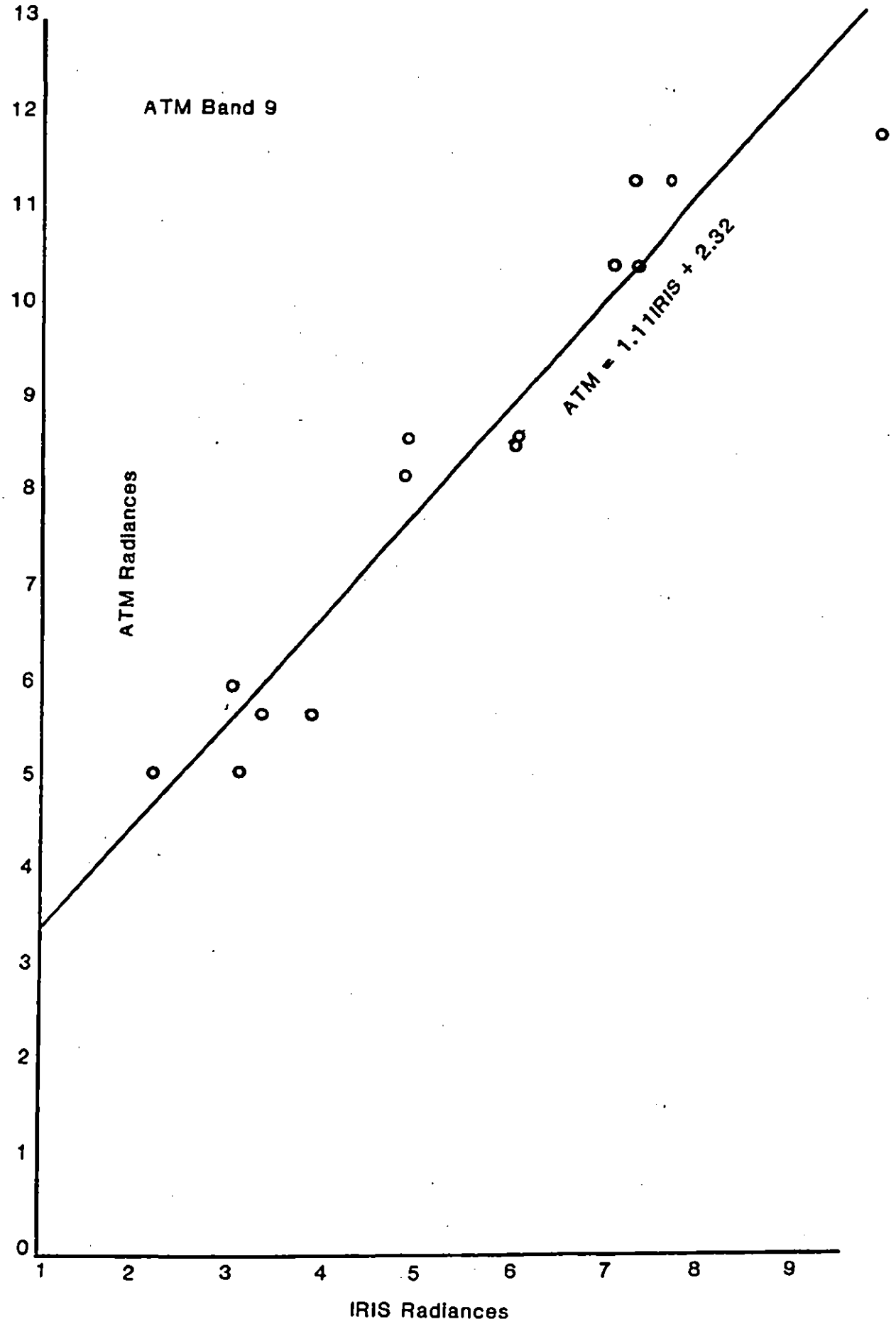
ATM Band 9
ATM = 1.11IRIS + 2.32
ATM Radiances
IRIS Radiances
0
1
2
3
4
5
6
7
8
9
10
11
12
13
1
2
3
4
5
6
7
8
9

ATM Band 10